MEMRO 2022

9th International Symposium On Middle Ear Mechanics in Research and Otology

June 21-25, 2022 Boulder, CO, USA

Organized by the University of Colorado School of Medicine,
Anschutz Medical Campus, Department of Otolaryngology

Conference Program and Abstracts

Welcome to MEMRO 2022

9th International Symposium on Middle Ear Mechanics in Research and Otology

Boulder, CO USA
June 21-25, 2022

It has been four eventful years since the last MEMRO meeting, in Shanghai China, where Colorado was selected to host of the 9th MEMRO meeting. Following MEMRO tradition, we seek to bring together middle ear scientists, engineers, and clinicians to discuss recent advances in middle ear physiology, biomechanics, surgical techniques, diagnostics, implants, computational models, imaging, and injury mechanisms. Our state goal was to increase clinician representation at MEMRO, and accordingly we chose "Advances in Middle Ear Science and OTO Surgery" as the meeting's topic, and offer an optional "Middle Ear Mechanics Seminar" for interested clinicians immediately prior to MEMRO.

The team selected to host the 9th MEMRO hails from the University of Colorado School of Medicine, located on the Anschutz Medical Campus in Aurora, CO, just East of Denver. We decided to host the meeting on the main campus of the University of Colorado in Boulder, CO, North West of Denver, to take advantage of the beautiful location at the base of the Rocky Mountains, with clear views of the nearby Flatirons immediately outside of the conference venue, and ready access to the University of Colorado main campus, Boulder CO entertainment and dining, and outdoor recreation opportunities. We hope that the majestic surroundings will attract presenters from around the world, and inspire lively discussions during the meeting.

MEMRO 2022 has received over 70 abstract submissions, and will include 5 keynote/plenary sessions, a session memorializing Richard Goode, 11 oral presentation sessions including 47 oral presentations, and 24 posters. We are quite pleased with the number and quality of the abstracts submitted given the worldwide events of the last three years, and anticipate an excellent meeting.

After such a fraught 3 years, where we have all lost family, friends, and colleagues during the COVID-19 pandemic, we are incredibly grateful to be able to extend a warm Welcome to Colorful Colorado. We hope you all enjoy a happy and healthy visit to our beautiful state.

Welcome to MEMRO 2022 in Boulder, CO, USA!

The MEMRO 2022 Organizing Committee,
Stephen Cass, Nathaniel Greene, John Peacock, and Daniel Tollin.

Contents

MEMRO 2022 is supported by funding from NIH NIDCD

NIH National Institute on Deafness and Other Communication Disorders

MEMRO 2022
Program at a Glance

Tuesday 21 June

08:00	Registration
13:30	Applied Middle Ear Mechanics Seminar for Clinicians Speakers: Steve Cass, Alex Huber, Karl-Bernd Huttenbrink, Aaron Remenschneider, Thomas Zahnert.
17:00	Welcome Reception

Wednesday 22 June

08:00	Registration
09:00	Opening Ceremony
09:30	Keynote Lecture (Alex Huber, UZH Zurich)
10:15	Coffee/Tea/Poster Session PS
10:45	Podium Session PD1 ME Biomechanics
12:15	Lunch/Poster Session PS
13:45	Plenary Lecture 1 (Luo Zhe-Xi, University of Chicago)
14:30	Podium Session PD2 ME Implants 1
16:15	Coffee/Tea/Poster Session PS
16:45	Podium Session PD3 Comparative Studies and Middle Ear Evolution

Thursday 23 June

08:00	Registration
09:00	Plenary Lecture 2 (Sumit Agrawal, Western University)
09:45	Podium Session PD4 Imaging
10:30	Coffee/Tea/Poster Session PS
11:00	Podium Session PD5 Bone Conduction 1
11:45	Podium Session PD6 Computational Models
12:45	Lunch/Poster Session PS
14:15	Podium Session PD7 Bone Conduction 2
15:15	Podium Session PD8 High Intensity Sound-Induced Hearing Damage and Protection
16:00	Coffee/Tea/Poster Session PS
16:30	Next MEMRO Presentations
17:00	Richard Goode Memorial (Geoffrey Ball, MED-EL)

Friday 24 June

08:00	Registration
09:00	Plenary Lecture 3 (Matt Mason, University of Cambridge)
09:45	Podium Session PD9 Physiology
10:15	Coffee/Tea/Poster Session PS
10:45	Podium Session PD10 ME Implants 2
12:15	Lunch/Poster Session PS (Committee meeting)
13:45	Plenary Lecture 4 (Stefan Stenfelt, Linköping University)
14:30	Podium Session PD11 Pathology
16:00	Group Photo & Coffee/Tea
16:30	Award Presentation/ Closing Ceremony
17:00	Meeting end, bus to Banquet
17:00	Reception at Chautauqua Dining Hall
18:00	Banquet Meal
19:00	Guest Speaker: Joe Sertich (Denver Museum of Nature and Science)
21:00	Last Call

MEMRO 2022
Detailed Program

Tuesday, June 21

12:00	Registration Opens

Applied Middle Ear Mechanics Seminar for Clinicians

13:30-14:10	Basics of middle ear mechanics for surgeons Karl Huttenbrink, M.D.
14:10-14:20	Questions and Discussion
14:20-14:40	Tympanoplasty Techniques Aaron Remenschneider, M.D.
14:40-14:50	Questions and Discussion
14:50-15:00	Coffee Break
15:00-15:20	The Ossicular Chain and Ossiculoplasty Thomas Zahnert, M.D./ Marcus Neudert, M.D.
15:20-15:30	Questions and Discussion
15:30-15:50	Otosclerosis and stapes surgery Alex Huber, M.D.
15:50-16:00	Questions and Discussion
17:00-19:00	Welcome Reception

Wednesday, June 22

8:00-17:00	Registration Opens
9:00-9:30	Opening Ceremony
9:30-10:15	Keynote Lecture Alex Huber, UZH Zurich Moderator: Stephen Cass
10:15-10:45	Coffee Break – Poster Session
10:45-12:15	**Podium Session PD1: Biomechanics of the Middle Ear** **Moderator: Sunil Puria**

PD1.1. The effect of prestrain in the tympanic membrane: measurement and modeling
Pieter Muyshondt, pieter.muyshondt@uantwerpen.be

PD1.2. Unified database and methods for METF validation in temporal bone experiments
Till Moritz Essinger, tillmoritz.essinger@ukdd.de

PD1.3. On the influence of morphology on middle ear transfer function
Matthias Bornitz, matthias.bornitz@ukdd.de

PD1.4. Quasi-Static and Vibrational Behavior of the Human Middle-Ear Ossicular Chain under Static Pressure Loads
Jae HoonSim, jaehoon.sim@usz.ch

PD1.5. Multiaxial Stiffness of the Human Stapedial Annular Ligament and Effects of Pretension in Ossiculoplasty
Merlin Schär, merlin.schaer@usz.ch

PD1.6. Contrary to previous reports, human stapes motion is piston-like to high frequencies and provides high-frequency cochlear input
Christopher McHugh, Christopher_Mchugh@meei.harvard.edu

12:15-13:45 Lunch and Poster Session

13:45-14:30 Plenary Lecture – Luo Zhe-Xi, University of Chicago
Moderator: John Peacock

14:30-16:15 **Podium Session PD2: Middle Ear Implants 1**

Moderator: Hannes Maier

PD2.1. Design, Fabrication, Benchtop, and Cadaveric Temporal Bone Testing of Ultraminiature MEMS Implantable Middle Ear Accelerometers
Karl Grosh, grosh@umich.edu

PD2.2. Outcomes of combining hearing implants with autologous auricular reconstruction in children with congenital aural atresia
Alex Bennett, a.bennett@doctors.org.uk

PD2.3. Intracochlear sound pressure measurement in human cadaver temporal bones during forward and backward stimulation of the cochlear using the floating mass transducer
David Stauske, david.stauske@medel.com

PD2.4. Investigation of a new type of hearing aid device – the hearing contact lens®
Michael Lauxmann, Michael.Lauxmann@Reutlingen-University.DE

PD2.5. Biomimetic Tympanic Membrane Implants with Tunable Mechanical and Oscillatory Properties Based on Simulation
Zhaoyu Chen, zhaoyu.chen@uniklinikum-dresden.de

PD2.6. Method for testing the dislocation resistance of middle ear prostheses
Martin Koch, martin.koch@uniklinikum-dresden.de

PD2.7. A new bio-compatible/degradable –sensor concept for middle ear pressure monitoring
Thomas Zahnert, Thomas.Zahnert@uniklinikum-dresden.de

16:15-16:45 Coffee Break – Poster Session

16:45-17:30 **Podium Session PD3: Comparative Studies and Middle Ear Evolution**

Moderator: Susan Voss

PD3.1. The Morphology of the Avian Bony Columella
John Peacock, john.2.peacock@cuanschutz.edu

PD3.2. A comparative study of elephant and human middle-ear sound transmission using 3D Laser Doppler Vibrometery

Caitlin O'Connell-Rodwell, Caitlin_Oconnell@meei.harvard.edu

PD3.3. Hearing capacities for accurate speech reception likely evolved before the human-chimpanzee split
Alexander Stoessel, alexander.stoessel@uni-jena.de

Thursday, June 23

8:00 Registration

9:00-9:45 Plenary Lecture – Sumit Agrawal, Western University
Moderator: Stephen Cass

9:45-10:30 **Podium Session PD4: Imaging Technologies**
Moderator: Dirk Beutner

PD4.1. Rabbit tympanic membrane thickness distribution obtained via optical coherence tomography
Pieter Livens, pieter.livens@uantwerpen.be

PD4.2. Study of the cochlear insertion area, relevant for mechanics and electrode insertion
Nicolas Verhaert, nicolas.verhaert@kuleuven.be

PD4.3. Intracochlear wave propagation analysis using optical coherence tomography vibrometry
Tristan Putzeys, tristan.putzeys@kuleuven.be

10:30–11:00 Coffee Break – Poster Session

11:00-11:45 **Podium Session PD5: Bone Conduction 1**
Moderator: Heidi Nakajima

PD5.1. Experimental Investigation of the Intracochlear Sound Pressure under Intracranial Stimulation and Bone Conduction Stimulation
Ivo Dobrev, ivo.dobrev@usz.ch

PD5.2. Vibration pattern of the bone encapsulating the inner ear during bone conduction stimulation
Stefan Stenfelt, stefan.stenfelt@liu.se

PD5.3. Is bone conducted stimulation closer to the cochlea more efficient?
Hannes Maier, Maier.Hannes@mh-hannover.de

11:45-12:45 **Podium Session PD6: Computational Models**
Moderator: Rong Gan

PD6.1. Model-Based Hearing Diagnosis based on Monte-Carlo Parameter Estimation and Artificial Neural Networks
Benjamin Sackmann, Benjamin.Sackmann@Reutlingen-University.de

PD6.2. Virtual Test Environment for Prostheses - Coupled Middle- and Inner-ear Model
Dmitrii Burovikhin, Dmitrii.Burovikhin@reutlingen-university.de

PD6.3. 3D Finite Element Model of the Entire Human Ear for Predicting Auditory Blast Injury
Rong Gan, rgan@ou.edu

PD6.4. Diagnostic support in tympanoplasty based on machine learning of numerical analysis results
Sinyoung Lee, sylee@bio.mce.uec.ac.jp

12:45-14:15 Lunch and Poster Session

14:15-15:15 **Podium Session PD7: Bone Conduction 2**

Moderator: Alex Huber

PD7.1. Can a promontory represent the cochlear response in bone-conducted hearing?
Namkeun Kim, nkim@sogang.ac.kr

PD7.2. Preliminary Experimental Investigation of the Relationship Between Temporal Bone 3D Motion and Intracochlear Pressure
Ivo Dobrev, ivo.dobrev@usz.ch

PD7.3. Estimation of promontory vibration by surface microphone measurements in bone conduction stimulation
Patrick Maas, pmaa@oticonmedical.com

PD7.4. Basilar membrane and organ of Corti vibration measured with OCT during bone conduction stimulation in guinea pigs
Stefan Stenfelt, stefan.stenfelt@liu.se

15:15-16:00 **Podium Session PD8: High Intensity Sound-Induced Hearing Damage and Protection**

Moderator: Ted Argo

PD8.1. Real-time Measurement of Stapes Motion and Intracochlear Pressure during Blast Exposure
Alexander Bien, bienag@gmail.com

PD8.2. Hearing Protection and Damage Mitigation in Chinchillas Exposed to Repeated Low-intensity Blasts
Shangyuan Jiang. Shangyuan.Jiang-1@ou.edu

PD8.3. Derivation of a Simplified Middle Ear Model Using System Identification
James Easter, james.easter@cuanschutz.edu

16:00-16:30 Coffee Break – Poster Session

16:30-17:00 Future MEMRO Presentations

17:00-18:00 Richard Goode Memorial
Geoffrey Ball, MED-EL

Friday, June 24

8:00 Registration

9:00-9:45 Plenary Lecture – Matt Mason, University of Cambridge
Moderator: Daniel Tollin

9:45-10:15 **Podium Session 9: Physiology**

Moderator: Daniel Tollin

PD9.1. Middle-ear Sound Transmission Delay and Attenuation due to Mechanically Pulling Tensor Tympany and Stapedius Muscles
Nam Hyun Cho, Namhyun_cho@meei.harvard.edu

PD9.2. Anatomical variations within the human middle ear based on clinical imaging data
Daniel Schurzig, daniel.schurzig@medel.com

10:15-10:45 Coffee Break –Poster Session

10:45-12:15 **Podium Session PD10: Middle Ear Implants 2**

Moderator: Jim Easter

PD10.1. A partial middle ear replacement prosthesis with a concentric ball joint in the headplate
Dirk Beutner, dirk.beutner@med.uni-goettingen.de

PD10.2. Optical Measurements of Eardrum Vibrations and Sound Propagation in the Ear Canal for the Fitting of Active Middle Ear Implants
Frank Boehnke, frank.boehnke@tum.de

PD10.3. Assessment of hearing rehabilitation and speech perception in Vibrant Soundbridge round window vibroplasty – The role of dynamic range
Susan Busch, busch.susan@mh-hannover.de

PD10.4. Determination of individual Maximum Power Output from clinical routine data in Vibrant Soundbridge round window vibroplasty
Hannes Maier, Maier.Hannes@mh-hannover.de

PD10.5. The Hannover Coupler V2: Audiological Outcomes of a new Round Window Coupler for the Vibrant Soundbridge
Nicole Knölke, knoelke.nicole@mh-hannover.de

PD10.6. Implantable Piezoelectric-Polymer Microphones for the Middle Ear
Aaron Yeiser, ayeiser@mit.edu

12:15-13:45 Lunch – Poster Session

13:45-14:30 Plenary Lecture – Stefan Stenfelt, Linkoping University
Moderator: Nathaniel Greene

14:30-16:00 **Podium Session PD11: Middle Ear Pathology and Diagnostics & Surgical Techniques & Reconstructions**

Moderator: Karl-Bernd Huttenbrink

PD11.1. Prevention of recurrent Cholesteatoma by respecting the pathophysiologic genesis: a new theory of the origin of a retraction pocket
Karl Bernd Huettenbrink, k-b.huettenbrink@uni-koeln.de

PD11.2. Analysing 3D Wideband Absorbance Immittance and Providing High Accuracy for 3. 3. Automated Diagnosis of Otitis Media with Effusion in Different Age Groups Using Advanced Machine Learning
Fei Zhao, fzhao@cardiffmet.ac.uk

PD11.3. Endoscopic Optical Coherence Tomography for Evaluation of Middle Ear Reconstruction
Joseph Morgenstern, joseph.morgenstern@ukdd.de

PD11.4 Training a Machine-Learning Differential Diagnostic Tool for Conductive Hearing Loss Using Mechanistic Models
Hamid Motallebzadeh, Hamid_Motallebzadeh@meei.harvard.edu

PD11.5. Improving the Quality of Ossicular Chain Reconstruction by Means of Real-time Monitoring - An Experimental Study
Christoph Müller, christoph.mueller@uniklinikum-dresden.de

PD11.6. Palate Myoclonus acoustic - a case report
Fang Wang, harryfangfang520@163.com

16:00-16:30 Group Photo – Coffee Break – Poster Session

16:30-17:00 Award Presentation/Closing Ceremony

17:00-18:00 Transportation to Chautauqua Dining Hall

17:00 Cocktail Hour and Banquet

19:00 Guest Speaker: Joe Sertich – Denver Museum of Nature and Science

Poster Session

PS1. Effect of Endolymphatic Hydrops and Mannitol Dehydration Treatment on Guinea Pigs
Shuqi Wang, forestmeow@163.com

PS2. Sound Transmission in the Avian Middle Ear
John Peacock, john.2.peacock@cuanschutz.edu

PS3. Coupling Varying Mass Loads to the Short Incus Process and the Effect on Middle Ear Transfer Function (METF)
Ivo Grüninger, ivogr@gmx.de

PS4. Determination of maximum power output in an active transcutaneous bone conduction implant
Mohammad Ghoncheh, Ghoncheh.Mohammad@mh-hannover.de

PS5. Interaural separation during hearing by bilateral bone conduction stimulation
Sudeep Surendran, sudeep.surendran@liu.se

PS6. Effect of Thiel conservation on bone conduction within the same specimen
Lukas Graf, Lukas.Graf@usb.ch

PS7. Effects of middle-ear perturbations on bone conduction hearing: a finite element study
Xiying Guan, xiying_guan@wayne.edu

PS8. Techniques to improve the efficiency of a middle ear implant: Effects of coupling method on intracochlear pressure
Nathaniel Greene, nathaniel.greene@cuanschutz.edu

PS9. Live Chinchilla Ear with Otitis Media with Effusion: A Holographic Study
Jeffrey Cheng, Tao_Cheng@meei.harvard.edu

PS10. Estimation of Location and Degree of Ossicular Fixation by Compliance Measurement
Hyeonsik YOU, hyeonsik420@gmail.com

PS11. Intracochlear pressure measurements at loudness levels for speech
Irina, Wils, irina.wils@kuleuven.be

PS12. Controlling stability of temporal bone experiments in a robotized setup
Michael Martin, m.martin@uni-tuebingen.de

PS13. Methodology for Reducing Measurement Artifacts in Laser Doppler Vibrometry Using a Customized Adapter Plate and an LED Microscope
Carmen Molenda, Carmen.Molenda@med.uni-muenchen.de

PS14. Technique for measuring three-dimensional vibration of the human tympanic membrane using a scanning laser Doppler vibrometer
Bastian Baselt, bastian.baselt@usz.ch

PS15. Quantitative Association of Middle-Ear Pressure Gains and Stimulus-Frequency Otoacoustic Emission Due to Middle-Ear-Parameter Modifications in a Mouse Model
Hamid Motallebzadeh, Hamid_Motallebzadeh@meei.harvard.edu

PS16. Ear-canal geometry measurements from human CT scans: New method and preliminary results
Susan Voss, svoss@smith.edu

PS17. Actuators & Sensors - The Origins of Transducerology
Geoffrey Ball, geoff.ball@medel.com

PS18. Systematic review and meta-analysis of audiological and patient-reported outcomes with the VIBRANT SOUNDBRIDGE
Severin Fürhapter, severin.fuerhapter@medel.com

PS19. Stepless Length Adjustable (SLA) Ossicular Replacement Prostheses (ORP) & Forces In The Middle Ear
Clemens Kuen, clemens.kuen@medel.com

PS20. Technical background of the Vibrogram in-situ measurement for the VIBRANT SOUNDBRIDGE
Hamidreza Mojallal, hamidreza.mojallal@medel.com

PS21. Development of a new stapes head coupler for the Vibrant Soundbridge
Kathrin Sonntag, kathrin.sonntag@medel.com

PS22. Design, Fabrication, Benchtop, and Cadaveric Temporal Bone Testing of Ultraminiature MEMS Implantable Middle Ear Accelerometers
Panagiota Kitsopoulos, pkitsop@umich.edu

PS23. Relevance of tympanic membrane lesion at different locations and of different sizes for the middle ear transfer function
Thomas Effertz, teffert@gwdg.de

PS24. Application of Wideband-Tympanometry for the Evaluation of Passive Middle-Ear Prostheses
Nicholas Bevis, nicholas.bevis@med.uni-goettingen.de

Oral Presentation Abstracts

Wednesday, June 22

PD1.1 *10:45 am Biomechanics of the Middle Ear*

The effect of prestrain in the tympanic membrane: measurement and modeling

Pieter Muyshondt, University of Antwerp
Pieter Livens, University of Antwerp
Joris.Dirckx, University of Antwerp

Background: Experiments on biological structures have shown that tissues retract when they are excised from the body. This retraction results from strains and stresses that exists in the normal state of the body, in the absence of external loads. These so-called prestrains and prestresses are believed to originate from the growth and remodeling of tissue. So far it has been unclear if the tympanic membrane (TM) contains any prestrain and prestress. Early measurements on human and mammalian TMs are inconclusive because the prestrains may be too small to be detected with old techniques. At the same time, it is unclear how TM prestrain would affect middle-ear (ME) mechanical behavior, both in normal and diseased conditions. In this work, the existence of prestrain in the TM is evaluated experimentally, and the effect of the measured prestrains on ME mechanical behavior is investigated using a modeling approach.

Methods: TM prestrain was measured by stereo digital image correlation on fresh cadaveric rabbit ears. To release prestrain locally, small straight incisions were created at different locations in the membrane with either a radial or circular orientation around the umbo. The change in strain upon incising the TM was determined by correlating images before and after creation of the incisions. To investigate the effect of the measured prestrains on ME mechanical behavior, a 3D finite-element model of the rabbit ME was developed based on detailed micro-computed tomography data and experimentally validated material parameters. To simulate different degrees of TM prestrain, a method was developed that updates the unstrained geometry iteratively until the prestrained geometry agrees with the given reference geometry of the ME. Next, the ME vibration response to sound-pressure loading was computed as a linear perturbation around the prestressed state. After validating the model outcome with respect to experimental data, the effect of different degrees of prestrain was investigated on the ME response for normal and diseased structural conditions.

Results and Discussion: During the prestrain experiments, sample dehydration was shown to significantly influence the recorded strain fields. To eliminate this effect, sufficient rehydration of the samples prior to each recording was necessary. The experiments demonstrated a release of prestrain around the incisions at different locations and orientations in the TM, although local variations in TM prestrain could not be related to incision location or orientation. The model simulations showed that the measured prestrains have a substantial impact on the normal umbo and footplate vibration response, displaying characteristics indicative of prestress stiffening. The effect of prestrain could be mimicked by appropriately scaling the elastic and damping parameters of the model, although the adjusted parameters may not be realistic compared to material properties measured in the literature. A model with a perforation in the TM was created to examine the role of prestrain on structural ME pathologies. The resulting change of the low-frequency response was found to be related to a release in TM prestrain upon perforation.

Conclusion: Prestrain in the TM leads to substantial prestress stiffening of the ME, affecting the vibration response. When the ME structure is altered by a disease or reconstruction, the state of prestrain may change accordingly and hence influence the ME response. To better understand diseased ME biomechanics and improve ME reconstruction in future studies, one should consider taking into account the effect of prestrain.

PD1.2 *11:00 am Biomechanics of the Middle Ear*

Unified database and methods for METF validation in temporal bone experiments

Till Moritz Essinger, TU Dresden - Medizinische Fakultät Carl Gustav Carus
Martin Koch, TU Dresden - Medizinische Fakultät Carl Gustav Carus
Hannes Maier, Medical University Hannover
Jae Hoon Sim, University Hospital Zürich, University of Zürich
Nathaniel Greene, University of Colorado
Liu Jie Ren, Fudan University
Matthias Bornitz, Technische Universität Dresden
Marcus Neudert, University Hospital Carl Gustav Carus at the Technische Universität Dresden

Introduction
Measurements of the middle ear transfer function (METF) in human temporal bone specimens are fundamental to the research of middle ear mechanics. These experiments are essential in the development of new instruments, surgical techniques, and prostheses as well as active hearing implants. When drawing conclusions from these measurements, it is imperative that the samples used are representative of the target population. Due to anatomical variation between subjects, this requires a standardized definition of "normal" sound transmission. The METF is the appropriate metric for this purpose. An important step towards a standardized range was undertaken by Rosowski et al. and the corresponding standard was widely adapted. However, the suitability of said range for the intended purpose has recently been called into question. Reliable statistics with a unified database are still lacking.

Methods
We present a statistical analysis of METF measurements in 478 temporal bones from five different international research groups. From these, we derive statistical parameters attributed to non-pathological sound transfer. This includes the mean, 95% confidence interval of the mean, and the 95% population-proportion tolerance interval. We also examine the differences between research groups and measurement methods using Welch's t-tests and linear mixed model analysis.

Results
We show how the different variables in the experimental setup and procedure affect the measurements and the statistical parameters of a sample group. We then group data for a clearly defined measurement method and calculate the target statistics.

Discussion
We propose that the intervals found may be used as an objective range for the validation of individual temporal bone specimens when measurements of the sound transfer from these are to be included in a statistical analysis. We also encourage the extension of the current database as more METF measurements become available. Finally, we provide a suggested procedure for measuring METFs using the methods described herein.

PD1.3 *11:15 am Biomechanics of the Middle Ear*

On the influence of morphology on middle ear transfer function

Matthias Bornitz, Technische Universität Dresden
Steffen Ossman, Carl Gustav Carus Faculty of Medicine, TU Dresden
Marcus Neudert, Technische Universität Dresden

Introduction: The middle ear transfer function (METF) is commonly used as a measure of middle ear functionality in experimental investigations and model simulations. From experimental investigations we know the large range (about 20dB) of the METF of normal middle ears. In simulation models we usually just have a mean middle ear concerning geometry and functionality. For the design of implants (passive and active) it is increasingly important to represent the range of normal middle ears in simulations. The METF in general is determined by geometry (or morphology) and material properties of the middle ear structures (tympanic membrane and ossicles). While the morphology can be determined relatively easily, it is quite time-consuming to determine material parameters. An interesting question is therefore: How much variation of the METF can one already describe with variations in morphology.

Methods: It was shown in various studies that the morphology of the middle ear displays large variations. Unfortunately most studies only published specific length measurements that do not capture the complete variation of shape. We used the statistical shape analysis - a commonly used approach in the field of anthropology - to describe the natural anatomic variations in the middle ear.

We evaluated micro-CT data of extracted, dried ossicles (malleus, incus and stapes) and of complete, unstained middle ear preparations. The voxel size of the imaging data was in the range between 10 and 19 µm (depending on the sample size). The relevant structures were semi-automatically segmented and further smoothed. Through a registration step the orientation bias was removed and a dense correspondence was established between the structures. The statistical shape model was then built by principal component analysis. The results were analyzed and compared to anatomical data. The geometric data was input into a finite element model of the middle ear and the middle ear transfer function was calculated.

Conclusion: The first three principal components (PC) already describe more than 50% of the anatomical variations; 6 PC describe 80% and 10 PC 90% of the anatomical variations. The PC are rather complex changes of middle ear morphology. The first PC for instance mainly describes the relative position of the umbo to the stapes footplate and a rotation of the manubrium.
There is no clear correlation between PCs and variations in METF. Although the first three PCs explain most of the morphological variance, they have little influence on the METF. The first PC accounts for just 1-2 dB change of the METF. The second PC gives a range of the METF of about 4 dB. In total, the morphologic variations account for approx. 10 dB of the METF range.

The range of METF can be described only partially with morphologic variations. Further influences come from material parameters and morphologic parameters that were not taken into account in the current study; like tympanic membrane thickness and annular ligament width and thickness.

PD1.4 *11:30 am Biomechanics of the Middle Ear*

Quasi-Static and Vibrational Behavior of the Human Middle-Ear Ossicular Chain under Static Pressure Loads

Jae Hoon Sim, University Hospital Zürich, University of Zürich
Birthe Warnholtz, University Hospital Zurich, University Zurich
Merlin Schär, University Hospital Zürich, University of Zürich
Lukas Prochazka, University Hospital Zurich, University Zurich
Ivo Dobrev, University Hospital Zürich, University of Zürich
Christof Röösli, University Hospital Zürich, University of Zürich
Alexander Huber, University Hospital Zürich, University of Zürich

Introduction: While opening of the eustachian tube regulates pressure difference between the external ear canal and the middle-ear cavity, the response is time-delayed. Therefore, such ventilation mechanism is not quick enough to response to rapid change of the surrounding pressure. Further, in the case that the eustachian tube is malfunctioning, the pressure difference is not released anymore. This study explores quasi-static and vibrational behavior of the human middle-ear ossicular chain under pressure difference between the external ear canal and the middle-ear cavity. While previous studies showed that flexibility of the incudo-malleal joint (IMJ) absorbs large quasi-static displacements of the tympanic membrane caused by abrupt change of the external static pressure, contribution of the IMJ flexibility to vibrational response of the middle ear was investigated in this study. In addition, quasi-static displacements of the middle-ear ossicles, which had been measured one or two-dimensionally in previous studies, were traced in three-dimensional space.

Methods: All the experiments were performed in human cadaveric temporal bones. First, to see effects of the IMJ flexibility on middle-ear sound transmission under static pressure loads, static pressures in the range of +/- 2 kPa were applied to the ear canal, and vibrational motions of the umbo and the stapes footplate center in response to acoustic stimulation were measured using a Laser Doppler vibrometer (LDV). The measurements were repeated for two conditions of the IMJ i.e., the IMJ with natural flexibility and the IMJ with artificially-reduced flexibility. The three-dimensional quasi-static displacements of the middle-ear ossicles were measured using a custom-made stereo camera system. Two cameras were assembled with a relative angle of 7-degrees, and were mounted onto a robot arm. Red fluorescent beads of a 100-μm diameter were placed on the middle-ear ossicles, and quasi-static position changes of the fluorescent beads under static pressure loads were traced by the stereo camera system. All the position changes of the ossicles were registered to the anatomical intrinsic frame, which were obtained from micro-CT imaging.

Results: With the reduced flexibility of the IMJ, attenuation in vibrational motion of the umdo and the stapes footplate by static pressure loads were enhanced. The additional attenuation was larger for the stapes footplate center under positive ear-canal pressures than those for other cases. While the umbo shows large quasi-static displacements toward both directions along the lateral-medial axis, the incus tip shows large displacement only toward to the lateral direction. Large relative rotational motion between the incus and stapes occurred at the incudo-stapedial joint, resulting in relatively small displacement of the stapes footplate.

Conclusions: The results of this study indicate an adaptive mechanism of the flexible IMJ to abrupt changes of surrounding static pressure by reducing the attenuation of the middle-ear sound transmission. Three-dimensional tracing of the middle-ear ossicular chain provides better understanding of the protective function of the human middle ear under static pressured loads as immediate responses.

PD1.5 *11:45 am Biomechanics of the Middle Ear*

Multiaxial Stiffness of the Human Stapedial Annular Ligament and Effects of Pretension in Ossiculoplasty

Merlin Schär, University Hospital Zürich, University of Zürich
Ivo Dobrev, University Hospital Zürich, University of Zürich
Christof Röösli, University Hospital Zürich, University of Zürich
Jae Hoon Sim, University Hospital Zürich, University of Zürich
Alexander Huber, University Hospital Zürich, University of Zürich

Introduction: A comprehensive understanding of the mechanical properties of the stapedial annular ligament (AL) is of vital importance for the optimization of reconstructive middle-ear surgery. The present work investigated the multiaxial nature of two different aspects related to AL mechanics: 1) multiaxial stiffness properties of the AL, and 2) preload effects in ossiculoplasty with different designs of partial ossicular replacement prostheses (PORPs), which are a consequence of AL pretension. Further, the experimental results were compared to model simulations.

Methods: The experiments were performed on fresh-frozen human cadaveric temporal bones. The multiaxial stiffness of the AL was measured at micro-Newton force levels, with the intact and severed stapedial tendon, and the force loading directions were retrieved in the anatomical reference frame of the stapes. The data were used to fit parameters in a numerical model, which featured a novel implementation of the preload effects not requiring a-priori assumptions about nonlinear stiffening of the AL. For the experimental investigation of the preload effects in ossiculoplasty with PORP, three different PORP designs were assessed, i.e., a fixed shaft with Bell-type interface, a ball-jointed shaft with Bell-type interface, and a ball-jointed shaft with Clip-type interface. To model anatomical variance and postoperative position changes, the PORP preloads were incrementally applied along four different directions (along the long and short axis of the stapes footplate and towards the medial and lateral direction). In addition, the combined effect of the preloads with concurrent pulling forces of the stapedial muscle was assessed. The middle-ear transfer function (METF) was measured with a laser-Doppler vibrometer at each condition.

Results: The stiffness of the AL was highest along the direction of piston-like motion, and more compliant for directions of rotational motion of the stapes. The stapedial tendon mainly increased the stiffness of rotational motion about the short axis of the stapes footplate, resulting in a decrease of the directional difference of the stiffness between opposing force-loading directions. In the experimental investigation of the preload effects in ossiculoplasty with PORP, the preloads attenuated the METF between 0.5 and 4 kHz. The largest attenuations were observed for the preloads towards the medial direction. The PORPs with a ball joint resulted in a considerable benefit for the preloads along the long axis of the stapes footplate. In contrast to the clip interface, the bell-type interface was prone to lose coupling to the stapes head for the preloads in the medial direction. The model simulations yielded similar trends as the experimental investigation. The stapedial muscle tension attenuated the METF as well, and reduced attenuation by the PORP preloads when the PORP preloads and the muscle-pulling forces were applied at the same time.

Conclusions: The experimental data indicates a direction-dependent attenuation of the METF with the PORP preloads, with the most detrimental effect resulting from the preloads towards the medial direction. The ball joint offers advantageous tolerance for angular positioning while the clip interface prevents PORP dislocations under the preloads in the lateral direction. The attenuation of the METF with the stapedial muscle tension decreases at higher preloads, which may need to be considered for interpretation of postoperative acoustic reflex tests. The viability of the novel preload implementation in the analytical model was confirmed based on the similar trends compared to the experimental data.

PD1.6 *12:00 noon Biomechanics of the Middle Ear*

Contrary to previous reports, human stapes motion is piston-like to high frequencies and provides high-frequency cochlear input

Christopher McHugh, Harvard Medical School, Mass Eye and Ear
Michael Ravicz, Massachusetts Eye and Ear
Nam Hyun Cho, Massachusetts Eye and Ear
Paul Secchia, Harvard University
Aleksandrs Zosuls, Boston University
Hideko Heidi Nakajima, Harvard Medical School, Mass Eye and Ear

Introduction: For decades, human stapes motion has been believed to be (a) primarily piston-like motion (into and out of the cochlea) with increasing amplitude below about 2 kHz, and (b) more complex (with significant rocking) at higher frequencies with a decrease in amplitude and large and sometimes irregular phase accumulation with frequency. This belief stems from multiple studies of stapes motion in human cadaveric temporal bones from several groups (including our lab), usually measured at a single location on the posterior crus or footplate with a laser-Doppler vibrometer (LDV) oriented at some angle to the piston direction. These studies form the basis of an American Society for Testing and Materials (ASTM) standard of typical human stapes velocity (Vs) (Rosowski et al., 2006, see Fig.1). The discrepancy between this high-frequency roll-off in Vs and good human hearing to high frequencies is an unresolved issue. Stapes rocking motion also confounds single-point measurements of stapes velocity. The standardization of stapes motion measurements was a topic of discussion at the 2015 MEMRO meeting in Aalborg, Denmark, but no resolution was reached.
Recently, our group has observed that higher Vs amplitude and smoother phase above 2 kHz can be achieved by careful preparation of the specimen to avoid ossicular-chain trauma. In this study, we test a hypothesis that the normal stapes motion is mostly piston-like to high frequencies, allowing for high-frequency sound transmission to the cochlear partition.

Methods: Fresh or previously frozen human cadaveric temporal bones were prepared more carefully than in conventional surgery. We accessed the middle-ear cavity via the facial recess, taking great care not to touch or suction near the stapes or the incus long process. Without noticeable displacement of the stapes, a small piece of retro-reflective tape was carefully placed on the stapes posterior crus as a target for Vs measurements. The single-beam LDV was focused on the stapes target directed as close to the piston motion as permitted. A probe tube microphone monitored sound pressure in the ear canal near the tympanic membrane (Ptm). A Thorlabs Ganymede III optical coherence tomography (OCT) device was focused through the round window to measure cochlear partition motion (Vcp) near the intersection of the bridge and basilar membrane.

Results and Discussion: Vs measured in this study is robust in magnitude and smooth in phase up to ~20 kHz, unlike the many previous reports in which stapes motion magnitude decreased above ~1.5 kHz. This evidence suggests that human stapes motion can be mostly piston-like up to the limit of hearing. Vs frequency response is also similar to Vcp measured with OCT. Stapes motion can, therefore, represent cochlear input up to 20 kHz.
We achieved robust high-frequency Vs by leaving the area near the incudo-stapedial joint untouched and avoiding surgical suction in the nearby area during specimen preparation. This suggests that in previous reports where stapes motion decreased above ~1.5 kHz, physical trauma during specimen preparation may have loosened the delicate ossicular chain.
Furthermore, our study suggests that conventional middle-ear surgical techniques, in which the stapes and long process of the incus are touched or suctioned, could reduce high-frequency hearing. Thus, surgical practice should be modified to preserve high-frequency hearing necessary for good speech perception, especially in noisy environments.
Supported by NIH/NIDCD R01 DC013303. We thank Anbuselvan Dharmarajan, Sunil Puria, and Kevin O'Connor.

PD2.1 *2:30 pm Middle Ear Implants 1*

Design, Fabrication, Benchtop, and Cadaveric Temporal Bone Testing of Ultraminiature MEMS Implantable Middle Ear Accelerometers

Panagiota Kitsopoulos, University of Michigan
Alison E. Hake, University of Michigan
Emily Z. Stucken, University of Michigan
Christopher M. Welch, University of Michigan
Karl Grosh, University of Michigan

Background: Hearing loss is a debilitating condition that affects over 5% of the world's population. Hearing aids (HAs) positively impact patients' lives, but HA adoption and use rates are very low. Negative issues associated with the external elements of traditional auditory prostheses, such as safety, appearance, and ease of use, are among those most cited by patients either for not adopting a HA or for abandoning their use. A completely implantable auditory prostheses (CIAP) could help to ameliorate these issues. For the same reasons, cochlear implant (CI) patients could also benefit from the development of a completely implantable device. Blocking progress toward this goal is the lack of a completely implantable acoustic sensor capable of matching or exceeding the performance of external microphones. Previous studies have indicated that, with their small size and performance, piezoelectric microelectromechanical systems (MEMS) accelerometers have the potential to function as implantable sensors within the middle ear, thus replacing the external components. A low-noise implantable accelerometer is yet to be built, but we are on the critical path towards meeting the necessary specifications.

Methods: Our ultraminiature accelerometer designs consist of proof-mass-loaded piezoelectric cantilever bimorph beams in either a single or dual resonance configuration. We test our sensors in benchtop experiments (actuation and sensitivity) where the output of the MEMS accelerometer was compared to that of a laser doppler vibrometer for calibration and verification. These experiments are used to validate analytical models that predict our sensors' performance due to different directional excitations. We have performed cadaveric temporal bones testing accessing the middle ear using a mastoidectomy with posterior tympanotomy approach to avoid disturbing the tympanic membrane) and affixing the accelerometer to the umbo.

Results: Previous results have validated the analytical model for transverse excitations. Our models now have identified a dual bandwidth sensor design that meets low noise and low mass specifications. Rapid prototyping has enabled us to develop packaging that encapsulates our sensor and fits within the middle ear cavity thereby allowing for quick experimental testing of new design concepts. Preliminary testing in cadaveric temporal bones with a commercial, ultraminiature, narrow bandwidth sensor shows promising results, and we are interested in extending this cadaveric experiment to our own prototypes.

Conclusion: Validated modeling and testing show promise for our small (<10mg) packaged piezoelectric MEMS accelerometers. While our theoretical results point the way forward, experimental validation of the packaged devices is needed to realize this promise.

PD2.2 *2:45pm Middle Ear Implants 1*

Outcomes of combining hearing implants with autologous auricular reconstruction in children with congenital aural atresia.

Alex Bennett, University of Edinburgh

Objectives: To describe how we combine hearing implants (BAHA Attract, Bonebridge or Vibrant Soundbridge) with autologous auricular reconstruction in children with Congenital Aural Atresia. To explain the clinical, audiological and radiological work-up and technical aspects of the procedure. To report the audiological and surgical outcomes.

Methods: Demographics, indication, operative details, surgical and audiological outcomes including the Children's Home Inventory for Listening Difficulties (CHILD) questionnaire were collected on all children undergoing hearing implantation with / or as part of a planned autologous auricular reconstruction.

Results: 8 Vibrant Soundbridges, 12 BAHA Attracts and 2 Bonebridges were implanted in children aged 5 – 15 (average 6) between December 2014 and March 2019. Implantation combined with: first stage auricular reconstruction = 2; final stage = 3; other ear procedure = 3; beforehand = 14. Single complication of skin necrosis following application of audio processor. No drop in bone conduction hearing following implantation. Average CHILD improvement from 4.6 to 6.8 (child scoring) and 4.7 to 6.6 (parent scoring).

Conclusion: Combined implantation with the first stage of reconstruction abandoned as the Temporo-parietal vascular flap required to cover the newly constructed ear meant inadequate cover of the implant. Now implant either before auricular reconstruction (sited with plastic surgical input to avoid the eventual site of ear and damage to its potential blood supply) or with the final stage. We have demonstrated no significant deterioration in the inner ear function and improved hearing with the CHILD questionnaire. Numbers too small to demonstrate benefit of one implant over another.

PD2.3 *3:00pm Middle Ear Implants 1*

Intracochlear sound pressure measurement in human cadaver temporal bones during forward and backward stimulation of the cochlear using the floating mass transducer

David Stauske, MED-EL Medical Electronics
Hamidreza Mohallal, MED-EL Medical Electronics
Hannes Maier, Medical University Hannover

Introduction: The Vibrant Soundbridge (VSB, MED-EL Medical Electronics, Austria) is currently the most widely used active middle ear implant for the treatment of sensorineural and mixed hearing loss. The core element of the implant is the floating mass transducer (FMT), which is coupled in “forward stimulation” either to the ossicular chain or stapes footplate or - in “backward stimulation” to the round window (RW) membrane. Depending on the treatment, various couplers are available and can be used to attach the FMT to middle ear structures or to the RW. Laser Doppler vibrometry (LDV) is the standard method to determine the output in forward stimulation mode [ASTM International, 2005]. However, LDV fails to provide correct output level results in reverse stimulation.

The objective of this experimental study was to determine the output of the FMT in reverse stimulation by combined LDV and intracochlear pressure (ICP) difference measurements in human temporal bones to provide reference output levels for both stimulation modes.

Material and methods: In fresh ASTM compliant human cadaver temporal bone preparations the FMT was first coupled to the short process of the incus and the equivalent output level was determined. Subsequently, the output level was determined for backward stimulation with the FMT coupled (A) by a spherical RW coupler and (B) by the Round Window Precision (RWP) coupler to the RW membrane. To ensure a defined coupling force at the RW membrane for the backward stimulation, a force sensor was implemented in the setup, which can be controlled with a micro-manipulator. In all configurations, LDV measurements at the stapes footplate and the intracochlear sound pressure between scala vestibuli (SV) and scala tympani (ST) were measured with micro-fiberoptic sensors to determine the equivalent sound pressure output level of acoustic and mechanical stimulation of the inner ear in both directions (n=10).

Preliminary results: Based on the preliminary results (n=5), the FMT generates the highest output level during forward stimulation, especially in the lower and mid-frequency range. In reverse stimulation mode the static coupling force between the FMT and the RW membrane had a significant influence on the sound transmission into the cochlear with both couplers. The results of this feasibility study still need to be extended by a comprehensive study.

ASTM International. Standard Practice for Describing System Output of Implantable Middle Ear Hearing Devices. ASTM F2504-052005. p. 1-6.

PD2.4 *3:15pm Middle Ear Implants 1*

Investigation of a new type of hearing aid device – the hearing contact lens®

Michael Lauxmann, University of Reutlingen
Dmitrii Burovikhin, University of Reutlingen
Benjamin Sackmann. University of Reutlingen
Ernst Dalhoff, University of Tübingen

The hearing contact lens® (HCL) is a new type of hearing aid devices. One of its main components is a piezo-electric actuator. In order to evaluate and maximize the HCL's performance, a model of the HCL coupled to the middle ear was developed using finite element approach. The model was validated step by step starting with the HCL only. To validate the HCL model, vibrational measurements on the HCL were performed using a Laser-Doppler-Vibrometer (LDV). Then, a silicone cap was placed onto the HCL to provide an interface between the HCL and the tympanic membrane of the middle-ear model and additional LDV measurements on temporal bones were performed to validate the coupled model. The coupled model was used to evaluate the equivalent sound pressure of the HCL. Moreover, a deeper insight was gained into the contact between the HCL and tympanic membrane and its effects on the HCL performance. The model can be used to investigate the sensitivity of geometrical and material parameters with respect to performance measures of the HCL and evaluate the feedback behavior.

PD2.5 *3:30pm Middle Ear Implants 1*

Biomimetic Tympanic Membrane Implants with Tunable Mechanical and Oscillatory Properties Based on Simulation

Zhaoyu Chen, Technische Universität Dresden, Germany
Lukas Benecke, Technische Universität Dresden, Germany
Matthias Bornitz, Technische Universität Dresden, Germany
Chokri Cherif, Technische Universität Dresden, Germany
Dilbar Aibibu, Technische Universität Dresden, Germany
Thomas Zahnert, University Hospital Carl Gustav Carus at the Technische Universität Dresden,
Marcus Neudert, University Hospital Carl Gustav Carus at the Technische Universität Dresden,

Introduction: Worldwide about 32 million people suffer from chronic otitis media, alone half of which are facing severe consequential hearing loss because of chronic tympanic membrane (TM) perforation. Most commonly, autologous grafts are used in TM reconstruction. However, apart from the limited availability and the increased surgical and infection risk, they cannot well replicate the full mechanical and oscillatory functionality of the human TM. Hence, biomimetic synthetic TM implants have been developed in ERCD, ENT-Clinic and ITM to overcome these drawbacks.

Materials and methods: The innovative TM implants were made from synthetic biopolymer polycaprolacton (PCL) and silk fibroin (SF) via by electrospinning technology. Radial and circular alignment of the synthetic and natural fibers was designed to mimic the unique fibrous structure of human TM. Additional precrystallized PCL microfilaments were incorporated into the fiber mats to enhance mechanical properties as required. One of the biggest challenges of developing a desired electrospun TM scaffold is that the acousto-mechanical properties depend directly on its complex and electrospinning process-related fiber structure. To tune the mechanical and oscillatory properties as desired, a multiscale simulation method combining the electrospinning process, the nano-/microscale fiber structure and macroscale acousto-mechanical properties of scaffolds was developed to predict as well as to validate the design of TM implants. The generated implants were experimentally characterized by tensile tests, laser Doppler vibrometer (LDV), cell culture, as well as light and scanning electron microscopy. These TM implants were further validated in vitro by performing TM reconstruction in human cadaver temporal bones.

Results: The studies showed that by manipulating the electrical field biomimetic fiber structures of human tympanic membrane can be achieved via electrospinning. The static and dynamic experiments have shown that the mechanical and oscillatory behavior of the TM implants can be tuned by adjusting the solution concentration, the SF and PCL mixing ratio and the electrospinning parameters based on simulation. By comparing with the human TM, candidates of TM implants could have comparable acousto-mechanical properties as human TM. In addition, the biocompatibility of the developed TM implants was demonstrated by culturing primary human keratinocytes and bronchial epithelial cells on the membranes over two weeks. Finally, in vitro experiments have shown that the TM with SF-PCLblend implants fully recovered the acoustic vibration when the perforation is smaller than 50 %. Furthermore, handling, medium-adhesion and transparency of the developed TM implants are similar to human TM.

Conclusion: The biomimetic fiber structure, the similar material stiffness and the biocompatibility of the developed implants result in comparable physiological and biological functions to human TM. Because these functions depend on the fiber structure, not only the form and size but also the mechanical and oscillatory functions are tunable in demand.

PD2.6 *3:45pm Middle Ear Implants 1*

Method for testing the dislocation resistance of middle ear prostheses

Martin Koch, Technische Universität Dresden, Medizinische Fakultät Carl Gustav Carus
Till Moritz Essinger, Technische Universität Dresden, Medizinische Fakultät Carl Gustav Carus
Matthias Bornitz, Technische Universität Dresden
Marcus Neudert, University Hospital Carl Gustav Carus at the Technische Universität Dresden,

Introduction
Active and passive prostheses for hearing rehabilitation are attached to the anatomical structures in different ways. Their positioning is usually stable enough to withstand movement of the ossicles due to athmospheric pressure changes and to the movement of the active components themselves. However, depending on the implant design there is the possibility of a dislocation due to an accident-related external force acting on the skull.

Material and methods
In this study a method is presented to experimentally quantify the risk of prosthesis dislocation due to the application of force to the skull. This is realised by means of drop tests with temporal bones attached to a mount in a calibrated test rig. The drop test was carried out with different spatial orientations of the temporal bone to simulate several specific impact directions. Acceleration sensors are used to measure and describe the impact process. A floating mass transducer of the Vibrant Soundbridge active middle ear implant attached to the ossicular chain as well as several passive ossicular replacement prostheses are applied as exemplary implants to highlight the method. The severity of the simulated accident is calculated using the Head Injury Criterion (HIC) adapted from automotive crash tests.

Results
HIC values of up to 1'000 were achieved using the test rig. This corresponds to a severe concussion or the Euro-NCAP classification "red". Photographic before/after comparisons as well as functional tests are undertaken to reveal any dislocation.

Discussion
The method can be applied to any other prosthesis in the middle ear. The necessity of such an experiment depends on the quality of the coupling and the weight of the prosthesis itself.

PD2.7 *4:00pm Middle Ear Implants 1*

A new bio-compatible/degradable –sensor concept for middle ear pressure monitoring

Thomas Zahnert, Technische Universität Dresden
Klara Mosshammer, Technische Universität Dresden
Theresa Lüdke, Technische Universität Dresden
Sarah Spitzner, Technische Universität Dresden
Daniel Firzlaff, Hochschule für Technik und Wirtschaft Dresden
Kathrin Harre, Hochschule für Technik und Wirtschaft Dresden
Hans Kleemann, Technische Universität Dresden
Marcus Neudert, Technische Universität Dresden
Karl Leo, , Technische Universität Dresden

Motivation: Ventilation problems of the middle ear are the most reason for the development of hearing problems and middle ear deseases in childhood. Until now, pressure in the middle ear is measured indirectly by using the impedance of the tympanic membrane (tympanometry). Direct methods are just described in scientific studies and would be harmful in clinical routine.

Method: Development of a new pressure-sensor design using a bio-compatible electronic device. The pressure sensitive capacitor is made of metallic electrodes and polydimethylsiloxane (PDMS) as anelastic dielectric material. A simple sample structure was developed consisting of a flexible, bio-compatible gelatin substrate coated with thin gold electrodes separated by a corrugated layer of PDMS. The capacitor is combined with a planar coil, which enables radio-frequency identification (RFID) technology for wireless data transmission

Results: The biocompatible pressure sensor can resolve pressure changes in the range of –7.5 kPa up to +7.5 kPa. Due to its compact design (area of 2 × 4 mm2) the sensor can be directly implanted in the human middle ear. Furthermore, the read-out of the pressure sensor can be conveniently done using wireless data communication technologies employing a plate capacitor with an elastic dielectric for pressure monitoring and a planar coil.

Conclusion: We demonstrate a sensor concept which is not only compatible but also degradable. Thus it allows the direct pressure measurements in the middle ear, avoiding additional surgeries device explanation.

PD3.1 4:45*pm* *Comparative Studies and Middle Ear Evolution*

The Morphology of the Avian Bony Columella

John Peacock, University of Colorado
Daniel Field, University of Cambridge
Daniel Tollin, University of Colorado
Garth Spellman, Denver Museum of Nature and Science

In birds, the middle ear consists of the tympanic membrane, one bone (the columella), the cartilaginous extracolumella, as well as one muscle and several ligaments. The columella is commonly described as a column-like bone which broadens at both ends leaving large fossae. At the basal end it attaches to the ovular footplate, and joins the extracolumella at its distal tip. However, almost all features of columellar morphology vary among extant birds. The shape of the shaft (long and slender vs short and broad), the basal region (narrow continuation of the shaft vs broad, hollow structure vs multiple crura as in the mammalian stapes), the distal region (narrow and rounded vs broad and pointed) and even the footplate itself (flat vs bulbous) display a wide range of forms.

We extracted the columella from ~128 taxonomically diverse species (representing over 50 family-level clades). The bones were imaged with a scanning electron microscope, and examined visually with an optical microscope. We present a comparative study of the morphology of the columella, begin to categorise its different forms and features, and examine whether the observed variation can be attributed to ecological or evolutionary factors.

PD3.2 5:00 *pm* *Comparative Studies and Middle Ear Evolution*

A comparative study of elephant and human middle-ear sound transmission using 3D Laser Doppler Vibrometery

Caitlin O'Connell-Rodwell, Mass Eye and Ear and Harvard Medical School
Jodie Berezin, Mass Eye and Ear and Harvard Medical School
Yihan Hu, Mass Eye and Ear and Harvard Medical School
Michael Ravicz, Mass Eye and Ear and Harvard Medical School
Sunil Puria, Harvard Medical School

Introduction: The auditory threshold of elephants is significantly better than that of humans below 64 Hz, comparable between 64 Hz to 1 kHz, and much worse at higher frequencies (Heffner and Heffner, 1982). In mammals, hearing ability is generally correlated to sound transmission through the middle ear (e.g., Puria et al, 1999). In comparison to human, the elephant tympanic membrane (TM) is larger by nearly a factor of 7, while its ossicles are more massive by nearly a factor of 10 (Hemilä et al., 1995). We explore whether the superior low-frequency hearing in elephants can be explained by better sound collection by their larger TM and better high-frequency hearing in humans by their lower-mass ossicles.

Methods: We measured 3-dimensional ossicular velocity in response to sound stimuli in thawed unfixed cadaveric temporal bones of elephants (African, n=1; Asian, n=3) and humans (n=3). Glass beads were placed at multiple locations on the ossicles, and velocity was measured with a 3D PolyTec laser-Doppler vibrometer (LDV) in response to ear canal tones from 6 Hz to 12 kHz. Approximately constant ear pressure (94 dB SPL) was generated and monitored with a probe-tube microphone near the TM. The orientation of the tympanic ring and stapes footplate were measured relative to the LDV measurement axes to project the measured 3D umbo velocity perpendicular to the plane of the tympanic ring (ossicular-chain input) and stapes velocity perpendicular to the footplate along the piston direction (cochlear input and proxy for hearing ability).

Results: The average elephant umbo velocity is approximately an order of magnitude greater than that in human between 20 and 300 Hz. The average stapes velocity in elephants is about 3-4 times greater than that in human in this frequency range, consistent with more sensitive hearing. Above 1 kHz, umbo velocity decreases by about -6 dB/oct in elephants, or by a factor of 10 at 10 kHz, while it is approximately constant in humans in the same frequency range. The stapes velocity in elephant is comparable to those in human above about 1 kHz. The functional ossicular lever ratio (ratio of stapes to umbo velocity) in elephant and human corresponds approximately to their anatomical lever ratio (ratio of the lengths of the incus-long-process to malleus-long-process) in both species below about 200 Hz, as expected. At higher frequencies, the functional lever ratio in human generally decreases as expected, but for elephant it increases to about 6 dB, which is unexpected.

Discussion: The elephant TM is the largest among terrestrial mammals, with approximately 7 times the area of the human TM, that should result in approximately 7 times higher umbo force for a given ear-canal sound pressure (Hemilä et al., 1995). Below 300 Hz, the higher stapes velocity in elephants than in humans can account for their improved hearing threshold. The 10 times greater ossicle mass could explain why umbo velocity in elephants decreases above 1 kHz. Given that the stapes velocities are similar in this frequency range, why humans hear better than elephants above about 1 kHz is not explained by current measurements. A possible explanation for why stapes velocity remains similar at higher frequencies while umbo velocity decreases (functional lever ratio increases) is that other modes of ossicular motion above 1 kHz may cause umbo velocity to be underestimated. For example, Puria and Steele (2010) proposed that an oscillating rotation about the inferior-superior axis of the malleus could also contribute to stapes motion, but this needs further analyses. These ossicular-motion measurements in a terrestrial animal with the largest TM and heaviest ossicles provide insight into the role of TM size and ossicular mass in hearing.

[Work supported by grant K01DC017812 (COR) from the NIDCD of the NIH, and The Amelia Peabody Charitable Foundation (SP).]

PD3.3 5:15 *pm* *Comparative Studies and Middle Ear Evolution*

Hearing capacities for accurate speech reception likely evolved before the human-chimpanzee split

Alexander Stoessel, Max Planck Institute for Evolutionary Anthropology Leipzig
Steffen Ossmann, Carl Gustav Carus Faculty of Medicine, TU Dresden
Matthias Bornitz, Technische Universität Dresden
Romain David, Natural History Museum, London
Marcus Neudert, University Hospital Carl Gustav Carus at the Technische Universität Dresden

The anatomy of the auditory periphery (ear region) in fossil hominins may shed light on the emergence of human spoken language. Humans differ from other great apes in several features of the outer, middle and inner ear including a shorter but wider bony external ear canal, a smaller tympanic membrane but larger stapes footplate size, and larger ear ossicle masses. However, the functional implications of these differences remain poorly understood as comparative audiometric data from great apes are scarce and conflicting. Here, we experimentally measure the combined sound transfer function of the external and middle ear of humans (12 temporal bones from eleven donors), chimpanzees (8 temporal bones from four individuals) and bonobos (5 temporal bones from three individuals), using laser-Doppler vibrometry from 0.2 to 10 kHz. This sound transfer function strongly affects hearing sensitivity. We find that that the magnitude of the average sound transfer function of panins (chimpanzees and bonobos) is generally higher than that of humans (+6.5 dB averaged over the studied frequency range), except for a small range between 3.5 and 5.1 kHz (-4.4 dB). The significantly ($p < 0.05$) greater sound transfer of panins represents 48.5% of the studied frequency range (logged), whereas the significantly higher sensitivity of humans represents only 0.6% of the same range. Therefore, to our surprise we find that chimpanzees and bonobos have a better sound transfer than humans in the frequency range of human speech (0.125–8 kHz). Given the relationship between sound transfer function and hearing sensitivity, our results suggest that the ability to receive speech frequencies accurately was already present in the last common ancestor of humans and chimpanzees. Hence, the unique configuration of the human auditory periphery cannot be used to infer the origins of spoken language. Instead the human configuration may be a by-product of evolutionary brain expansion to preserve hearing sensitivity.

PD4.1 9:45 am *Imaging Technologies*

Rabbit tympanic membrane thickness distribution obtained via optical coherence tomography

Pieter Livens, University of Antwerp
Joris Dirckx, University of Antwerp

The thickness distribution of the tympanic membrane (TM) contributes significantly to its mechanical behavior. When the TM is made to vibrate under incident sound, the thickness distribution determines the inertial behavior of the membrane. When the TM is subjected to large quasi-static pressure variations, the thickness determines the amount of out-of-plane bending. Therefore, computer models of the TM, and subsequently the entire middle ear chain, are sensitive to the TM thickness.

However, determining the TM's thickness remains challenging. Average TM thickness values have often been used in numerical simulations of the middle ear in humans. Due to the lack of precise data, values ranged from 30 to 150 μm. Often, an average value of 74 μm is adopted. Clearly, the range of possible thickness values introduces an uncertainty in the computational results.

For the non-human middle ear, even less data is available. The New Zealand white rabbit, for example, has been used as animal model in several experimental and modeling studies but TM thickness data are hardly available in literature. Only one investigation has measured the TM thickness in rabbits and only one location was investigated, while the thickness distribution is assumed to be heterogeneous. Frequency response curves under sound pressure, and displacement curves under quasi-static pressures are available in literature. From these data, the TM's stiffness can be determined. Knowing the TM stiffness would provide fundamental knowledge on rabbit TM structure. Additionally, a comparison with the human TM can then be made, which provides insight into the structure-function relation of the TM between species.

Using optical coherence tomography (OCT), we imaged five left and five right TMs of New Zealand white rabbits. From these data, ten individual thickness distribution maps were computed with a through-thickness resolution of 1.4 μm. In addition, the average thickness distribution of the New Zealand white rabbit was computed. It was found that the general structure of the TM was similar to humans. The TM is thickest at the umbo and decreases towards the TM annulus. However, where the TM connects to the TM annulus, it increases again in thickness. Compared to humans, the thickness distribution of the rabbit TM is more symmetrical around the umbo and is generally thinner.

PD4.2 10:00 am *Imaging Technologies*

Study of the cochlear insertion area, relevant for mechanics and electrode insertion

Nicolas Verhaert , KU Leuven
Anastasiya Starovoyt, KU Leuven
Tristan Putzeys, KU Leuven
Lore Kerkhofs, KU Leuven
Greet Kerckhofs, KU Leuven and UCLouvain
Grzegorz Pyka, KU Leuven
Tiago Rocha Félix, Cochlear Deutschland GmbH & Co KG

Introduction: With softer electrode arrays, Ecoch G monitoring and minimal traumatic surgery, more often residual hearing can be preserved in case of cochlear implantation (CI). Many subjects, however, loose the residual hearing after a period of two years after CI. A thorough understanding of the cochlear microstructures at the level of the insertion area, inside of the cochlea, is crucial. This could help improving the insertion process and avoid microtraumata that induce late onset fibrosis higher up in the cochlear duct. A commonly available, however, non-destructive method for reliable insertion trauma evaluation remains a challenge. Furthermore, there is a need for scalable models to enable controlled, repeatable insertion experiments.
Micro-focus Computed Tomography allows for non-destructive 3D visualisation. In combination with a hafnium-substituted Wells-Dawson polyoxometalate (Hf-POM) it can differentiate between intracochlear fluid and soft tissues. In this study we investigated the relevant intracochlear microstructures of fresh-frozen human cochleae.

Methods: contrast-enhanced microCT imaging (CE-µCT) for the evaluation of in total seven fresh-frozen human cadaveric cochleae was performed. The CE-µCT results were validated by comparison to histological images. In four of these cochleae, trauma was induced after the first imaging, followed by imaging. µCT images of two cochleae were used to produce 3D printed models of the scala tympani. Their anatomical accuracy was quantified as the geometric deviation of the printed 3D model from the original cochlea, expressed as the Root Mean Square Error (RMSE). Insertion forces were registered. Round window thickness and profile is investigated.

Results: CE-µCT allowed visualizing not only the mineralized, but also the soft tissues within the cochlea. The anatomical accuracy of 3D printed scala tympani models was within the limits of cochlear anatomical variability with RMSE $\leq$ 0.11mm. The maximum insertion forces were comparable for full electrode insertion in 3D models (median; IQR = 86.84mN; 38.36mN) and in fresh-frozen cochleae (median; IQR = 106.08mN; 71.72mN). Micro-architecture of the cochlea will be revised in details such as the role of secondary spiral ligament and the length of the Rosenthal's canal. Relevant for MEMRO is the description and thickness measurement of the round window membrane.

Conclusions: Our study reports on CE-µCT imaging as a novel non-invasive imaging method for the evaluation of fresh human cochleae including the round window. It enables detailed, quantitative 3D assessment of electrode insertion trauma. Additionally, CE-µCT images are a reliable base for development of anatomically and mechanically accurate, scalable cochlear models as will be shown in the presentation. The micro-architecture of the insertion area will be rethinked, in terms relevant for CI insertion.

PD4.3 10:15 am *Imaging Technologies*

Intracochlear wave propagation analysis using optical coherence tomography vibrometry

Tristan Putzeys, KU Leuven
Lore Kerkhofs, KU Leuven
Anastasiya Starovoyt, KU Leuven
Nicolas Verhaert, KU Leuven

Background: Understanding the mechanics of cochlear microanatomy and acoustomechanical stimulation pathways, such as air and bone conduction, is being approached from multiple angles. Such as via intracochlear pressure measurements and extracochlear vibrometry (Nakajima et al., Fierens et al., Grossöhmichen et al., Dobrev et al., and many others), intracochlear vibrometry via cochleostomy and different forms of fitting the data to appropriate models such as finite element analysis and lumped element modelling (Stenfelt et al., Rosowski et al.). While Laser Doppler vibrometry is often used for recording and visualizing pressure waves, it is limited to extracochlear structures, e.g. stapes, round window membrane (RWM) and promontory, unless the cochlea is altered. Here we propose to use the emerging technology of Optical Coherence Tomography (OCT) vibrometry (Van der Heijden et al., Nakajima et al., Starovoyt et al. and others) to inspect human intracochlear structures of interest, such as the basilar membrane (BM) and the osseous spiral lamina (OSL), without the need for round window perforation or opening the otic capsule, and to deconvolute the recorded signals into travelling waves.

Methods: A Thorlabs Telesto SD-OCT system uses infrared light to probe 2-3 mm into the hook region of the cochlea and reconstructs a depth profile based on the optical interference spectrum, the resulting image is similar to an ultrasound. It was used alongside custom external hard- and software for triggering the OCT scans and synchronization with a stimulation source, i.e. an insert phone or a bone transducer. The synchronization allows for ‘snapshots’ of the cochlear microanatomy at specific points during stimulation, yielding high time-resolution. Comparing two snapshots with a small time difference results in a synchronized velocity map across all visible structures. Recording this velocity distribution for a full period of stimulation allows for deconvolution into left- and right-travelling waves (for a 2D cross section) visualizing net transfer of pressure waves.

Results: At AC stimulation levels of 60 to 80 dB HL in a cadaveric human temporal bone OCT vibrometry allowed velocity measurements of the RWM, the OSL and the BM. When looking at the OSL, both a rigid and a mobile response were found (Similar to the model of Raufer et al.), depending on the stimulation frequency. It was also found that below 2 kHz left- and right-travelling waves on the basal part of the OSL had equal amplitude, while above 2 kHz the wave travelling towards the BM dominates.

Conclusions: Recording and deconvoluting the velocity using OCT vibrometry across multiple intracochlear structures in a synchronized (simultaneous) manner, without altering the cochlea, allows for a novel approach to both visualize travelling waves and to analyze pressure wave propagation with potential to untangle the intracochlear stimulation micro-pathways.

PD5.1 11:00 am *Bone Conduction 1*

Experimental Investigation of the Intracochlear Sound Pressure under Intracranial Stimulation and Bone Conduction Stimulation

Ivo Dobrev, University Hospital Zürich, University of Zürich
Tahmine Farahmandi, University of Zurich
Flurin Pfiffner, University of Zurich
Christof Röösli, University Hospital Zurich, University of Zurich

Background: The frequency-dependent contributions of the non-osseous bone conduction pathways are poorly understood, especially the fluid pathway. The aim of this work is to measure and investigate sound pressure propagation from the intracranial space to the cochlear fluid.

Methods: Stimulation was provided sequentially to the bone (BC) or directly to the intracranial contents (hydrodynamic conduction or HC) in four cadaver heads. Each ear was tested individually for a total of 8 samples. The intracochlear sound pressure levels were monitored via custom-made intracochlear acoustic receivers (ICAR), while intracranial pressure was generated and monitored via commercially available hydrophones. A version of the ICAR was optimized for research purposes under BC stimuli, specifically to reduce the mechanical coupling between the sensing part and the external support structure. In parallel, the spatial motion of the cochlear promontory and stapes were measured via a 3D Laser Doppler Vibrometer (3D LDV). The cadaver heads are continuously irrigated, in order to keep the skull cavity full of fluid (free of air pockets) and kept at a physiological static pressure of 10-15cm water column equivalent, to ensure fluid reaches all soft tissues.

Results: The effectiveness of the attachment of the ICAR to the bony surface, was critical for reducing the relative motion between the sensor and the cochlear fluid, responsible for pressure readout artifacts of up to 10-25dB, particularly in scala vestibuli. Comparing absolute values, without actuator calibration, within the typical audiometric frequency range (0.5-4 kHz), the differential stapes motion, under BC, could be compared to an “equivalent” stapes motion from a 100-120dB SPL AC stimulus, while the HC induced only 70-90dB SPL motion “equivalent.” However, regardless of these major differences in the magnitude of motion, the BC and HC produced almost identical differential stapes motion, when normalized by the promontory motion. Based on that, it is hypothesized that BC and HC could produce similar cochlear fluid volume velocity, and potentially similar sensation level, if the bone velocity level is matched.
Similarly, when the intracochlear pressure is normalized by either the motion of the otic capsule or the differential stapes motion, the magnitudes and phases of the resultant complex ratios were very similar under BC and HC stimuli. Specifically, above 3 kHz, the phase showed a trend for a lead of intracochlear pressure relative to stapes, and a delay relative to the otic capsule wall motion. This suggests that the stapes could be driven by the cochlear fluid, which in turn is driven by the motion of the cochlear walls, experiencing either rigid-body-like motion (fluid inertia) or deformation (otic capsule compression). This phenomenon appears to be similar for BC and HC.
When comparing the ratios between the intracranial pressure, intracochlear pressure and otic capsule motion, major differences could be identified between the BC and HC. Under HC, the cochlear fluid appears to be activated by an osseous pathway, rather than a direct non-osseous pathway from the cerebrospinal fluid (CSF). However, the osseous pathway itself is activated by the acoustic pressure within the CSF.

Conclusions: Data at high frequencies indicates that the skull bone surrounding the brain and CSF could play a role in the interaction between the CSF and the cochlea, under both stimulation conditions, while inertia is a dominant factor at low frequencies. Further work should be focused on the investigation of the solid-fluid interaction between the skull bone walls and the intracranial content.

PD5.2 11:15 am *Bone Conduction 1*

Vibration pattern of the bone encapsulating the inner ear during bone conduction stimulation

Stefan Stenfelt, Linköping Uniiversity
Srdan Prodanovic, Linköping Uniiversity
Mohammad Ghoncheh, Medical University Hannover
Hannes Maier, Medical University Hannover

Background: Bone conduction hearing is hearing of sounds that are transmitted through the tissues of the head, such as soft tissue, skull bone, and fluid. The skull vibrations interact with the structures forming pathways for the vibrations that ultimately causes a pressure difference of the inner ear fluids across the cochlear partition and thereby a motion of the basilar membrane resulting in an excitation of the sensory cells. Clinical as well as experimental studies and numerical simulations have shown that the vibration of the bone encapsulating the inner ear generates the hearing sensation. However, it is not clear how the vibration of the bone surrounding the inner ear is transformed to a motion of the inner ear fluids. This is here investigated by vibration experiments in human cadaver heads.

Results: The analysis is based on separating the vibration of the bone surrounding the inner ear in three modes: translational, rotational, and compressional motion. Each mode has three spatial dimensions meaning that the vibration of the inner ear is described by nine parameters. The results are presented in a local coordinate system of the inner ear to facilitate interpretation of the vibration modes. Translational and rotational motion generates inertial effects while compressional motion generates motion based on space alteration. Three-dimensional velocity data at bony positions around the inner ear were measured with a three-dimensional laser Doppler vibrometer in four human cadaver heads (seven ears) when the stimulation was a vibration at the mastoid. The 3D vibrations and coordinates of the measurement positions were fed into a minimum square algorithm to estimate the nine parameters of the bony motion surrounding the inner ear.

Conclusion: Results from the preliminary analysis indicate that the translational motion dominates at low frequencies while rotational motion contributes the most at mid-frequencies. Compressional motion increases with frequency and gives the most contribution at the highest frequencies. These preliminary data are in line with results from numerical simulations indicating that inertial effects dominate at low and mid frequencies, while compressional responses are important at high frequencies for hearing bone conducted sound.

PD5.3 11:30 am *Bone Conduction 1*

Is bone conducted stimulation closer to the cochlea more efficient?

Hannes Maier, Medical University Hannover
Nils Prenzler, Hannover Medical School
Rolf Benedikt Salcher, Hannover Medical School
Max Eicke Timm, Hannover Medical School
Bernd Waldmann, Cochlear Deutschland GmbH & Co KG
Thomas Lenarz, Hannover Medical School and Cluster of Excellence Hearing4all
Tiago Rocha Félix, Cochlear Deutschland GmbH & Co KG

Introduction: For percutaneous bone conduction devices (BCDs), there are well established standard methods to determine the output [CENELEC, 2019]. For transcutaneous BCDs, however, methods are lacking to determine the output, in terms of equivalent hearing level, e.g. to investigate alternative stimulation sites. Here, intracochlear pressure (ICP) differences in human head preparations are a potential method to determine the output. However, previous research has indicated that relative movements between pressure probe and cochlea are a source of measurement artifacts [Borgers et al., 2019]. In this project, we developed and evaluated in temporal bones a method to determine the size of the artifact arising from relative motions. Furthermore, we measured the stimulation efficiency of bone conducted stimulation at the standard implantation site of the transcutaneous device Osia® (Cochlear Ltd.) at the surface of the skull compared to two stimulation sites closer to the cochlea.

Methods: The artifact estimation method was evaluated in 10 fresh frozen human temporal bones using bone conduction (BC) stimulation with a modified OSI200 actuator (Cochlear™ Osia®). The artifact is the intracochlear pressure caused by the relative movement between sensor and skull. This relative movement was determined with two sequential laser Doppler vibrometry (LDV) measurements on sensor and promontory, while the ICP sensor was intentionally vibrated. The transfer function from relative movement to ICP can then be calculated, and used to estimate the size of the artifact in experiments with unintentional relative movement caused by bone conduction stimulation. The effectiveness of fixing the pressure sensors by glue for the mitigation of artifacts was evaluated in five temporal bones during bone-conduction (BC) stimulation. The effect of stimulation closer to the cochlea was investigated in 6 ears, in three fresh frozen human cadaver head preparations. After creation of a posterior tympanotomy BC stimulation was performed with a modified B81 (Radio Ear) vibrator at a position ~50 mm horizontally behind the ear canal at the skull surface (Osia® conventional position), on the lateral semicircular canal (LSCC), and at a position superior to the stylomastoid foramen (SSMF) at the depth of the cochlea. During BC stimulation at these sites to determine the output between 0.1 to 10.0 kHz the aforementioned artifact size estimation procedure was used.

Results: Application of glue to cochleostomies reduced both relative motion and the ICP magnitude measured while vibrating the sensors, but the effect on the transfer function was minor. In the cadaver head experiments the ICP signals measured in scala vestibuli and scala tympani were 10 to 40 dB above the estimated artifact level at frequencies above approx. 0.5 kHz. Compared to the standard stimulation site at the skull surface, the output was 5 - 10 dB higher at the two investigated positions (LSCC, SSMF) below the skull surface level closer to the cochlea between 0.5 – 10 kHz. This finding was supported by similar results using LDV measurements on the promontory.**Conclusion:** The artifact in ICP measurements during BC stimulation can be estimated from the relative movement between sensor and cochlea. The transfer function was insensitive to the reduction of the relative motion by glue. The tested alternative stimulation positions closer to the cochlea yielded an increase in output level of 5 – 10 dB between 0.5 to 10 kHz, below 0.5 Hz results were dominated by the artifact.

References
Borgers C, Fierens G, Putzeys T, van Wieringen A, Verhaert N. Reducing Artifacts in Intracochlear Pressure Measurements to Study Sound Transmission by Bone Conduction Stimulation in Humans. Otology & Neurotology. 2019;40(9):e858-e67.
CENELEC. IEC 60118-9 Electroacoustics – Hearing aids – Part 9: Methods of measurement of the performance characteristics of bone conduction hearing aids. 2019.

PD6.1 11:45 am *Computational Models*

Model-Based Hearing Diagnosis based on Monte-Carlo Parameter Estimation and Artificial Neural Networks

Benjamin Sackmann, University of Reutlingen
Michael Lauxmann, University of Reutlingen
Dmitrii Burovikhin, University of Reutlingen

Simulation models of the middle ear have rarely been used for diagnostic purposes due to their limited predictive ability with respect to pathologies. One big challenge is the large uncertainty and ambiguity in the choice of material parameters of the model.

Typically, the model parameters are determined by fitting simulation results to validation measurements. In a previous study, it was shown that fitting the model parameters of a finite-element model using the middle-ear transfer function and various other measurable output variables from normal ears alone is not sufficient to obtain a good predictive ability of the model on pathological middle-ear conditions. However, the inclusion of validation measurements on one pathological case resulted in a very good predictive ability also for other pathological cases. Although the found parameter set was plausible in all aspects, it was not yet possible to draw conclusions about the uniqueness and the accuracy or the uncertainty of the parameter set.

To answer these questions, statistical solution approaches are used in this study. Using the Monte Carlo method, a large number of plausible model data sets are generated that correctly represent the normal and pathological middle-ear characteristics in terms of various output variables like e.g., impedance, reflectance, umbo, and stapes transfer function. Subsequent principal component analyses (PCA) allow to draw conclusions about correlations, quantitative limits and statistical density of parameter values.

Furthermore, applying inverse PCA yields numerous plausible parameterizations of the middle-ear model, which can be used for data augmentation and training of a neural network which is capable of distinguishing between a normal middle ear and pathologies like otosclerosis, malleus fixation, and disarticulation based on objectively measured quantities like impedance, reflectance, and umbo velocity.

PD6.2 12:00 pm *Computational Models*

Virtual Test Environment for Prostheses - Coupled Middle- and Inner-ear Model

Dmitrii Burovikhin, University of Reutlingen
Michael Lauxmann, University of Reutlingen
Benjamin Sackmann, University of Reutlingen

In order to evaluate the performance of different stapes prosthesis types, a coupled finite element (FE) model of human ear was developed. First, the middle-ear FE model was developed and validated using the middle-ear transfer function measurements available in literature including pathological cases. Then, the inner-ear FE model was developed and validated using tonotopy, impedance, and level of cochlea amplification curves from literature. Both models are based on pre-existing research with some improvements and were combined into one coupled FE model. The stapes in the coupled FE ear model was replaced with a model of a stapes prosthesis to create a reconstructed ear model that can be used to estimate how different types of protheses perform relative to each other as well as to the natural ear. This will help in designing of new innovative types of stapes prostheses or any other type of middle-ear prostheses as well as to improve the ones that are already available on the market.

PD6.3 12:15 pm *Computational Models*

3D Finite Element Model of the Entire Human Ear for Predicting Auditory Blast Injury

Rong Gan, University of Oklahoma
John Bradshaw, University of Oklahoma
Marcus Brown, University of Oklahoma
Shangyuan Jiang, University of Oklahoma

Introduction: Blast-induced hearing loss is one of the most prevalent types of disabilities among Service members and Veterans. Blast overpressure (BOP) causes tympanic membrane (TM) rupture, middle ear ossicular chain disarticulation, and hair cell damage in the cochlea. While middle ear injury can be examined non-invasively, observing damage in the inner ear is more challenging. This paper reports a 3D finite element (FE) model of the entire human ear with the two and a half turns of cochlea to mimic the anatomic structure of a three-chambered, fluid-filled cochlea. The model was successfully used to predict biomechanical injuries of the middle ear and cochlea induced by BOP waves.

Methods: The 3D FE model of the human ear consists of the ear canal, TM, middle ear ossicular chain with suspensory ligaments and muscle tendons, middle ear cavity, and spiral cochlea with three chambers (scala vestibula, scala media, and scala tympani) separated by the basilar membrane (BM) and Reissner's membrane (RM). The computational simulation was performed using Fluent and Mechanical in ANSYS with fluid-structure coupled analysis in the time domain. The material properties of structural components were similar to those used in our previously published ear models and the RM was assumed as a viscoelastic material. The BOP waveforms recorded from blast tests in human cadaver temporal bones were applied at the entrance of the ear canal as input blast pressure.

Results and Discussion: The model-derived results include the blast pressure near the TM in the ear canal and pressures inside the cochlear fluid; the displacements of the TM, middle ear ossicles, and cochlear BM; and the energy flux entering the cochlea through the stapes. Based on model-predicted results, two injury criteria are identified as 1) middle ear injury metric presented by the failure strain of two vulnerable middle ear tissues: the TM and incudostapedial joint, and 2) auditory risk units (ARUs) presented by summation of cochlea basilar membrane displacements from the base turn to apex. The total energy flux entering the cochlea calculated from the cochlear pressure and stapes movement serves as a supplemental index to assess the auditory blast injury.

Conclusions: The 3D FE model of the human ear can serve as a standardized model to predict the ear's immediate response to blast exposure through biomechanical changes of the ear tissues and their functions. The usability of the model to accurately determine the blast-induced damage in the middle and inner ear has been demonstrated by two injury criteria with the assessment of energy flux into the cochlea.

Acknowledgement: This work was supported by DOD W81XWH-14-1-0228.

PD6.4 12:30 pm *Computational Models*

Diagnostic support in tympanoplasty based on machine learning of numerical analysis results

Sinyoung Lee, The University of Electro-Communications
Yoji Morita, The University of Electro-Communications
Sho Kanzaki, Keio University Hospital
Takuji Koike, The University of Electro-Communications

Introduction: The tympanoplasty surgery is one of the cures for conductive hearing loss caused by ossicular fixation. A mobility of the ossicles has been evaluated for determining the operative procedure during the surgery, because a preoperative diagnosis of the part of fixation in most patients is difficult to be made by tympanometry or diagnostic imaging. The assessment of ossicular mobility is usually made with palpation by surgeon, and quantitative evaluation of the condition of the ossicles is difficult. Parts and degrees of fixation are different among patients, and identification of the part of fixation is difficult particularly in the case of combined fixation. Therefore, we have been developing an intra-operative assessment system which can provide an objective and quantitative assessment of the mobility of each ossicle during middle ear surgery[1]. A database of the quantified ossicular mobility considering each case of pathology is necessary to improve the reliability of the evaluation. Thus, we are also constructing a numerical analysis database of changes in ossicular mobilities caused by each case of ossicular fixation with developing the assessment system. In this study, compliance changes caused by each case of ossicular fixation were simulated using a finite-element model of human middle ear, and an effective measuring method of ossicular mobility for diagnosis was investigated by a clustering analysis in machine learning using the simulation results.
The finite-element model of human middle ear (Fig. 1) was reconstructed following the model of Koike et al.[2]. Each parameter of the model was determined based on the reported values. The unknown parameters were determined by conforming calculation results to the values of the measurements[3]. Fixation of ossicles were represented by increasing the stiffness of the ossicular ligaments in the intact model by 10 times to 1000 times. The stiffening degrees were determined by considering the measurements of changes in ossicular velocities caused by artificial fixation of temporal bones[3]. Singular fixation cases and combined fixation cases were calculated. Compliances at each ossicle were calculated as the ratio of the displacement to a point load in the direction perpendicular to the tympanic membrane (Fig. 1). Each data set of the fixation cases was composed of three features, i.e. standardized compliances of each ossicle. Clustering analysis for the data sets was performed using Ward's method. One of scatter plots of the clustering analysis is shown in Figure 2. Singular and combined fixation data with fixation by 10, 100, 1000 times of the intact model were used. The data was divided into three groups as below: Group 1, almost normal or mild fixation around malleus or incus; Group 2, SAL fixation in addition to mild fixation around malleus or incus; and Group 3, severe fixation around malleus or incus regardless of SAL fixation. A blue point in figure 2 shows the data of a virtual patient prepared for diagnosis. Here, it is assumed that only SAL of the virtual patient is 4 times stiffer than the normal one. The blue point is located between Group 1 and Group 2.

Conclusion: Thus, in this case, it is estimated that SAL is mildly stiff, and the ligaments which support the malleus and the incus are almost normal. This result shows that clustering analysis in machine learning can assist surgical procedure of the tympanoplasty.
This work was supported by Strategic Core Technology Advancement Program 2017 (Supporting Industry Program), and AMED under Grant Number 20he0122007j0001.

[1] T. Koike, et al., Development of Intra-operative Assessment System for Ossicular Mobility and Middle Ear Transfer Function, Hear. Res., 2019.
[2] T. Koike, et al., Modeling of the human middle ear using the finite-element method, J. Acoust. Soc. Am., 2002.
[3] H. Nakajima, et al., Experimental ossicular fixations and the middle ear's response to sound: Evidence for a flexible ossicular chain, Hear. Res.

PD7.1 2:15 pm *Bone Conduction 2*

Can a promontory represent the cochlear response in bone-conducted hearing?

Namkeun Kim, Sogang University
Jongwoo Kim, Sogang University

Information: Due to the difficulty in measurement of a basilar membrane (BM) movement in bone-conducted (BC) hearing, a promontory is generally considered as the representative position to show the BM velocity corresponding to BC inputs. In the proper BM velocity calculation for BC hearing, the representative position velocity, which is called the reference velocity, should be subtracted from the BM velocity to obtain the pure BM motion. The BM velocity subtracting the reference velocity is called the relative BM velocity. In this study, using the 3D finite element (FE) model of a human head including auditory periphery, the relative BM velocity was calculated through the promontory and BM velocities in BC simulation, and it was used to obtain the best frequency (BF) map. The model was validated by comparison of intracochlear pressure and promontory velocities of the model corresponding to BC stimulation with experimental results. The consistency of the BF map with the previous study can be a good indicator of adequacy of the promontory as a reference position in BC hearing. In addition, more candidate positions to measure the reference velocity were selected in the simulation, and the velocities of the positions were used as the reference velocity for BF map calculation.

Results: The results showed that the BF map could be consistent with the previous study when the osseous spiral lamina was used as the reference point. In other words, contrary to general expectations, there was limitation for the promontory velocity to become the reference velocity in BC hearing. Since the reference points on the osseous spiral lamina were varied according to the BM position showing the maximum velocity corresponding to input frequencies, a rotational motion did not distort the relative BM velocity. However, the promontory velocity could not be a proper reference velocity because it could not effectively remove the rotational motion of the whole head structure from the BM motion in BC hearing.

PD7.2 2:30 pm *Bone Conduction 2*

Preliminary Experimental Investigation of the Relationship Between Temporal Bone 3D Motion and Intracochlear Pressure

Ivo Dobrev, University Hospital Zürich, University of Zürich
Tahmine Farahmandi, University of Zurich
Flurin Pfiffner, University of Zurich
Christof Röösli, University Hospital Zurich, University of Zurich

Background: The temporal bone, including the otic capsule, undergoes a complex 3D motion pattern that depends on the frequency of the BC stimulation.

Methods: Preliminary measurements were conducted in a single fresh frozen cadaver head, where the both medial and lateral bone surfaces of the temporal bone have been exposed. The skull bone was mechanically excited in the frequency range of 0.1- 10 kHz via the actuator of a bone conduction hearing aid (BCHA). Stimulation was sequentially applied to the ipsilateral mastoid and classical BAHA location (~5cm posterior of the ear canal) via a conventional transcutaneous (5-N steel headband) and percutaneous (BI300) coupling. In the first stage of the experiments (days 1-2), the intracochlear sound pressure (ICSP) levels, in the scala tympani and scala vestibuli, were recorded via custom-made intracochlear acoustic receivers (ICAR). A version of the ICAR was optimized for research purposes under BC stimuli, specifically to reduce the mechanical coupling between the sensing part and the external support structure. The 3D motion of the ipsilateral promontory and stapes were also recorded, sequentially, via a 3D laser Doppler vibrometer (LDV). The cadaver head was continuously irrigated to prevent drying or fluid loss of the cochlear. At the second stage of the experiments (days 3-4), three-dimensional motions were monitored (scanned), across the lateral and medial (intracranial) sides of the skull at the ipsilateral temporal bone, via the 3D LDV, moved by a customized robotic positioner. A total of 70-100 measurement points (~5 mm pitch) were measured across each side of the bony surface of each temporal bone, under each stimulation condition. The different measurement points were registered to a common anatomical coordinate system, based on an automated segmentation of a tomographic reconstruction (0.3mm voxel) of the skull. Due to the complex geometry of the measured skull surface, several “scans” needed to be done, where each one included the location of 4-7 registration markers (1mm diameter wire). Any erroneous registration measurements were automatically detected and excluded.

Results: The temporal bone surface, surrounding the otic capsule, remains rigid-like up to 5 kHz, in contrast to the parietal plate, which showed deformations above 1 kHz, with an onset of the deformations first near the stimulation region, already at 0.5 kHz. Wavelength of the wave patterns across the skull base decreased with frequency, with ~ 10cm at 6 kHz, and reaching ~3cm at 20kHz. This corresponded to an approximately constant wave speed of ~ 600m/s. The magnitude of the complex ratio of the differential ICSP and the promontory motion (normalized ICSP) was not affected in a major way (within 3-7dB) by coupling or stimulation location above 2-3 kHz, when wave motion across the whole skull becomes a major part of the head response. At lower frequencies, stimulation at the mastoid produced 10-15dB higher intracochlear pressure, per unit of promontory motion, than at the BAHA location, with a smaller effect of coupling. The normalized ICSP, relative to skull deformation amount, decreases with frequency up to 2kHz for the skull base, and up to 10 kHz for the otic capsule surface, reaching a similar magnitude above 12 kHz for both regions.

Conclusions: The area around the otic capsule appears rigid up to significantly higher frequencies than the rest of the skull surface, resulting in primarily inertial loading of the cochlear fluid. With the onset of deformations across the otic capsule, an increase in differential ICSP, per unit of promontory motion, is observed, suggesting a combined effect of cochlear wall deformation and translation.

PD7.3 2:45 pm *Bone Conduction 2*

Estimation of promontory vibration by surface microphone measurements in bone conduction stimulation

Patrick Maas, Oticon Medical
Mohammad Ghoncheh, Medical University Hannover
Stefan Stenfelt, Linköping Uniiversity
Hannes Maier, Medical University Hannover

Purpose: Bone conduction (BC) hearing systems are used to treat patients with conductive and mixed hearing losses. A major challenge, however, is the objective determination of BC systems' output performance on human heads. Especially, with technological advances towards semi-implantable BC systems, in situ output performance verification becomes inevitable. Surface microphone (SM) recordings offer a non-invasive alternative method for evaluation of BC vibrations. The objective of this study was to benchmark non-invasive SM recordings on the forehead against the gold standard of Laser Doppler Vibrometry (LDV) on the cochlear promontory (CP) for BC output evaluation in human cadaver heads.

Materials and Methods: For reference, the output performance of percutaneous bone anchored hearing systems (Ponto 3, Oticon Medical) was evaluated on a skull simulator (SKS-10, Interacoustics). The devices were implanted on the intended placement at 55 mm superior-posterior to the ear canal opening in five (10 ears) human cadaveric heads. LDV (OFV 534, Polytec) measurements were performed to determine the vibration response on the ipsilateral cochlear promontory. The cochlear promontory was exposed through small triangular perforation of the ear drums. Radiating sound from the head was measured with the SM hold in place by a head band on the middle of the forehead. The SM has the structure of a stethoscope with a microphone placed in the apex of the cone and was calibrated before experiments against a probe microphone (ER7C, Etymotic) on the skin.

Results: The results show the output performance of the bone conduction hearing system on the cochlear promontory and on the forehead. The average sound pressure levels recorded by the SM were approximately between 40 and 100 dB SPL at a minimum signal-to-noise-ratio of 12 dB. The recorded SPLs on the forehead follow similar trend in frequency as CP velocity magnitudes. The correlation and linear regression analysis suggests a linear relation between frequency compensated SPLs measured on the forehead and velocity magnitudes on the ipsilateral cochlear promontory. An error distribution analysis indicates that CP vibration can be estimated non-invasively with an accuracy of approximately 10 dB (standard deviation) in a frequency range 0,1 to 10 kHz by surface microphone measurements.

Conclusions: Our results suggest that the non-invasive surface microphone offers an accuracy of estimating CP vibrations within 10 dB compared to invasive LDV measurements for technical and diagnostic use in clinical settings.

PD7.4 3:00 pm *Bone Conduction 2*

Basilar membrane and organ of Corti vibration measured with OCT during bone conduction stimulation in guinea pigs

Stefan Stenfelt, Linköping Uniiversity
Mingdou Zhao, Linköping Uniiversity
Srdan Prodanovic, Linköping Uniiversity
Anders Fridberger, Linköping University

In hearing by bone conduction, vibrations of the skull bone interact with the outer, middle, and inner ear that ultimately cause an excitation of the inner ear fluids generating a hearing response. The same sensory cells that are responsible for hearing with air conduction stimulation are responsible for hearing bone conducted sound. This has been demonstrated in experiments where an air conducted sound is cancelled by a bone conduced sound. Even so, there are differences in the cochlear stimulation between air and bone conducted sound. While in air conducted sound the generation of cochlear fluid flow is primarily through the vibration of the stapes, in bone conduction the entire framework vibrates resulting in multiple sources of fluid flow generation. How this difference affects the vibration of the basilar membrane and organ of Corti is currently unknown. Here, this is investigated by measurements of the vibration of the basilar membrane and organ of Corti together with the bony walls of the cochlear ducts when stimulation is by air and bone conduction. The experiments are conducted in guinea pigs where the vibrations of the structures are obtained by an optical coherence tomography (OCT) measurement system. The OCT measures the structures inside the cochlea through the round window enabling vibration measurements of the most basal part of the guinea pig cochlea. The preliminary data shows basilar membrane vibration with bone conduction stimulation that is similar to the air conduction response with the additional vibration of the bone. A more detailed analysis of the vibration will be presented. This is the first direct measurement of the vibration response of cochlear structures in an active inner ear.

PD8.1 3:15 pm *High Intensity Sound-Induced Hearing Damage and Protection*

Real-time Measurement of Stapes Motion and Intracochlear Pressure during Blast Exposure

Alexander Bien, University of Oklahoma Medical Center
Shangyuan Jiang, University of Oklahoma
Rong Gan, University of Oklahoma

Introduction: Hearing damage induced by exposure to a blast and high-intensity sound is a severe health concern affecting a significant fraction of military personnel and civilians. Blast-induced auditory injuries are primarily caused by the overwhelming amount of energy transmitted through the middle ear and entering the cochlea. The energy absorbed by the middle ear damages the middle ear tissues and causes conductive hearing loss, while the energy transmitted into the cochlea overstimulates the hair cells and upper-level structures and causes sensorineural hearing loss. However, the amount of energy entering the cochlea has not been quantitatively measured, which obscures the damage formation mechanism in ears exposed to blast and impedes the development of hearing protection devices. In this study, we simultaneously monitor the movement of the stapes footplate (SFP) and the pressure in the scala vestibuli (SV) during blast exposure using dual laser Doppler vibrometry established in our laboratory. The SFP motion and SV pressure (Psv) characterize the energy transduction from the middle ear to cochlea, and provide a quantitative assessment of the damage to the cochlea under blast exposure.

Methods: Five fresh human temporal bones (TB) were involved in this study. The TB was mounted to the "head block" which is a fixture to simulate a real human skull and placed under the blast apparatus inside an anechoic chamber. The pressure sensor P0 was mounted approximately 1 cm lateral to the ear canal opening to monitor the pressure entering the ear canal and the pressure sensor P1 was inserted into the ear canal to measure the pressure at the tympanic membrane. The SV was surgically accessed through the facial recess and a 3D-printed adaptor was inserted to connect a piezoelectric sensor to the SV for measuring the pressure (Psv). Two laser doppler vibrometers (LDVs) were placed outside the chamber and the LDV1 measured the movement of the TB and the LDV2 measured the movement of the SFP. The actual velocity of the SFP was obtained by subtracting the velocity measured from the LDV1 from the velocity measured from the LDV2. The LDVs, P1, and Psv signals were triggered by P0 and recorded at a sampling rate of 1 MHz.

Results: The P0, P1, Psv, and velocities of SFP and TB were simultaneously measured from each TB. The P0 waveform was similar to Friedlander waveform typical of free-field blast exposure. The P1 peak value was about 2 times higher than the P0, demonstrating the amplification function of the external auditory canal. The peak pressure value of Psv was approximately 5 times higher than the value of P0. The velocities of TB and SFP were consistent with the results published by Jiang et al. (Hear Res, 2021). The time delay of the first negative peak of the SFP velocity was 0.03 ms earlier than the first positive peak of the Psv signal, indicating the positive Psv pressure was caused by the compression of the cochlear fluid when the SFP moved into the cochlea. Results measured from 5 TBs were consistent entering the cochlear enables future studies to investigate the blast-induced conductive and sensorinwith each other with individual differences.

Conclusions: For the first time, SFP movement and Psv have been successfully measured simultaneously during blast exposure. The experimental data characterized the response of the human middle ear and inner ear to blast load, which can improve the understanding of how injuries are formed during blast exposure. The approach to quantitative assessment of the energy eural hearing loss independently.

Acknowledgements: This work was supported by DOD grant W81XWH-14-1-0228.

PD8.2 3:30 pm *High Intensity Sound-Induced Hearing Damage and Protection*

Hearing Protection and Damage Mitigation in Chinchillas Exposed to Repeated Low-intensity Blasts

Shangyuan Jiang, University of Oklahoma
Sarah Sanders, University of Oklahoma
Rong Gan, University of Oklahoma

Introduction: High-intensity sound or blast-induced hearing loss is one of the most prevalent types of occupational diseases among Service members and Veterans. To date, there is no therapeutic treatment for blast-induced progressive hearing damage. We recently conducted a study on therapeutic function of Liraglutide, the long-acting glucagon-like peptide-1 receptor (GLP-1R), to mitigate the auditory injury after blast exposure in animal model of chinchilla (Jiang et al., Ann Otol & Rhin, 2021). However, the mechanisms behind liraglutide treatment in ears with and without hearing protection devices (HPDs) remain unclear. In this study, the electrophysiological measurement after blast exposure and histological examination of brain tissues along the ascending auditory pathway were performed in chinchillas with ears open or protected by HPDs (e.g., earplugs). The goal is to investigate the hearing damage mitigation provided by liraglutide treatment and the effect of HPDs on liraglutide's therapeutic function over different time courses after blast exposures.

Methods: Young adult chinchillas were divided into two groups: ears open and ears plugged with foam earplugs. All animals were assigned to three experimental groups: pre-blast liraglutide treatment, post-blast drug treatment, and blast control to expose 6 consecutive blasts at 3-5 psi (or 20-35 kPa) on Day 1. The 7-day-long liraglutide treatment started 2 days before Day 1 in the pre-blast drug group and immediately after the blast in the post-blast drug group. There was no drug treatment for the blast-control animals. The auditory brainstem response (ABR), distortion product otoacoustic emission (DPOAE), and middle latency response (MLR) were measured on Day 1 pre- and post-blast and on Days 4, 7, 14, and 28 after blast. Chinchillas were sacrificed on Day 14 or Day 28 and their brain tissues were harvested for immunofluorescence images. Statistical analyses were performed on experimental data to determine hearing restoration in relation to the drug treatment, HPD protection, and post-blast recovery time.

Results: Changes in ABR threshold, DPOAE level, and MLR amplitude after the blast exposure in liraglutide treated animals indicated that the post-blast hearing function was ameliorated by the liraglutide treatment over the time course. In the open ear group, the drug-treated chinchillas show longer-lasting hearing restoration than the blast controls. In the plugged group, the liraglutide treatment facilitated hearing restoration at the early stage of the experiment. Electrophysiological and immunofluorescence results indicated that the therapeutic function of the drug treatment was associated with pathological changes that occurred in multiple regions in the auditory system at different time points.

Conclusions: The blast-induced hearing damage in protected ears was obviously less than that of open ears, but the damage mitigation in both open and plugged ears with liraglutide treatment can be detected. The finding suggested that the potential effect of liraglutide on hearing restoration after repeated blast exposures showed the relation to the injury in the peripheral auditory system in addition to the central auditory system. This study provided a preliminary investigation on therapeutic solution to various types of blast-induced hearing damage with great potential.
Acknowledgements: This work was supported by DOD grant W81XWH-19-1-0469.

PD8.3 3:45 pm *High Intensity Sound-Induced Hearing Damage and Protection*

Derivation of a Simplified Middle Ear Model Using System Identification

James Easter, University of Colorado
Nathaniel Greene, University of Colorado
Theodore Argo, Applied Research Associates, Inc.
Tim Walilko, Applied Research Associates, Inc.
Daniel Tollin, University of Colorado

Introduction: Our study of acoustic injury from very high-pressure events (e.g. blast) has created a need for a simple, computationally efficient middle ear model able to accept a predicted pressure input in the EAC after attenuation by hearing protection and then to return energy input (SV pressure and cochlear volume velocity) to the inner ear. This energy input will be used in turn with a damage model mapping it to hair cell and synaptic injury, and ultimately to loss of auditory function.

Method: employed to derive the simplified model draws upon a powerful set of techniques developed within the discipline of System Identification. These combine an experimental design methodology to yield the most useful guiding data set with a decision process for candidate model selection, optimization within the selected model family, model validation and useful simulation. A nonlinear model may be found in this way that gives accurate prediction of a chosen output variable, without attempting representation of physical quantities within its structure.
The input data were a set of pressure waveforms recorded from experiments using a mobile shock tube (ARA, Littleton, CO). Simulated blast waves with peak pressures of 1 14 psi (171 194 dB SPL) were recorded at the skin surface and within the EAC of cadaveric human specimens. Parallel experiments were conducted in human temporal bones using a blast emulator delivering high pressure (120–145 dB SPL) pure tones from 10 Hz to 12800 Hz directly to the EAC. Stapes velocities were recorded by laser Doppler velocimetry (Polytec, Inc.), while SV and ST pressures were measured with fiber optic probes (FISO, Inc.).
The data from each of the 43 frequencies at a given presentation level were used as input to System Identification Toolbox (Mathworks, Inc.), yielding a nonlinear Hammerstein-Wiener model optimized for that frequency. The individual models were then combined to yield a composite model giving good prediction of SV pressure in response to EAC pressure across the spectrum of interest. The composite model was validated against shock tube pressure data, and found to capture both the sharp rise time and long duration characteristic of blast waves.
This model will be used in concert with the hearing protection and neurophysiological injury modules developed for this project to improve prediction of auditory degradation from high-pressure events.

[1]Department of Otolaryngology, University of Colorado School of Medicine, Aurora, CO, USA.
[2]Department of Physiology and Biophysics, University of Colorado School of Medicine, Aurora, CO, USA
[3]Applied Research Associates, Inc., Littleton, CO, USA.

PD9.1 9:45 am *Middle Ear Physiology*

Middle-ear Sound Transmission Delay and Attenuation due to Mechanically Pulling Tensor Tympany and Stapedius Muscles

Nam Hyun Cho, Massachusetts Eye and Ear
Michael Ravicz, Massachusetts Eye and Ear
Sunil Puria, Harvard Medical School

Introduction: The three-bone flexible ossicular chain in mammals may allow independent alterations of middle-ear (ME) sound transmission via its two attached muscles. The stapedius (ST) muscle, which has its insertion on the stapes posterior crus, is known to stiffen the stapes annular ligament. The tensor-tympani (TT) muscle, which has its insertion on the malleus neck, is thought to increase tension of the tympanic membrane (TM). It is well documented in several species that middle ear sound transmission has a wide bandwidth and a delay, including cat (Puria and Allen, 1998), gerbil (Olson, 1998), chinchilla (Ravicz and Rosowski, 2013), and human (O'Connor and Puria, 2006). Changes in eardrum stiffness were previously shown to affect middle-ear delay at low frequencies (O'Connor et al., 2017). We hypothesize that the ME muscles can modulate the gain and latency of ME sound transmission. We studied this question in human cadaveric temporal bones by mechanically pulling on each muscle and measuring sound transmission.

Methods: In unfixed thawed human-cadaver temporal bones (N=3), the middle-ear cavity and facial recess were opened to access the TT and ST bodies. Forceps gripped the TT near the bony tunnel near the malleus and the ST body to apply known amounts of static pull in their natural direction with a load cell and micromanipulator. Tones between 0.1 and 10-kHz generated by a loudspeaker were delivered to a glass-backed ear-canal coupler with a calibrated microphone to measure ear-canal pressure (Pec) near the TM. A Thorlabs Ganymede-III-HR 905-nm optical coherence tomography (OCT) system with custom VibOCT software measured the umbo motion Vu through the coupler. Stapes velocity Vs was measured on a reflective target on the posterior crus with a laser-Doppler vibrometer. From these measurements, we determined Vu/Pec and Vst/Pec. For frequencies between 200-500 Hz, we fit straight lines to the phase of these measurements and compute the group delay as the negative of the slope for each muscle pull that ranged from 10-100 gram force, a physiologically likely range.

Results: A static TT muscle pull produced a frequency-independent attenuation in sound-driven umbo and stapes motion magnitude of 12-15 dB at frequencies below about 1 kHz for the highest pull forces. The baseline ME delay was reduced (phase increased) by 150-250 us. A static ST muscle pull attenuates the stapes motion by 6-7 dB below about 0.6 kHz and the baseline ME delay was reduced by 30-100 us. The ST muscle pull affected mostly the stapes motion and not the umbo motion, while TT muscle pull affected the umbo motion and stapes motion roughly equally.

Discussion: These are the first results to demonstrate that sound transmission delay through the human ME is altered by TT and ST muscle pulls that mimic muscle activation. Although both muscles were not pulled together in the present study, the results suggest that ME transmission could be attenuated by up to 20 dB and baseline delay reduced by up to 300 us when both muscles are simultaneously pulled. For humans, the maximum interaural time difference produced by the head is about 800 us. Thus, a 300-us reduction in delay can affect the interaural time significantly. This suggests that a role for TT and ST muscle activity might be to modify sound-localization cues. Recent studies showed that horizontal saccadic eye motions cause bilateral changes in EC pressure that were hypothesized to be produced by the TM being moved by the two ME muscles (Gruters et al., 2018). Muscle-induced changes in ME-transmission delay may provide a way of mechanically changing interaural time- and level-difference cues to help the brain work synergistically with the visual system to perform sound localization.

Work supported by Amelia Peabody Charitable Fund (to SP).

PD9.2 10:00 am *Middle Ear Physiology*

Anatomical variations within the human middle ear based on clinical imaging data

Daniel Schurzig, Hannover Medical School
Moritz Becker, Hannover Medical School
Max Eicke Timm, Hannover Medical School
Hannes Maier, Medical University Hannover
Athanasia Warnecke, Hannover Medical School

Background: The anatomical variability of the human middle and inner ear plays an important role for hearing restoration with middle ear and cochlear implants. Patients with conductive hearing loss typically undergo middle ear reconstruction surgery in which sound conduction from the tympanic membrane to the stapes footplate is restored. This is commonly done by using passive prostheses to replace damaged or missing ossicles and thereby close the functional disruption from outer to inner ear. Anatomical variations require these implants to be available in various sizes, allowing for an exact fit of the implant to the individual requirement of a patient. This study was conducted in order to investigate to which extent commonly available implant sizes match the anatomical variations of the human middle ear. Furthermore, correlations between different dimensions were investigated to check if a general size categorization of the human middle ear is feasible.

Materials & Methods: High resolution cone beam computed tomography images (CBCTs) of 50 patients (100 ears) were retrospectively examined. Fiducials were manually placed on 10 anatomical landmarks as reference points to compute the width and height of the tympanic membrane, the distance from the tympanic membrane to the stapes footplate and head, the height of the stapes, the angle between stapes and tympanic membrane as well as the overall width and height of the tympanic cavity.

Results: All dimensions indicate a high variation of the human middle ear with hardly any interrelation between the different dimensions. Even dimensions like width and height of the tympanic membrane (which should intuitively correlate very well) show an R2 value of only 0.22, indicating that not only the size but also the shape of the tympanic membrane varies substantially. The ranges of commonly available implant sizes were found to cover the range of anatomical dimensions in the majority of cases.

Conclusion: The high anatomical variation and lack of correlations between dimensions indicates that a general size categorization of the human middle ear is not straight forward, but that a detailed anatomical assessment of each individual middle ear structure is required prior to implantation. The currently available implant portfolio comprehensively covers nearly all anatomical size requirements.

PD10.1 10:45 am *Middle Ear Implants 2*

A partial middle ear replacement prosthesis with a concentric ball joint in the headplate

Dirk Beutner, University of Göttingen
Thomas Effertz, University of Göttingen
Nicholas Bevis, University of Göttingen

A partial middle ear replacement prosthesis with a concentric ball joint in the headplate
In passive middle ear prosthetics, rigid implants have proven successful in reconstructing the ossicular chain. However, these cannot fully replicate the physiology of the ossicular chain. Pressure fluctuations cause high stresses in rigid passive prostheses, which can result in dislocation, protrusion and pre-tension in the annular ligament resulting in unsatisfactory hearing results.
In collaboration with MED-EL, we developed a new passive middle ear prosthesis that features a balanced, centered ball joint between the headplate and shaft of the prosthesis. We compared the sound transmission properties of this new prosthesis with those of a standard rigid prosthesis. Using Laser-Doppler-Vibrometry (LDV), we measured the sound-induced velocity of the stapes footplate relative to a given acoustic stimulus.
The new prosthesis showed equivalent sound transmission characteristics compared to the rigid prosthesis, while retaining the ability to compensate for pressure fluctuations due to its ball joint. This ensures good transmission properties even during displacements of the tympanic membrane.
This development is a further step towards a physiological reconstruction of the ossicular chain.

PD10.2 11:00 am *Middle Ear Implants 2*

Optical Measurements of Eardrum Vibrations and Sound Propagation in the Ear Canal for the Fitting of Active Middle Ear Implants

Frank Boehnke, Technical University Munich
Katja Böck, Technical University Munich
Tobias Strenger, Universität Augsburg

Background: Middle ear implants (MEI) are for the medical rehabilitation of the hearing function in case of sound conduction hearing losses as well as cochlear hearing losses and their combinations.

Objectives: An objective tool to reach the best fitting of the external worn sound processors is essential for patients who do not want or cannot participate in the fitting process.

Methods: In addition to Laser-Doppler-Vibrometry (LDV) measurement the sound pressure was measured distant to the eardrum to attain additional information for comparison. Three groups of patients with different middle ear characteristics were examined.

Results: Because of the large spreading of measuring results even within a patient group with similar eardrum and middle ear conditions it is difficult to develop characteristic diagrams which represent the mean values of eardrum displacements with different sound processor adjustments being the base for normative data courses. In addition to measurement results a numerical analysis of the one-dimensional pressure wave propagation was conducted.

Conclusions and Significance: The LDV measurements can be used as a tool for fitting sound processors by finding individual maximum eardrum velocities in the frequency range 125 Hz to 8 kHz. In comparison to acoustical measurements the optical measurements have advantages concerning lower variations of measurement values, higher spectral resolution, and robustness against disturbing acoustic noise, especially at low frequencies. The numerical analysis allowed the confirmation of measured results and is therefore useful to reconstruct pathological conditions, which are impossible or difficult to measure.

Böck K, Böhnke F, Rahne T, Strenger T (2022) Optical measurements of eardrum vibrations and sound propagation in the ear canal for the fitting of active middle ear implants. Acta-Otolaryngologica, doi.org/10.1080/00016489.2022.2038388.

PD10.3 11:15 am *Middle Ear Implants 2*

Assessment of hearing rehabilitation and speech perception in Vibrant Soundbridge round window vibroplasty – The role of dynamic range

Susan Busch, Hannover Medical School and Cluster of Excellence Hearing4all
Thomas Lenarz, Hannover Medical School and Cluster of Excellence Hearing4all
Hannes Maier, Medical University Hannover

Background: The dynamic range (DR) of hearing is the loudness input range accessible to the patient, defined as the difference between the hearing threshold and the uncomfortable loudness level. In human speech, the minimum dynamic range is proposed to be in the range of 30 to 35 dB (French & Steinberg, 1947), although some studies suggest a DR of 40 dB or higher for sufficient speech understanding (Studebaker & Sherbecoe, 1999; De Gennaro et al., 1981). In patients with hearing implants, the DR covered by the device depends on the bone conduction threshold and the maximum power output (MPO) of the implant. The active middle ear implant Vibrant Soundbridge provides a variety of coupling possibilities of the floating mass transducer (FMT) to treat patients with mild to moderate-severe hearing losses. The FMT can be attached to structures of the ossicular chain or to the oval or round window. The aim of this study was to determine the relationship between covered dynamic range and word recognition score in patients implanted with the VSB in round window application.

Methods: For our retrospective analysis, 69 patients, implanted with the Vibrant Soundbridge at the round window at the Medical School Hannover (Germany), were selected and analyzed in two steps. First, individual frequency-dependent maximum power output (MPO) of the Vibrant Soundbridge was determined for each patient based on the patients' audiological data (see accompanying presentation H. Maier). Secondly, the dynamic range (DR) was calculated for each patient and frequency as the difference between MPO and bone conduction threshold. In addition to the absolute DR, a weighted dynamic range (WDR) was calculated based on the Speech Intelligibility Index (SII) which weights audible speech cues by their importance at each frequency (ANSI S3.5-1997). The word recognition score (WRS) in quiet was correlated to the absolute and weighted DR across the frequencies 0.5, 1.0, 2.0 and 4.0 kHz.

Results: As a first order approximation of the intelligibility function a linear regression was determined between WRS and DR ($RDR^2 = 0.926$, $RWDR^2 = 0.929$) with a strong correlation between predictor and outcome variable ($rDR = 0.962$, $rWDR = 0.964$). Word recognition scores in quiet (n=67) improved with increasing dynamic range. A significant shift in performance was detected above a DR of 20 dB with a mean WRS of $\geq 77.3\%$ ($\pm$ 16.1% standard deviation) and a mean WRS of $\leq 51.7\%$ ($\pm$ 29.6 dB standard deviation) below 20 dB. A mean WRS of $> 80\%$ can be found in patients with a DR between 30 and 40 dB or higher. The mean difference between the SII-weighted DR and the absolute DR was only minor (1.2 dB) and ranged from -1.1 to 3.2 dB.

Conclusion: The individual DR could be successfully determined from patients' clinical data only. Our results show that a DR below the proposed 30 dB can yield in sufficient word recognition but increasing DR further improves the mean speech outcome and reduces the variability within the data.

References

French, N.R., and Steinberg, J.C. (1947). Factors governing the intelligibility of speech sounds. J Acoust Soc Am 19, 90-119.
Studebaker, G.A., Sherbecoe, R.L., McDaniel, D.M., and Gwaltney, C.A. (1999). Monosyllabic word recognition at higher-than-normal speech and noise levels. J Acoust Soc Am 105, 2431-2444.
De Gennaro, S., Braida, L.D., and Durlach, N.I. (1981). A statistical analysis of third-octave speech amplitude distributions. J Acoust Soc Am 65, 16-16.
ANSI S3.5-1997. American National Standard methods for calculation of the speech intelligibility index (American National Standards Institute, New York).

PD10.4 11:30 am *Middle Ear Implants 2*

Determination of individual Maximum Power Output from clinical routine data in Vibrant Soundbridge round window vibroplasty

Hannes Maier, Medical University Hannover
Thomas Lenarz, Hannover Medical School and Cluster of Excellence Hearing4all
Susan Busch, Hannover Medical School and Cluster of Excellence Hearing4all

Introduction: The frequency specific maximum power output (MPO) at cochlear level of all acoustic devices, such as conventional hearing aids as well as bone conduction devices and active middle ear implants, belongs to the most important parameters that are crucial for speech intelligibility and patient benefit. It defines the upper border of the input loudness range above threshold that can be made accessible to the patient. Optimally, technical limits exceed the useful patient's dynamic range but in a majority of cases and pathologies, technical limitations prevent the use of the entire residual input range of patients due to too low MPO. Although technical limitations are encountered in all classes of acoustic devices, the situation in active middle ear implants (AMEI) is aggravated by a pronounced variability in stimulation efficiency. Various methods to measure the MPO in patients have been developed, such as using acoustic output saturation in the external ear canal [Zwartenkot et al., 2012; Mertens et al., 2014] or recordings of surface emitted sound [Hodgetts et al., 2018]. Nevertheless, all these approaches require non-standard additional measurements. In this study, we present a method to determine individual MPO from clinical audiometry routine data in round window stimulation with the Vibrant Soundbridge.

Methods: In our retrospective study, 69 patients, implanted with the Vibrant Soundbridge at the round window at the Medical School Hannover (Germany), were analyzed. Using the bone conduction threshold, the direct threshold determined by the device, and technical data provided by MED-EL the MPO was determined for individual combinations of implants (VORP502, VORP503) and processors (Samba, Amadé) as well as processor variants (Hi, St, Lo, LoLo). To analyze the effect of coupling mode independently of these parameters, patients were divided into four groups: (A) without coupler (N = 29), (B) the spherical coupler (N = 18), (C) the soft coupler (N = 11) or (D) the custom-made "Hannover coupler" (N = 11) and the MPO was normalized to a specific implant processor combination (Samba Hi, VORP503).

Results: The MPO frequency dependence was similar for coupling types (A-D) with a maximum at 1.5 kHz. Only at 3 kHz significant differences between group A and C were found (t-test, p =0.044). The average MPO over speech relevant frequencies (0.5, 1.0, 2.0, 4.0 kHz) was 76.8 ± 15.2 dB HL for group (A) (mean value ± standard deviation), 82.6 ± 7.3 dB HL for group (B), 71.6 ± 13.8 dB HL for group (C), and 78.7 ± 12.6 dB HL for group (D). Despite the minor differences in avg. MPO for the different coupling modes, the variability in group (B) was significantly reduced compared to groups (A) and (C). Although the variability in group (D) was generally small, two outliers contributed to an increased spread which might be due to the group composition that included patients with multiple previous revisions.

Conclusion: The individual MPO could be successfully determined from patients' clinical data only and permits an in-depth analysis of individual patient outcomes. Beside technical characterization of devices our findings form the basis to determine the patients' dynamic range coverage. This allows a detailed interpretation of audiological results (see accompanying presentation S. Busch) and improved clinical decision criteria.

References

Hodgetts W, Scott D, Maas P, Westover L. Development of a Novel Bone Conduction Verification Tool Using a Surface Microphone: Validation With Percutaneous Bone Conduction Users. Ear Hear. 2018
Mertens G, Desmet J, Snik AFM, Van de HPH. An Experimental Objective Method to Determine Maximum Output and Dynamic Range of an Active Bone Conduction Implant: The Bonebridge. Otology & Neurotology. 2014
Zwartenkot JW, Snik AFM, Kompis M, Stieger C. Gain and maximum output of implantable hearing devices in patients with moderate to severe sensorineural hearing loss. JHS. 2012

PD10.5 11:45 am *Middle Ear Implants 2*

The Hannover Coupler V2: Audiological Outcomes of a new Round Window Coupler for the Vibrant Soundbridge

Nicole Knölke, Hannover Medical School
Hannes Maier, Medical University Hannover
Susan Busch, Hannover Medical School and Cluster of Excellence Hearing4all
Thomas Lenarz, Hannover Medical School and Cluster of Excellence Hearing4all

Introduction: The Floating Mass Transducer (FMT) of the Vibrant Soundbridge (VSB) can be coupled to different parts of the ossicular chain or to the round window. To place the FMT against the round window membrane (RWM), biological and artificial materials have been used to improve the vibratory transmission into the cochlea1. Furthermore, new couplers like the RW Coupler2 and the RW Soft Coupler3 were developed. The coupling of the FMT to the round window still results in varying audiological outcomes. Main reasons are the mismatch of the diameter of the FMT and the RW membrane, the surgically challenging placement of the FMT at the RW, and the undefined force between FMT and the RWM. A new custom made design, the Hannover Coupler version 14 (HC1), was developed to overcome these obstacles by (a) adapting the coupler geometry to the round window (RW) niche (b) stabilizing the FMT, and (c) controlling static coupling force to the RW. Based on the experiences with the HC1, a redesigned and optimized CMD version termed “Hannover Coupler v2” (HC2) was developed. In this study we observed the performance of the HC2 in a small series of clinical applications.

Material and Methods: Ten patients with mixed hearing loss and a history of multiple ear surgeries, intended for the RW application of the VSB, received the HC2. The audiological outcomes was assessed up to 6 months (6M) based on preoperative and postoperative hearing thresholds, word recognition score (WRS) obtained with the Freiburg monosyllable test at 65 dB SPL and the speech recognition threshold in quiet and noise (Oldenburg sentence test, OLSA, 50% threshold, noise at 65 dB). The effective gain (BC threshold minus sound field threshold) and the coupling efficiency (BC threshold minus in situ threshold) were calculated.

Results: The median WRS (n=10) improved significantly from 0% to 80% (Wilcoxon signed rank test, $p = 0.006$). The median speech reception threshold (SRT) (n=8) in noise improved significantly from 11.6 dB SNR to -2.4 dB SNR (Wilcoxon signed rank test, $p = 0.023$), and in quiet significantly from 79.6 dB SPL to 44.4 dB SPL (Wilcoxon signed rank test, $p = 0.016$). The average effective gain of -1.3 dB indicated a closure of the air bone gap. The determined average coupling efficiency of 23.3 dB was within the acceptance range suggested by the manufacturer. A significant, but clinically not relevant change in BC threshold was observed at 4 kHz (t-test, $p = 0.037$) and 6 kHz (t-test, $p = 0.019$) at the 6M follow-up. One revision surgery had to be performed during the study period, which was neither device nor surgery related.

Conclusion: All ten patients were safely implanted with the VSB in conjunction with the HC2. They achieved a significant improvement of their speech recognition in quiet and in noise, despite multiple previous ear and revision surgeries. The speech recognition with the HC2 even exceeds published results of the RW coupling without a coupler and with the RW Soft Coupler.

References
1 Olszewski L, Jedrzejczak WW, Piotrowska A, Skarzynski H. Round window stimulation with the Vibrant Soundbridge: Comparison of direct and indirect coupling. Laryngoscope. 2017;127:2843-2849.
2 Zahnert T, Mlynski R, Löwenheim H, et al. Long-Term Outcomes of Vibroplasty Coupler Implantations to Treat Mixed/Conductive Hearing Loss. Audiol Neurotol. 2018;23:316-325.
3 Rahne T, Skarzynski PH, Hagen R, et al. A retrospective European multicenter analysis of the functional outcomes after active middle ear implant surgery using the third generation vibroplasty couplers. Eur Arch Otorhinolaryngol. 2021;278:67-75.
4 Müller M, Salcher R, Lenarz T, Maier H. The Hannover Coupler: Controlled Static Prestress in Round Window Stimulation With the Floating Mass Transducer. Otol Neurotol. 2017;38:1186-1192.

PD10.6 12:00 pm *Middle Ear Implants 2*

Implantable Piezoelectric-Polymer Microphones for the Middle Ear

Aaron Yeiser, MIT
Annesya Banerjee, Harvard University
John Zhang, MIT
Lukas Graf, Harvard Medical School, Mass Eye and Ear
Christopher McHugh, Harvard Medical School, Mass Eye and Ear
Yew Song. Harvard Medical School, Mass Eye and Ear
Ioannis Kymissis, Columbia University
Elizabeth Olson, Columbia University
Hideko Heidi Nakajima, Harvard Medical School, Mass Eye and Ear
Jeffrey Lang, Electrical Engineering and Computer Science

Introduction: Cochlear implants are the most successful neuroprothesis to date restoring hearing in the deaf, with over 700,000 deployed around the world by 2019. However, cochlear implants still rely on external microphones next to or behind the pinna, which have cosmetic and functional drawbacks. This hardware cannot take advantage of the direction–sensitive frequency response of the pinna. We present two implantable piezo- electric microphone designs that directly sense motion of umbo, which compare favorably against existing implantable microphones.

Sensor design overview: Polyvinylidene difluoride (PVDF) is an excellent piezoelectric material for detecting motion of the middle ear, as it is biologically inert and orders of magnitude more compliant than common piezoelectric ceramics. Our lab has developed two principal PVDF microphone designs for the middle ear shown in Figure 1, which we have named the drum-mic and the cantilever-mic. While many other implantable microphones like the Envoy Esteem detect motion of the incus through point contact with a needle, our designs are robust and compliant enough to directly capture motion of the umbo where motion is large and mostly one-dimensional.

Motion of the umbo causes the PVDF membrane of the drum-mic to stretch generating an electrical signal detected by a custom low noise amplifier. The cantilever-mic is constructed from two layers of PVDF sandwiching a Kapton base layer. Umbo motion induces a bending moment, producing a differential charge output detected by the same amplifier. The cantilever's integral ground shield and differential output provide excellent protection against electromagnetic interference (EMI).

Methods: Microphone performance is tested in a previously frozen human temporal bone. We implant the microphones, attach a tube to the sealed ear canal, and induce sound pressure to the ear canal with a Beyerdynamic speaker. With a broadband input stimulus, a calibrated probe-tube Knowles EK3103 reference microphone in the ear canal, and laser doppler vibrometry (LDV) measuring umbo motion, the sensitivity of the PVDF microphone and its effect on middle ear dynamics can be accurately measured. The experimental setup is illustrated in Figure 2.

Figure 3 shows a technique we are developing to measure the sensor's response to external sound by emulating a human pinna sealed to the ear canal.

Results: Our sensors exhibit high sensitivity to ear canal pressure—in particular, the cantilever-mic yields a low noise floor, shown in Figure 4. The drum-mic's lack of EMI shielding or waterproofing and higher parasitic capacitance results in more sensor noise, although some of the noise when wet could be alleviated with an insulating coating. Figure 5 shows noise performance compared to a high quality commercial hearing aid microphone. Equivalent input noise (EIN) is computed by averaging noise over a 1/3-octave bandwidth and then dividing by measured pressure sensitivity. Over the bandwidth 100 Hz to 8 kHz the cantilever-mic's overall EIN is 45 dB SPL, the drum-mic's is 59 dB SPL, and the Sonion 65GC31's is 24 dB SPL.

PD11.1 2:30 pm *Middle Ear Pathology & Diagnostics and Surgical Techniques & Reconstructions*

Prevention of recurrent Cholesteatoma by respecting the pathophysiologic genesis: a new theory of the origin of a retraction pocket

Karl Bernd Huettenbrink, University Clinic Cologne, Germany

Cholesteatoma surgery consists of two steps: eradication of the squamous epithelium and reconstruction. Modern techniques of eradication improve the results, but recidives still remain a concern. The frequency of residual recidives is solely dependent of the surgeon's proficieny to remove all epithelial cells, quite similar to carcinoma surgery. However, the development of a recurrent recidive, which constitutes a new, original cholesteatoma, is unpredictable, as conventional surgery will only repair the defects, but not remedy the pathophysiologic origin of the disease. Therefore, in order to effectively reduce the risk of recurrency, the causes for the development of a cholesteatoma should be cleared.

It is undisputed by most otologists that a cholesteatoma develops from a retraction pocket whose self-cleaning is disrupted by migration of the epithelium. As the keratin accumulates, destructive breakdown of the bone tissue under the perimatrix develops as a result of the bodies' frustrated attempt to enzymatically dissolve this foreign body. Thus, to prevent the development of a recurrence, it is important to prevent this early phase, the development of a retraction pocket.
Until now, however, explications of the cause of a retraction pocket have been very controversial: the tube's dysfunction with the development of a negative pressure in the tympanic cavity, which is often considered responsible (e-vacuo-theory), is not correct. However, many findings from clinical observations, supported by results from animal experiments, showed that there was always an inflammation of the mucosa under a developing retraction pocket.
The new idea explaining the genesis of a retaction pocket is that the tympanic membrane , which has the potency of horizontal migration, appears to actively migrate toward the focus of inflammation in the tympanic cavity to cover and control the inflammation. This principle of controlling inflammation in a cavity is also found elsewhere in the body, such as in the abdomen with the migration of the omentum majus. An irritationless retraction pocket , as is often seen as an incidental finding, should therefore not be regarded as pathology per se, but as a sign of successful healing of a previous inflammation in the middle ear. Only when self-cleaning no longer occurs does the 2nd phase begin, the development of a cholestatoma.
Therefore, in order to prevent the re-development of a retraction pocket, it is essential in the context of a cholesteatoma surgery, after the removal of the epithelium, to avert a renewed mucosa inflammation. The experience gained in surgery of the nasal sinuses can be used for this purpose: It is crucial to ensure unobstructed drainage from the mucosa-lined cavities. Surgery should therefore prevent bottlenecks in the path of mucosal drainage towards the tube ("tensor fold") or scarring on the promontory, by inserting thin silicone sheets. This warranty of unimpeded drainage, along with the creation of stable walls, is the decisive measure for preventing recurrent cholesteatoma recurrence, thus based on the pathophysiology of cholesteatoma genesis.

PD11.2 2:45 pm *Middle Ear Pathology & Diagnostics and Surgical Techniques & Reconstructions*

Analysing 3D Wideband Absorbance Immittance and Providing High Accuracy for Automated Diagnosis of Otitis Media with Effusion in Different Age Groups Using Advanced Machine Learning

Fei Zhao, Cardiff Metropolitan University
Emad M Grais, University of Sheffield
Leixin Nie, Institute of Acoustics of Chinese Academy of Sciences
Tariq Rahim, Cardiff Metropolitan University

Otitis media with effusion (OME) (also known as 'Glue Ear') is one of the most common causes of childhood hearing impairment and disability. It is estimated that more than 80% of children will have otitis media before the age of 10. This places a significant cost burden on the NHS with approximately 200,000 children with OME seen annually in primary care. Delayed diagnosis and poorly managed cases can result in severe and persistent OME with surgical treatment becoming the only management option, leading to long waiting times, and excessively high costs for the NHS. A simple, fast, objective, reproducible and non-invasive measurement called Wideband Absorbance Immittance (WAI) significantly improves the sensitivity for diagnosing childhood OME, and thereby reduces inappropriate diagnosis and costs associated with this condition. However, the main challenge is that the WAI dataset contains thousands of values, so that it is a difficult task for clinicians to classify the middle ear as normal or abnormal in the clinical setting. AI approaches are well-suited to understand and interpreting results in terms of pattern-recognition, which maximises the potential for WAI use in the clinical environment as an effective and accurate diagnostic tool. A recent study indicates that AI applications provide effective automatic diagnostic tools for OME. The major contribution of this study is the use of Machine Learning (ML) tools to better understand and interpret WAI data and further the exploration of age effect on the characteristics of WAI at frequency- pressure domain in normal and ears with otitis media with effusion (OME). The easy to use, accurate and automated diagnostic tool provides practical guidance to clinicians to recognize the importance and clinical meaning of WAI regions that are closely associated with middle ear transfer function, and thereby further facilitate clinical effectiveness.

PD11.3 3:00 pm *Middle Ear Pathology & Diagnostics and Surgical Techniques & Reconstructions*

Endoscopic Optical Coherence Tomography for Evaluation of Middle Ear Reconstruction

Joseph Morgenstern, Technische Universität Dresden
Jonas Golde, Technische Universität Dresden
Lars Kirsten, Technische Universität Dresden
Matthias Bornitz, Technische Universität Dresden
Edmund Koch, Technische Universität Dresden
Thomas Zahnert, Technische Universität Dresden
Marcus Neudert, Technische Universität Dresden

Introduction: Endoscopic optical coherence tomography (eOCT) enables non-contact high-resolution three-dimensional imaging of the tympanic membrane and adjacent areas of the middle ear, as well as oscillation measurement using Doppler OCT. This allows for better assessment of the outcome of tympanoplasty in patients postoperatively.

Material/methodology: Twenty patients were examined by eOCT after tympanoplasty. A near-infrared laser in the wavelength range around 1300 nm with a working range of 8 mm was used. The thickness of the tympanic membrane or reconstruction and the coupling of the prostheses were determined. In addition, the vibration behavior of the reconstructed tympanic membrane and prostheses was evaluated. The results were compared with audiometric data.

Results: The measurement could be performed in all patients. According to the tympanic membrane thickness and the circumference of the reconstruction, the tympanic membranes showed different vibration patterns and vibration amplitudes. The reconstruction thickness could be determined up to a thickness of 800 µm, the largest thickness of the reconstruction over a prosthesis was 700 µm. The results correlate with audiological outcome.

Conclusion: eOCT provides enhanced diagnostic capabilities, especially by determining vibration behavior, tympanic membrane morphology, and prosthesis coupling. This allows identification of causes for postoperatively impaired sound transmission as well as approaches for further improvement of tympanic membrane reconstruction.

PD11.4 3:15 pm *Middle Ear Pathology & Diagnostics and Surgical Techniques & Reconstructions*

Training a Machine-Learning Differential Diagnostic Tool for Conductive Hearing Loss Using Mechanistic Models

Hamid Motallebzadeh, Harvard Medical School
Michael Deistler, University of Tübingen
Florian Schönleitner, Technische Universität München
Annesya Banerjee, Harvard University
Jakob Macke, University of Tübingen
Sunil Puria, Harvard Medical School

Introduction: Conductive loss stems from a diverse set of possible pathologies, such as superior-canal dehiscence (SCD), ossicular fixation, or ossicular disarticulation. These distinct pathologies can result from similar physical traumas and exhibit similar symptoms, which means that in most cases x-ray-based imaging and exploratory surgeries are used to confirm a suspected pathology. Wideband tympanometry (WBT) could become a cost-effective tool for noninvasively diagnosing ME pathologies. However, the task of mining complex WBT datasets for reliable indicators of ME pathologies has proven challenging. Machine learning (ML), with its powerful pattern-recognition and classification capabilities, may provide a reliable methodology for doing this. However, only very limited attempts have been made thus far to incorporate ML into ME assessments, mainly due to the lack of large-enough WBT datasets of confirmed pathologies that are usually required to train ML algorithms. Simulation data from reliable mechanistic models such as finite-element (FE) models can compensate the need for such large clinical dataset.
Methods: We have implemented simulation-based inference (SBI), a powerful tool for objective parameter identification of an FE model whose behavior is consistent with experimental data. A middle-ear (ME) FE model was reconstructed from uCT images of a sample on which three sets of measurements were available: stapes velocity, ear-canal impedance and absorbance. Seven parameters of the ME model were selected to train the SBI neural network (NN) to detect the probability distributions of their values in normal and three pathological conditions: cochlear load (associated with SCD), stiffness of mallear ligament and stapes annular ligament (associated with ossicular fixation), and ossicular joints (associated with ossicular disarticulation) in addition to other influential parameters such as damping, and stiffness of tendons and eardrum. The baseline (normal ear model) was tuned by SBI in a following procedure: First a plausible range of normal values were established for each parameter from data reported in the literature. Sets of randomly selected values from those ranges were fed into the FE model and simulation data were extracted. Parameter sets and associated simulation data were fed into the SBI. The SBI learns the association between model parameters and simulation outcomes. Then the reference experimental data were fed to the trained NN and it returned probability distribution for each parameter value. To mimic the pathological cases, new simulations were performed with parameter values beyond the normal ranges.
Results: For our first baseline model we performed 10,000 simulations for 7 parameters. Upon giving the NN the mean experimental stapes-velocity and WBT data, it inferred parameters that can reproduce matching responses in the baseline FE model. We also performed validation tests on the trained NN to evaluate its performance. The learning curve analysis shows that for the selected parameters, training set of 2000 simulations would be enough to minimize the differences between the model response and reference experimental data, however, larger dataset improves the specificity of the prediction. The noise-level analysis shows that the NN performance is robust to the model and experimental uncertainties even up to 10 times of the standard deviations of the experimental data. SBI was able to predict the mimicked pathological conditions of SCD, ossicular fixation and discontinuity by exporting the associated parameter values beyond the normal ranges.
Conclusion: SBI is a promising tool to predict the probability distribution of the parameters of mechanistic models which represent auditory responses. From the probability distribution of these parameters, it should be possible to determine whether the ME is normal or pathological and, if pathological, which anatomical structure(s) the pathology stems from.

PD11.5 3:30 pm *Middle Ear Pathology & Diagnostics and Surgical Techniques & Reconstructions*

Improving the Quality of Ossicular Chain Reconstruction by Means of Real-time Monitoring - An Experimental Study

Christoph Müller, University Hospital Carl Gustav Carus at the Technische Universität Dresden
Korinna Lorenz, University Hospital Carl Gustav Carus at the Technische Universität Dresden
Marie-Luise Polk, University Hospital Carl Gustav Carus at the Technische Universität Dresden
Matthias Bornitz, Technische Universität Dresden
Marcus Neudert, University Hospital Carl Gustav Carus at the Technische Universität Dresden
Thomas Zahnert, University Hospital Carl Gustav Carus at the Technische Universität Dresden

Introduction: The intraoperative positioning of the passive middle ear prosthesis during tympanoplasty with ossiculoplasty is essential for the postoperative sound transmission and the postoperative hearing outcome. The reconstruction quality of the ossicular chain can be evaluated intraoperatively using a real-time monitoring system (RTM system). In this experimental study, the benefit of a RTM system was investigated for the implantation of partial (PORP) and total (TORP) prostheses.

Methods: Laser Doppler vibrometry was used to measure the middle ear transfer function (METF) in 13 human temporal bones. The vibration excitation of the ossicular chain was performed acoustically using a loudspeaker in the external auditory canal and electromagnetically using a magnet placed on the umbo. The measurements began with the intact ossicular chain, followed by real-time monitoring guided ossicular chain reconstruction with PORP and TORP. The RTM was realised by permanent LDV measurments at the stapes fooplate during the prosthesis coupling process.

Results: Electromagnetic and acoustic excitation of the intact and the reconstructed ossicular chain provided comparable results. The use of the RTM system significantly improved the quality of the ossicular chain reconstruction. The METF increased by 8 dB (standard deviation: ± 12 dB) over the entire frequency range after implantation of the PORP and positioning control by the RTM system. When using the TORP, the METF could be improved by 11 dB (standard deviation: ± 13 dB).

Conclusion: The RTM system is a very effective method for intraoperative quality control of ossiculoplasty. The intraoperative use of a RTM system should be a routine part of every tympanoplasty with ossiculoplasty. The RTM system is also excellent for educational purposes for the surgical training of young ear surgeons in the temporal bone laboratory.

PD11.6 3:45 pm *Middle Ear Pathology & Diagnostics and Surgical Techniques & Reconstructions*

Palate Myoclonus acoustic - a case report

Fang Wang, Technical University Munich
Markus Wirth, Technical University Munich
Maria Buchberger, Technical University Munich
Frank Boehnke, Technical University Munich

Palatal myoclonus (PM) is an uncommon clinical disease characterized by a contraction of the palatal muscles including the levator veli palatini and the tensor palatini muscle. The contractions lead to the rapid opening and shutting of the Eustachian tube, which produces a clicking tinnitus that is usually audible by the examiner. Palatal myoclonus should be distinguished from middle ear myoclonus, another form of objective tinnitus. Here, we describe a nine year old boy with essential palatal myoclonus tinnitus who was successfully treated with botulinum toxin (BT) injections. The results of the tympanometry and subjective as well as objective audiometry were also normal. The click noise was measured in the external auditory canal with 77 dB SPL (or 0.141 Pa) peak value, using an electret microphone. We took botulinum toxin (Botox®, Allergan) injection into the area of the lateral soft palate. It was done in narcosis since he did not take it well in local anesthesia. There occurred slight difficulties with swallowing developed after the injection, but dissolved completely after one week. His symptoms suspended in the next few days and the patient had been free of symptoms for three months. This case report discusses common questions about myoclonic induced OT clicking tinnitus and provides answers, and we intended to establish future diagnostic and treatment guidelines for palatal myoclonus.

1. Deuschl G, Toro C, Valls-Sole J, Zeffiro T, Zee DS, Hallett M. Symptomatic and essential palatal tremor: Clinical physiological and MRI analysis. Brain 1994; 117: 4: 775–788.
2. Sismanis A, Pulsatile tinnitus, Otolaryngologic Clinics of North America 2003;36(2):389–402.
3. Krause E, Heinen F, Gürkov R. Difference in outcome of botulinum toxin treatment of essential palatal tremor in children and adults. American Journal of Otolaryngology 2010;31(2): 91-95. 37
4. Penney SE, Bruce IA, Saeed SR. Botulinum toxin is effective and safe for palatal tremor: Journal of Neurology 2006; 253:857-860.
5. Carman KB, Ozkan S, Yarar C, et al. Essential palatal tremor treated with botulinum toxin. Pediatric Neurology 2013, 48(5): 415-417

Poster Sessions

Wednesday, June 22 through Friday, June 24

PS1

Effect of Endolymphatic Hydrops and Mannitol Dehydration Treatment on Guinea Pigs

Shuqi Wang, Fudan University
Chenlong Li, Department of Facial Plastic Reconstruction Surgery, Eye & ENT Hospital of Fudan University
Liu Jie Ren, fudan University
Wenjuan Yao, Shanghai University
Tianyu Zhang, Fudan University
Jingqi Xu, Fudan University
Lili Chen, Fudan University
Youzhou Xie, Fudan University
Peidong Dai, Fudan University

This study investigated the development of hearing loss on guinea pig EH models, as well as the effect of dehydration treatment. By combining analogical observations and objective measurement of hearing loss (ABR and LDV measurement of RWM vibration), The highlights of this study are:

1.EH induced hearing loss progressed with the development of EH, it starts at low frequencies, and later involves medium to high frequencies.
2.EH increases the cochlear impedance, causing conductive dysfunction. This dysfunction can be cured by dehydration treatment in early stage. But irreversible sensorineural component becomes significant for long-time EH.
3.Early dehydration treatment is suggested for reserving hearing.

This study gives an overview of the development of hearing loss in EH, and partly revealed the mechanical basis and biological influences of EH. Moreover, the investigation of dehydration treatment may provide a reference for clinical practice.

PS2

Sound Transmission in the Avian Middle Ear

John Peacock, University of Colorado
Garth Spellman, Denver Museum of Nature and Science
Daniel Tollin, University of Colorado

The middle ear of birds consists of a tympanic membrane which is joined the cartilaginous extracolumella, which in turns joins to the bony columella. This system is very different from that seen in mammals and, with the addition of a cartilaginous element, has more flexibility than the mammalian system. The transmission of sound energy through this system has not been well described, and thus the contribution of its increased flexibility to hearing capability is not clearly understood.

To study this, we made measurements of sound transmission through the middle ear in the American Crow (Corvus brachyrhynchos) using laser Doppler vibrometry. We measured the amplitude and phase of sound evoked displacements of the middle ear at the tympanic membrane, extracolumella, and columella. We studied the contribution of parts of the extracolumella to sound transmission by making measurements before and after manipulation of the structures.

PS3

Coupling Varying Mass Loads to the Short Incus Process and the Effect on Middle Ear Transfer Function (METF)

Ivo Grüninger, Ludwig-Maximilians-Universität München
Joachim Müller, Ludwig-Maximilians-Universität München

Background: Modifications of the ossicular chain (OC) as oscillating system, e.g. due to middle ear surgery, lead to changes of its dynamic behaviour and therefore of the METF and the resulting sound transmission. The implantation of (active) middle ear implants (AMEI) regularly requires such modifications to the OC. Using e.g. a floating mass transducer as active part of such a device and coupling it to the OC modifies the oscillating system by adding mass. While clinical results for different coupling techniques of an AMEI to the OC have been reported repeatedly, the effects of mass loads coupled to the OC on the middle ear dynamics are less well described. Previously published data including FE-analysis and experimental results using laser doppler vibrometry (LDV) after loading the OC at different sites, show a decrease of stapes foot plate (FP) displacement, especially for higher frequencies.
To our best knowledge, experimental data regarding the effects of systematically loading varying masses to the short incus process (SIP) are lacking so far. In this study, we therefore aim to examine the effect of mass loading the SIP on the METF and the resulting motions at the SIP and the stapes FP. This data might help to further understand the effects of coupling implants at the SIP on sound transmission and might be useful for further development of future generations of middle ear implants.

Material and methods: Laser-doppler vibrometry in eight human fresh frozen temporal bones and mass loads between 0 – 100 mg coupled to the short incus process. Movement was measured for frequencies between 100Hz and 8.5kHz at the stapes FP as well as at the SIP in the direction perpendicular to the axis through the incudomalleolar joint and the long incus process. Parametric function fitting was used to assess the effects on the METF.

Results: Our data shows a decrease of stapes and incus velocity especially for high frequencies and a shift of characteristic frequency towards lower frequencies with increasing mass loads. Descriptive data and first modelling results are presented.

PS4

Determination of maximum power output in an active transcutaneous bone conduction implant

Mohammad Ghoncheh, Medical University Hannover
Susan Busch, Hannover Medical School and Cluster of Excellence Hearing4all
Thomas Lenarz, Hannover Medical School and Cluster of Excellence Hearing4all
Hannes Maier, Medical University Hannover

Introduction: The maximum hearing level provided by percutaneous or active transcutaneous bone conduction device (BCD) is one of the main factors that determine the treatment success in patients with conductive or mixed hearing loss. The current common clinical approach is based on the indication range in terms of bone conduction (BC) thresholds provided by the manufacturers. Objective measurement methods such as sound pressure measurements using a probe microphone in the external auditory canal (van Barneveld et al., 2018) or on the forehead using a surface microphone (Hodgetts et al., 2018) have been introduced to determine maximum power output of the active transcutaneous BCDs that are not directly accessible after implantation. Here, we present a method to determine the MPO of a transcutaneous active BCD in terms of hearing level using only patients' audiological data from clinical routine examinations.

Method: 71 patients (average age 43 ± 19 yrs. ranging from 5 to 84 years) implanted with the Bonebridge (MED-EL, Innsbruck, Austria) between 2011 and 2020 were included in this study. We determined the MPO of the Bonebridge in terms of hearing level (dB HL) using the BC and direct threshold of the patient together with corresponding force levels at hearing threshold and the maximum force output of the device. The MPOs were divided into two groups with MPOs of ears with better BC threshold on the ipsilateral (implanted) side in group A and MPOs of ears with the better BC threshold on the contralateral ear in group B.

Results: The obtained average MPOs were in the range between 50 to 75 dB HL for frequencies from 0.5 to 6 kHz in group A with better BC threshold on the ipsilateral ears. The variability of the data was approximately 8 to 11 dB (standard deviations) across measured frequencies (0.5-6 kHz). The average MPOs in group B with better contralateral ears were in the range from 52 to 76 dB HL. The standard deviation within this group of patients was between 5 and 10 dB. The average MPO in both groups have a similar trend. However, the difference between groups were significant at 3 and 6 kHz (t-test; $P=<0.05$) indicating that the BC sound travelling across the skull is subjected to transcranial attenuation.

Conclusion: Our proposed method demonstrates that the MPO of individual patients with a transcutaneous bone conduction device can be determined using audiological data of the patients. Additionally, it emphasizes that masking of the contralateral ear during direct threshold measurements would be a useful addition in clinical audiology.
Reference

Hodgetts, W., Scott, D., Maas, P., Westover, L., 2018. Development of a novel bone conduction verification tool using a surface microphone: Validation with percutaneous bone conduction users. Ear Hear. 39, 1157–1164. https://doi.org/10.1097/AUD.0000000000000572
van Barneveld, D.C.P.B.M., Kok, H.J.W., Noten, J.F.P., Bosman, A.J., Snik, A.F.M., 2018. Determining fitting ranges of various bone conduction hearing aids. Clin. Otolaryngol. 43, 68–75. https://doi.org/10.1111/coa.12901

PS5

Interaural separation during hearing by bilateral bone conduction stimulation

Sudeep Surendran, Linköping University
Stefan Stenfelt, Linköping University
Liu Jie Ren, Fudan University
Wenjuan Yao, Shanghai University
Tianyu Zhang, Fudan University
Jingqi Xu, Fudan University
Lili Chen, Fudan University
Youzhou Xie, Fudan University
Peidong Dai, Fudan Unviersity

Cross head transmission (CHT) inherent in bone conduction (BC) is one of the most important factors that limit the performance of BC binaural hearing compared to air conduction (AC) binaural hearing. In AC, CHT is imperceptible due to the clear separation between the right and left ear pathways enabling the brain to process these signals independently leading to a clear understanding of the nature and position of the sound source(s). In this study, the prominence of CHT in BC hearing is addressed using the fact that ipsilateral cochlear excitation can be canceled by controlled bilateral BC stimulation.
A cancellation experiment was conducted on 20 participants with normal hearing at 13 third-octave frequencies in the range of 250 - 4000 Hz. Ipsilateral (IL) BC cochlear excitation was canceled by varying the level and phase of IL stimulation with respect to that of contralateral (CL) BC stimulation provided at 40 dBHL. The technique employed multiple stages of masking enabling adjustments of the stimulation level and phase until the tones got canceled in the IL ear. The cancelation was made initially for stationary BC stimulation at the mastoid followed by cancellation of transient stimulations at the mastoid. To accelerate the process, the cancellation parameters obtained from stationary stimulations (Interaural Level Difference (ILD) and Interaural Phase Difference (IPD)) were employed to set the initial conditions for transient stimulations to obtain its cancellation parameters (ILD and Interaural Time Difference (ITD)). Frequencies, where the participants were unable to achieve cancelation, were excluded from the final analysis.
At cancellation, the median ILD falls from around 5 dB at the low frequencies to reach a minimum level of -2.9 dB at 1 kHz in the mid-range frequencies and then increases at high frequencies reaching a maximum level of 9.5 dB at 2 kHz before slightly falling at 4 kHz. The unwrapped IPD shows an overall increase with frequency starting with 85° at 250 Hz reaching around one cycle separation at 630 Hz (327.5°) leading to multiple cycle separation at high frequencies (820.5° at 3125 Hz). The ITD shows an overall fall from lower to higher frequencies, though some minor deviations were observed at around the mid frequencies. It initially falls from 3 ms at 250 Hz to 1.2 ms at 800 Hz, rises in the mid-range frequencies to reach 1.4 ms at 1250 Hz before falling towards the higher frequencies reaching 0.825 ms at 4 kHz.
The deviations observed in the cancellation parameters show that at mid frequencies, CL stimulation contributes equally well or even more compared to that of IL. The study reveals that the ILDs for both types of stimulations are the same. It was also observed that the IPDs could not be exactly translated to ITDs for the same frequency implicating that the nature of stimulation mattered during cancellation. The similarities in the patterns of the cancellation parameters with frequency for different subjects, though with a few individual deviations, show the potential for the development of a generalized transfer function for the cancellation of CHT. This would enable BC to achieve a similar performance as compared to AC which could improve the quality of life of many BC hearing aid users and widen the scope of the applications of BC hearing.

PS6

Effect of Thiel conservation on bone conduction within the same specimen

Lukas Graf**,** Harvard Medical School, Mass Eye and Ear
Andreas Arnold, Spital Münsingen
Sandra Blache, University Basel, Basel, Switzerland
Flurin Honegger, University Basel Hospital, Basel, Switzerland
Magdalena Müller-Gerbl, University Basel, Basel, Switzerland
Christof Stieger, University Basel Hospital

Background and aims: Conserved specimens do not decay and therefore allow long-term experiments and permit to overcome limited access to fresh (frozen) temporal bones for studies on middle ear mechanics. We used a Thiel conservation which is mainly based on a watery solution of salts. In contrast to pure Formalin, the Thiel conservation aims to preserve the mechanical proprieties of human tissue. Regarding its influence on the middle ear, our previous investigations using air conduction stimulation showed that the transfer function to the stapes and the round window of Thiel conserved whole head specimens deteriorates by 10dB in the mid-frequency range compared to fresh frozen specimens and remains stable over a year. With bone conduction, sound reaches the cochlea through multiple pathways. The aim of this study is to examine the effect of Thiel conservation on bone conduction in the same specimen before and after conservation.
Methods: Seven ears of four fresh frozen whole heads were stimulated with a direct, electrically driven, bone anchored hearing system (Baha SuperPower). The motion for bone conduction stimulation was measured with a single point laser Doppler vibrometer (LDV) at the promontory, the ossicular chain, and the round window through a posterior tympanotomy. After the initial experiments, the entire whole heads were embalmed in Thiel solution. In order to enable direct comparison between fresh frozen and Thiel, in our experimental setup the Thiel conservation did not include intravascular and intrathecal perfusion. The measurements were repeated 3 and 12 months later.
To determine the effect of freezing, defrosting, and embalming on the whole heads, CT scans were performed at different stages of the experimental procedure. Additionally, three extracted temporal bones were measured by LDV on the promontory and embalmed in Thiel solution to investigate the direct impact of Thiel solution on the bone.
Results: The averaged magnitude of motion on the promontory increased in whole head specimens by a mean of 10.3 dB after 3 months of Thiel embalming and stayed stable after 12 months. A similar effect was observed for motion at the tympanic membrane (+7.2 dB), the stapes (+9.5 dB), and the round window (+4.0 dB). In contrast to the whole head specimens, the transfer function of the extracted temporal bones did not change after 3 months of Thiel embalming (-0.04 dB in average). CT scans after conservation showed a significant brain volume loss mostly >50% as well as a remarkable change of consistency and structure of the brain. Partial changes could already be observed after 1-2 days of defrosting. In an additional experiment, a pure substitution of brain mass and weight by Thiel fluid did not lead to a new deterioration in sound transmission. In contrast, a frozen whole head showed a distinctively reduced transfer function before defrosting.
Discussion: For our setup, sound transmission of bone conduction in the same whole head specimens significantly increased after Thiel conservation. Such an increase was not observed in extracted temporal bone specimens.
Due to brain changes in the CT scans, we investigated the consequences of the brain volume and structure loss as well as the brain before defrosting. The loss of volume alone could not explain the increase of sound transmission as we did not observe a difference when the volume was replaced with Thiel fluid. However, complete defrosting of the entire brain seems to have a major influence. Beside the destructive effect of freezing to the brain, our modified conservation method without perfusion failed to preserve the brain structure.
Conclusion: investigations of bone conduction in whole heads for fresh frozen and defrosted as well as Thiel conserved specimens depend on the condition of the brain, rather than on Thiel-related effects to the mechanics inside the temporal bone.

PS7

Effects of middle-ear perturbations on bone conduction hearing: a finite element study

Xiying Guan, Wayne State University
Junfeng Liang, Wayne State University
Hamid Motallebzadeh, Harvard Medical School
Sunil Puria, Harvard Medical School

Introduction: Bone conduction (BC) hearing refers to the perception of sounds when the skull is set in vibration at auditory frequencies. While the BC vibration simultaneously stimulates the outer, middle, and inner ear, the middle ear is thought to have little contribution to BC hearing because early studies shown that the BC thresholds in patients with otosclerosis – fixation of the stapes footplate – are normal except at 2 kHz where the BC threshold is increased by 10-15 dB, known as Carhart's notch. However, the studies in the past 15 years shown that the notch can present at 0.5, 1, and 2 kHz and the amplitude of the notch can be as much as 25 dB HL. We hypothesize that the middle ear has a greater contribution to BC at a wider frequency range than previously thought, and the contribution can be influenced by the mechanical conditions of the middle ear. We tested the hypothesis using a finite element (FE) model of a human ear.

Methods: The FE human ear model, previously developed using CT scans and simulated using the Actran software, was adapted into the COMSOL software. The model consists of the ear canal, the ossicular chain, the middle ear soft tissues, and the simplified inner ear as the scala media was merged with the scala vestbuli. BC excitation was simulated by applying a rigid-body vibration to the model in the stapes piston-motion direction. The BC-evoked intracochlear pressures at the basal cochlea in the scala vestibuli (PSV) and scala tympani (PST) and the differential pressure (PDIFF = PSV-PST) were simulated at 0.1-10 kHz under normal and perturbed conditions in the middle ear. The perturbations include fixing the stapes footplate to the oval window, stiffening the malleus-incus joint, stiffening the malleus-incus joint and the incus-stapes joint, and increasing the mass of the malleus and incus by 100 mg.

Results: The model predicts that 1) fixation of the footplate reduces PDIFF by 5-15 dB at 0.2-2 kHz and the maximum reduction occurs at 0.4-0.5 kHz; 2) stiffening the malleus-incus joint does not affect PSV or PST; 3) stiffening both ossicular joints leads to a small fluctuation (less than 3 dB) in PSV and PST over the tested frequencies; 4) increasing the mass of the malleus and incus increases PSV, PST, and PDIFF by as much as 20 dB below 300 Hz and 5-8 dB above 300 Hz.

Conclusion: The simulated effect of footplate fixation suggests that the middle ear contributes to BC hearing at 0.2-2 kHz, a frequency range wider than that suggested by Carhart's original finding. Adding mass to the ossicles may produce a noticeable increase in BC sensitivity while stiffening the middle-ear joints has little effect on BC.

This work is supported by NIH/NIDCD R21DC017251.

PS8

Techniques to improve the efficiency of a middle ear implant: Effects of coupling method on intracochlear pressure

Nathaniel Greene, University of Colorado
Herman Jenkins, University of Colorado
Daniel Tollin, University of Colorado
James Easter, University of Colorado

Hypothesis: Coupling a middle-ear transducer directly to the stapes will most effectively transmit sound pressure into the cochlea.

Background: Active middle ear implants (AMEIs) effectively treat moderate to severe sensorineural, mixed, or conductive hearing loss by vibrating the ossicular chain with an electric actuator. Previous work in our laboratory has shown that the effectiveness of an AMEI at producing motion in the stapes depends jointly on the coupling mechanism and the exact placement of the actuator along the ossicular chain (Deveze et al. 2013). Here, we extend those results by measuring intracochlear pressure concurrently with stapes motion during AMEI input.

Methods The AMEI was coupled to the ossicular chain using the following methods: 1) placing the tip of the transducer in contact with the incus body (baseline), 2) with áWengen clips crimped to the transducer and attached to the incus long process (ILP), and 3) after chain disarticulation, a bell-shaped prosthesis crimped onto the transducer and placed in contact with the head of the stapes. Performance of the AMEI in each condition was assessed by measuring the pressure in scala vestibuli (PSV) and scala tympani (PST), using fiber-optic pressure sensors, concurrently with stapes velocity (va) via a single-axis laser-doppler vibrometer, and comparing computed maximum equivalent ear canal sound pressure levels (LEmax).

Results: Consistent with our previous report, coupling to the ILP or stapes produced similar or substantially improved stapes velocity relative to the baseline coupling condition; however, intracochlear pressure did not always show a comparable increase in performance with alternative coupling methods, suggesting that velocity of stapes capitulum alone is not sufficient to fully characterize coupling efficiency.

Conclusion: Intracochlear pressure as well as stapes velocity varies with different coupling methods of the AMEI to the ossicular chain. Further research assessing clinical outcomes is necessary to elucidate the qualitative benefits of various coupling techniques.

PS9

Live Chinchilla Ear with Otitis Media with Effusion: A Holographic Study

Jeffrey Cheng, Massachusetts Eye and Ear, Harvard Medical School
Haimi Tang, Worcester Polytechnic Institute
Cosme Furlong, Worcester Polytechnic Institute
Melissa Castillo-Bustamante, Massachusetts Eye and Ear, Harvard Medical School
John Rosowski, Massachusetts Eye and Ear, Harvard Medical School
Aaron Remenschneider, Massachusetts Eye and Ear, Harvard Medical School

Otitis Media with Effusion (OME) is a common middle ear disease in children, which can cause hearing loss and learning disability if not diagnosed and treated promptly. Mechanisms associated with OME induced hearing loss include: (i) Viscous damping of middle-ear motions; (ii) Reduction of middle-ear air space; (iii) Static-middle-ear-pressure induced changes in tympanic membrane (TM) shape and compliance; (iv) Increased TM thickness and stiffness due to chronic inflammation. However, the frequency dependence of OME induced hearing loss and the effects of effusion level and position remain unclear. Traditional diagnostic tools of OME, such as tympanometry and wide-band acoustic immittance, are based on average TM motion and do not detect partial effusion, nor do they describe the relation between the location of effusion and localized TM motions. We developed a High-speed Digital Holographic (HDH) system to study the surface motion of the TM in live chinchillas with OME.

The left ears of ten chinchillas were injected with Lipopolysaccharide (LPS) to induce OME; the right ears served as controls. Auditory brainstem responses (ABR) and distortion product otoacoustic emissions (DPOAE) were measured before the LPS injection, and 5 days post injection just prior to holographic measurements. The middle-ear inflammation and effusion was monitored daily via endoscopy. HDH was used to record the shape and the acoustic-click-induced displacement of about 60% of the TM surface in live chinchillas. Frequency and impulse analyses were performed on the measured displacement datasets to derive TM motion parameters that are compared between the control and OME ears. Correlation analyses between the TM shape and motion parameters, middle ear inflammation status and functional hearing tests will assess the clinical utility of the HDH system.

Preliminary results suggest the shapes of the TM in OME and normal ears are similar, even though significant effusion levels were observed behind the TM in OME ears. Our measurement technique is highly sensitive to the level of effusion, as the regions of the TM surface in contact with effusion showed largely reduced motions, and the reductions in the mechanical responses are correlated with elevated ABR and DPOAE hearing thresholds measured in OME ears. A comparison of motion parameters between the control and OME ears showed localized changes of resonance frequencies, motion magnitude and damping in the OME ears. Assessment of the clinical diagnostic value of our HDH system is ongoing.

PS10

Estimation of Location and Degree of Ossicular Fixation by Compliance Measurement

Hyeonsik You, The University of Electro-Communications
Sinyoung Lee, The University of Electro-Communications
Yuuka Irie, The University of Electro-Communications
Yuki Shimizu, The University of Electro-Communications
Sho Kanzaki, Keio University Hospital
Chee Sze Keat, Mechano Transformer Corp.
Takenobu Higo, Leadence Corp.
Kenji Ohoyama, Leadence Corp.
Hajime Ikegami, Daiichi Medical Co., Ltd
Takuji Koike, The University of Electro-Communications
Masaaki Hayashi, Daiichi Medical Co., Ltd

Assessment of ossicular mobility during tympanoplasty surgery is important, because a surgical procedure is determined based on the mobility of each ossicle, and the degree of improvement of the mobility affects the prognosis for recovery of hearing level. However, an objective measurement of the ossicular mobility has up to now been rarely performed during the surgery, and the assessment of ossicular mobility is made by palpation in most cases. Palpation is inherently subjective and may not always be reliable, especially in milder degrees of ossicular fixation and in the case of combined fixation. We have developed a hand-held probe and evaluation software that can provide an objective and quantitative assessment of the mobility of each ossicle during middle ear surgery. However, there are difficulties to establish the criteria for ossicular fixation, because it is hard to obtain the data from patients with confirmed ossicular condition and hard to mimic various fixation with cadavers. Therefore, we have been investigated the mechanics of the middle ear using the finite-element method to simulate ossicular fixation. In this study, we measured ossicular mobility at several point on the ossicles, and compared with the numerical analysis. And then, effective diagnostic methods for fixation using our measurement system were investigated.
The hand-held probe consists of a piezoelectric force censor, a high precision piezoelectric actuator and an ear pick, which is usually used in ear surgery. The rear end of the ear pick is connected to the actuator via the force sensor. When the tip of the ear pick contacts one of the ossicles, the actuator vibrates the ear pick at 30 Hz, and reaction force is measured with the force sensor. The ossicular mobility is quantified as compliance which is the ratio of displacement and applied force at each measuring point.
The measurements were performed on two normal fresh cadaver ears. Exposure of the middle-ear ossicular chain, which included near full view of the stapes footplate, was made by a mastoidectomy with posterior tympanotomy. Measurements were made at five points on the ossicles shown in Fig. 1, which were accessible by the approach method, and the measurement points were decided in consideration of the areas that doctors often palpate (1. head of the malleus, 2. long leg of the incus, 3. upper part of posterior crus of the stapes in mediolateral direction, 4. upper part of posterior crus of the stapes in vertical direction, 5. basal part of posterior crus of the stapes).
A finite-element model of the middle ear was created, and the compliance at each point of the ossicles was calculated using the CFD-ACE+ (ESI Corp). Measurement and simulation results are shown in Fig.1. Although the absolute values are slightly different, both results show similar tendencies.
Next, the effects of the fixation of the middle ear ligament on the compliance were estimated using the model. Changes in compliance caused by various fixation states were calculated, and the features of each state were analyzed. These features suggest that it is possible to diagnose the location and degree of fixation by measuring compliance at each ossicle. The numerical simulation analysis can improve the accuracy of evaluation in our assessment system, and it can provide valuable information of the status of the ossicles to the surgeons.
This research was supported by AMED under Grant Number 20he0122007j0001.

PS11

Intracochlear pressure measurements at loudness levels for speech

Irina Wils, KU Leuven
Alexander Geerardyn, KU Leuven & UZ Leuven
Tristan Putzeys, KU Leuven
Guy Fierens, KU Leuven & Cochlear Ltd.
Kathleen Denis, KU Leuven
Nicolas Verhaert, KU Leuven

Background: Intracochlear pressure measurements, typically measured with fiber-optic pressure sensors, evaluate cochlear drive and thus hearing sensation. Hence, they allow investigating the fundamental mechanisms of sound transmission and evaluating the preclinical performance of acoustic hearing implants. Previous studies had to simulate at high intensities (80-120 dB SPL) to obtain a reasonable signal-to-noise ratio. Hence, linearity is assumed to draw conclusions about lower stimulation intensities, such as during normal conversation (60 dB SPL). However, stimulating at lower levels would be beneficial to verify this linearity. It would also facilitate the investigation of non-osseous bone conduction pathways and harmonic distortion. One possibility to enable low-intensity measurements is to reduce noise.

Methods: The methods for measuring intracochlear pressure are similar to those reported by Borgers et al. (2019). The commercially available fiber optic pressure sensors (FOP M-260, FISO Technologies, Canada) measure pressure. However, instead of the previously used two-channel signal conditioner (VELOCE 50, FISO Technologies, Canada), an OCT Common-Path interferometer (INT-COM-1300, Thorlabs Inc., USA) is used to convert the optical signal into an electrical signal. In addition, lock-in amplifiers (SR830, Stanford Research Systems, USA) are used to measure, amplify and filter the signal. This system is tested in a calibration setup, where the pressure sensor is submerged in a vibrating water column. After initial characterization, the technique is verified with a temporal bone, where stimulation is provided with an insert phone. Two pressure sensors are inserted into the cochlear scalae vestibuli and tympani. Pressure is measured while the vibrating water column and the insert phone produce pure tones at multiple frequencies (250-6000 Hz) and varying intensity (45-118 dB SPL for the water column and 40-90 dB HL for the insert phone). Finally, the measured pressure is compared to the noise floor via a Welch test for significance ($\alpha = 0.05$).

Results: The lowest intensity for which the measured pressure was significantly different from the noise floor was determined for each frequency with both setups. Regarding the calibration setup, these intensities range from 73 to 90 dB SPL, while for the setup with the temporal bone, they range from 50 to 80 dB HL depending on the signal frequency. Since stimulation for the temporal bone setup occurs in the ear canal, a 20 dB difference is expected from the calibration setup due to the middle ear gain. Furthermore, the temporal bone setup showed that for the whole mid-frequency range (800-4000 Hz), stimulation intensities as low as 60 dB HL result in pressure measurements significantly different from noise.

Conclusions: The reported measurement system enables intracochlear pressure measurements at physiological stimulation intensities as low as 60 dB HL, which is 20 dB lower than the current state-of-the-art. Thus, this updated technique will allow investigating linearity at clinically relevant stimulation intensities, non-osseous bone conduction pathways, and harmonic distortion.

PS12

Controlling stability of temporal bone experiments in a robotized setup

Michael Martin, University of Tübingen
Stephan Kempa, University of Tübingen
Ernst Dalhoff, University of Tübingen

Introduction: In-vitro temporal bone (TB) experiments are often used to investigate stapes velocity in response to some rehabilitative intervention with passive or active implants. In these applications, drying of the thawed TB is often of limited importance, because overall experimental time can be kept short. In other applications, it can be desirable to extent measurement time in order to acquire data of more than one structure of interest, possibly several measurement angles, or treatment conditions. For the development of a robotized TB measurement setup, we investigate the establishment of a standard procedure to ensure the stability of mechanical middle-ear (ME) properties. In the robotized setup, the use of glass beads is preferred in order to achieve high signal-to-noise ratio more for Laser-Doppler measurements. Therefore, it is undesirable to flush the ME with saline more often than needed. Here, we investigate the time dependence of the drying process under controlled conditions and methods to prolong stability of the preparation.

Method: After TBs are taken out of the freezer, they are kept in saline for 1/2 hour before the start of the measurements. TBs are measured with a robotized setup every 25 Minutes at the same physiological landmarks under robotized control of measurement location and direction (umbo, stapes head, long process of the incus, round window). To process the data, the vibration-to-pressure transfer functions are calculated based on raw velocity data recorded from LDV and sound pressure from ER7C probe-tube microphone. The TB experiments are performed with different preservation methods. As preservation medium paraffin and low-viscosity silicone are investigated.

Results: Significant changes in ME-transfer functions are noticed over time, if no interventions are undertaken.

Conclusion: A regularly control measurement is implemented in the TB experimental protocol for early detection changes in the ME-transfer function and subsequent intervention in order to re-moisten the tympanic membrane. Alternatively, preservation techniques can be applied to prolong intervention-free periods.

PS13

Methodology for Reducing Measurement Artifacts in Laser Doppler Vibrometry Using a Customized Adapter Plate and an LED Microscope

Carmen Molenda, Ludwig-Maximilians-Universität München
Joachim Müller, Ludwig-Maximilians-Universität München
Ivo Grüninger, Ludwig-Maximilians-Universität München

Background: "In present middle ear research, the temporal bone model has become an integral part of the research methodology. For the investigation of middle ear mechanics, measurement by laser Doppler vibrometer has become firmly established. (Rosowski 1990; Müller & Schön 1994, Chien 2006; Strenger et al. 2018). While LDV-Measurements offer great accuracy, sometimes the experimental set-up for best possible results can be challenging. In addition to the LDV itself, an ear microscope is also needed for middle ear research. For research purposes, often microscopes are used which are out of clinical service and no longer used in clinicsdespite
they are far away from end of life. However, one of the potential sources for artifacts is the lightning or lightning source of the microscope on which the LDV is mounted to focus the laser beam on the desired target. Warming and consecutive drying of the specimen and its middle-ear structures as well as direct measuring artifacts due to vibrations from the cooling - system for the light source, might occur.

Methods and Results:"We report our experience reducing these artifacts by developing a customized adapter plate allowing to mount a Laser Doppler Vibrometer Type CLV-2534 (Polytec GmbH, Germany) to an new and inexpensive ATMOS iView PRO Microscope (ATMOS MedizinTechnik GmbH & Co. KG, Germany). The laser beam is focused using a micro manipulator Type A-HLV-MM30 (Polytec GmbH, Germany). By using a microscope with LED-technology as lightning source, instead of a microscope with a conventional lightning source, no cooling system is necessary and artifacts due to an for example a ventilator were distinctly reduced. In a measurement run with 500 measurement repetitions, we were able to impressively demonstrate that the artifacts were drastically reduced when using the LED microscope with the LDV compared to a conventionally used microscope (Zeiss - OPMI). Even with small measurement series (n=25), the interference artifacts could already be visibly reduced. Further, warming and drying out of middle-ear structures can be slowed down.

Summary: working with an LED microscope in the research laboratory is a comparatively affordable method with potential to be used in OR since the ATOMOS is specified for. Thus, by means of an adapter plate, the LDV can be easily integrated into the experimental setup and the LED lightning source offers significant advantages over the conventional lamps installed on microscopes. The LED microscope can significantly reduce the measurement artifacts and simultaneously allows the examination of the specimen (e.g. a temporal bone) to be examined more gently due to the lack of heat development. sys

PS14

Technique for measuring three-dimensional vibration of the human tympanic membrane using a scanning laser Doppler vibrometer

Bastian Baselt, University Hospital Zürich, University of Zürich
Merlin Schär, University Hospital Zürich, University of Zürich
Ivo Dobrev, University Hospital Zürich, University of Zürich
Alexander Huber, University Hospital Zürich, University of Zürich
Jae Hoon Sim, University Hospital Zürich, University of Zürich

The motion of the tympanic membrane (TM) converts acoustic waves in air to mechanical vibration of the middle-ear ossicular chain. It shows a simple in-phase motion at low frequencies and complex motion patterns with several spatial nodes at high frequencies. While many previous studies investigated functional roles of the TM for middle-ear sound transmission, the obtained knowledge is still insufficient to explain how various motion of the TM in the frequency domain contributes to middle-ear sound transmission. For instance, it is not clear how the complex motion of the TM at high frequencies leads to torsional motion of the malleus. While most measurements of vibrational motion of the TM have been done in two-dimensional planes, three-dimensional motion needs to be measured to reveal contribution of the TM to middle-ear mechanics thoroughly. This study provides techniques to measure three-dimensional motion of the TM using a laser Doppler vibrometer (LDV), which has been used widely to measure vibrational motion of the middle-ear structures.

Techniques to measure three-dimensional motion of the TM in cadaveric temporal bones were developed based on two-dimensional measurement of vibrational motion of the membrane using an infra-red scanning LDV (short wavelength infrared scanning vibrometer, Optomet, Germany). The infra-red scanning system was used to enhance reflectivity of the laser beam on semi-transparent surface of the TM. The TM only with the malleus manubrium was isolated, and acoustic stimuli was imposed with an artificial ear canal. The vibrational motion of 150-200 points on the TM was measured from the medial side (i.e., from the middle-ear cavity side), with five different orientations of the LDV head. Information on each orientation was obtained from coordinates of the robot arm on which the LDV was mounted, and coordinates of all the measurement points in the corresponding LDV measurement frame were recorded. Then, all the measured motion and coordinates of the measurements points with the five orientations were registered into a reference measurement frame. A common grid was generated on the reference measurement frame, motion on a common grid was interpolated from the registered motion, and three-dimensional motion components at each grid point were calculated. To register the obtained three-dimensional motion components into an anatomical intrinsic frame, three-dimensional features of the TM and the manubrium were obtained using micro-computed tomography (micro-CT) imaging, and an anatomical frame based on a plane from the annulus of the tympanic membrane and an axis along the manubrium was extracted. Correlation between the anatomical frame and the reference measurement frame was calculated from coordinates of external reference points in both frames. Once the three-dimensional components were obtained with respect to the anatomical intrinsic frame, the components normal and tangential to the TM surface were calculated for further analysis. The surface profile of the TM was obtained from micro-CT imaging as well.

The established technique provides a way to measure in-plane components as well as out-of-plane components of the TM motion for a complete picture of TM vibration, and thus is expected to contribute to thorough knowledge about vibratory functions of the TM, in normal and reconstructed middle ears.

PS15

Quantitative Association of Middle-Ear Pressure Gains and Stimulus-Frequency Otoacoustic Emission Due to Middle-Ear-Parameter Modifications in a Mouse Model

Hamid Motallebzadeh, Harvard Medical School
Sunil Puria, Harvard Medical School

Introduction: Sounds in the ear canal (EC) travel through the middle ear (ME) in the "forward" direction on their way to the cochlea. Inside the cochlea of a healthy ear, complex electro-mechanical processes within the organ of Corti (OoC) generate sounds that propagate through the cochlear fluids and travel through the ME in the "reverse" direction back toward the EC. These sounds emitted by the cochlea and measured in the EC are called otoacoustic emissions (OAEs). However, much remains to be understood about how OAEs are generated within the cochlea, how they are shaped by traversing through the ME, and how they are measured. Insight into how OAEs are shaped by the ME will better enable us to interpret their relationship to pathologies of the cochlea and ME.

Methods: We developed a coupled 3D finite-element model of the mouse EC, ME, ME cavity, and cochlea. The cochlea incorporates a repeating pattern of Y-shaped structures of outer-hair-cell (OHC) and phalangeal-process attached to Deiters' cell, sandwiched between the basilar membrane and reticular lamina. The ME pressure gains, impedances, and reflectances at the sound-delivery–EC and stapes–cochlea interfaces were calculated. The modified ME pressure gains were calculated by excluding the reflectances at the EC and stapes. Stimulus-frequency OAEs (SFOAE) generation was achieved in the model by introducing random perturbations to the electromechanical gain supplied by the OHCs within the OoC. We performed ME-parameter sensitivity analyses relating the changes in the ME pressure gains and SFOAE amplitudes due to modifications of the: (1) stapes-annular-ligament stiffness, (2) eardrum stiffness, and (3) ossicular mass.

Results: The main characteristics such as the ME pressure gains, EC, ME, and cochlear impedances, and EC and stapes reflectances were calculated. The basic characteristics of EC and stapes reflectances are comparable to those of human. Both have magnitudes that are close to 1 at low frequencies, reach their minimum at the ME resonance, and are again close to 1 at the highest frequencies. For the active model, stapes reflectance could be greater than one in the 60–70 kHz range due to cochlear amplification, but the general trends in EC reflectance are virtually unaffected by cochlear amplification. Modified ME pressure gains follow a pattern similar to the conventional pressure gains; they start with low magnitudes at the lowest frequencies, increase to the maximum gain around the ME resonance frequency (10–13 kHz), and after a plateau in the 60–80 kHz region, drop again by 100 kHz. The modified gains, however, lack the sharp peaks that appear in the forward (and consequently round-trip) pressure gains, which happen due to the occurrence of the standing waves inside the EC. The model confirms the dual mechanisms required for SFOAE generation: cochlear amplification and linear reflections due to random perturbations within the cochlea. We also quantitatively illustrated that the ME round-trip pressure gain needs to be modified in order to explain the SFOAE variations due to ME-parameter modifications. Increasing and decreasing the stapes annular ligament and eardrum stiffness by a factor of eight changes SFAOEs by up to 30 dB in the 10-30 kHz frequency range, while the ME round-trip gain does not account for this change. This discrepancy on average can be up to +/- 10 dB. Removing ear canal and stapes reflections (as in previous work) diminishes the discrepancy and allows one to quantitatively associate OAE changes to round-trip ME gain.

Conclusion: Introducing random perturbations to the OHC gain generated stimulation-frequency OAEs in a finite-element model of the mouse cochlea coupled to a middle ear. Consistent with previous work, we quantitatively illustrate that changes to the ME parameters and the resulting ME pressure gains determine how OAEs are modified, as long as only incident pressures are considered without reflections.

PS16

Ear-canal geometry measurements from human CT scans: New method and preliminary results

Susan Voss, Smith College
Soomin Myoung2, University of Massachusetts Chan Medical School
Auden Balouch, University of Massachusetts at Amherst
Hannah Durkee, Smith College
Mealaktey Sok, Smith College
Aaron Remenschneider, University of Massachusetts Chan Medical School
Douglas Keefe, Boys Town National Research Hospital, Omaha, NE
Nicholas Horton, Amherst College

Peripheral sound flow through the ear canal, as well as the specific application of wideband acoustic immittance (WAI) measurements, depend on ear-canal geometry. Yet, there are few data that describe canal geometry; published measurements from babies and children do not exist and recent measurements suggest that average adult ear canals are systematically larger at the WAI probe location than industry-chosen areas, by an average factor of about 1.3.

Using the medical imaging software OsiriX, a method to use multiplanar reconstructions of high-resolution CT images was developed to make measurements along the ear canal. The new method will be described here and includes clear definitions for the canal's termination, central axis, and entrance, and applies them to measure the cross-sectional area along the central axis. De-identified CT scans were obtained retrospectively through the University of Massachusetts Medical School; both they and Smith College granted exemptions from IRB oversight.

Preliminary results include measurements of canal geometry from CT scans of adult, child, and infant ears. In general, left and right ears from a given subject are far more similar than measurements across subjects. In adult ears, canal areas vary substantially at the first-bend location where WAI probes likely sit. The new method yielded consistent results from three independent and blinded researchers (APB, HD and MS) on six ears.
Multiplanar CT reconstruction provides a new and repeatable method to describe ear-canal geometry.

Application of this method to a larger population of subjects of all ages will enable a far better description of individual ear-canal geometry as well as variability across subjects. Furthermore, descriptions of ear canals of all ages will support the development of accurate WAI measurements.

Supported by: R15 DC014129-02 from the NIDCD. A similar but not identical poster was presented at the American Auditory Society Meeting in February 2022.

PS17

Actuators & Sensors - The Origins of Transducerology

Geoffrey Ball, MED-EL (former Stanford University, University of Oregon & Symphonix)
Stefan Rainer, BU Vibrant MED-EL

Abstract: The heart of the technology is always the transducer. We present a large array of our earliest electromagnetic transducer designs and the evolutions of our transducer in what we call "The Origins of Transducerology". We highlight what turned out to be our largest transducer design success designs. A highlight what shall be turned out to be significant design mistakes that we had to overcome and how they were discovered and corrected. We will also discuss our many design ideas that could not be realized due to technological realization limitations or because of significant design issues. We highlight our "best of" as well as the designs that "got away" and that could have been better. The first FMT designs had several significant issues that had to be solved, and then improved, and the revised and re-designed over and over until we achieved optimized results. The trade-offs, constraints and positives and negatives for many of our favorite designs will be displayed. We had to learn from many design mistakes, resolve them and then repeat. And we had to find the resources and talent that could build our devices and many times we had to build the tooling and machines to build the devices. This poster should be of interest to electro-mechanical transducer engineers and researchers in biomechanics that are looking at ways to improve actuator and sensor applications in their research and for studies of hearing. We show pictorially how the designs were realized from conception to final implantable grade form. In our experience, the full realization of new transducer designs for active middle ear and active bone conduction systems is far from being "easy peasy" and very few groups have been able to achieve design, regulatory and reliability success.

Methods – Transducers and Actuators that conceptionally seemed ideal often turned out to have unforeseen design flaws that could only be discovered by taking design concepts through an entire product/project development process from conception to the full approved device realization. One is the example of the first conceptions of the FMT, which on paper, should not have worked. Yet they did in fact "work" which was due to the fact that they could not be constructed to be perfectly "balanced". The first Symphonix "push-pull" dual coil devices were built with the "springs" in the exact opposite the direction of what they should have been and thus caused what we labeled "transducer drop out" whereas the drive level was decreased to low levels the magnet would collide with the housing and the devices would "go non-linear" at lower levels. Transducerology proponents would typically expect that non-linearities would occur at much higher levels, or at over-voltage levels. With the first that FMT's were to be produced for clinical use "drop out" was discovered. This delayed the first implants as we had to re-design the transducers and re-validate them all over again before they could be used in patients. Drop out could not have been known prior to the execution of a full transducer and system development. We shall show several other examples of similar findings in our presentation.

Discussion – Many transducers and sensor design's that "look great on paper" as we used to say often will have key design flaws that can only be learned during the work toward true device actualization. In the field of hearing we have seen many cases of proposed designs by groups that have never completed a complete development cycle and often proclaim the superiorities of said designs far to early. In our experience the only way you can truly discover potential pitfalls and the real value of design proposals is by design through to final production of working devices. Our experience that sometimes designs can work fine all the way up until the manufacturing validation phase (aka just before

PS18

Systematic review and meta-analysis of audiological and patient-reported outcomes with the VIBRANT SOUNDBRIDGE

Severin Fürhapter, MED-EL
Michael Urban, MED-EL
Thomas Dejaco, MED-EL
Klaas Kieswetter, MED-EL
Francesca Scandurra, MED-EL
Karin Rose-Eichberger, MED-EL

Background: Twenty-six years after its first implantation, the VIBRANT SOUNDBRIDGE (VSB) still leads the field of active middle ear implants. Researchers all around the globe have thoroughly investigated the implant's safety and performance, leading to hundreds of peer-reviewed publications. With this growing body of evidence, however, keeping track of the bigger picture becomes more challenging.

Methods: Based on a systematic literature review in the National Library of Medicine literature database (PubMed), clinical outcomes from 219 primary publications on the VSB middle ear implant system were included and plotted as raw mean unaided/aided or improvement scores. From a subset of 72 publications, meta-analyses were conducted to estimate pooled mean scores across publications. Mixed models and model selection were used to explore the effects of potential demographic and clinical predictors on each outcome. Specifically, a meta-analysis was conducted on sound field hearing thresholds, word recognition score at conversational speech level, speech recognition threshold in noise, the Abbreviated Profile of Hearing Aid Benefit questionnaire, and the daily use of the audio processor.

Results: Both, the raw means and pooled estimates from meta-analyses consistently showed similar average outcomes and levels of variation among studies. Overall, pediatric patients and patients with conductive hearing loss were associated with better aided results in sound-field hearing thresholds and word recognition scores compared to adults and patients with sensorineural or mixed hearing loss. The site of FMT coupling had no effect on any outcome summarized here, thus highlighting the surgical flexibility of the middle ear implant system.

Conclusion: Overall, the reviewed literature on the VSB provides compelling evidence for long-term hearing improvement, by hearing thresholds, speech in quiet and speech in noise tests, measurable benefit in hearing-related quality of life, accompanied by high wearing comfort and patient satisfaction, as measured by daily use of the device.

PS19

Stepless Length Adjustable (SLA) Ossicular Replacement Prostheses (ORP) & Forces In The Middle Ear

Clemens Kuen, MED-EL Medical Electronics
Edwin Waool-Kornherr, MED-EL Medical Electronics
Thomas Lechleitner, MED-EL Medical Electronics
Uwe Steinhardt, MED-EL Surgical Solutions GmbH

ORP are well-established medical products used to restore the mechanical sound transmission from the tympanic membrane to the oval window, of the human middle ear. For tympanoplasty prostheses the functional length of an ORP is one of the most critical factors for acoustical signal transportation. Therefore, SLA systems are of special interest, they allow the surgeon to intraoperatively adapt the devices to the required functional length. The objective of the current study is to investigate if the SLA prosthesis from MED-EL (currently not FDA approved in USA) can withstand typical forces within the human middle ear.

Assessment of the surgical usability was performed to assess that appropriate design & performance has been achieved. Literature was reviewed to define forces which can occur during the lifetime of an ORP. Destructive pull tests, with partial & total ORP (mXACT PRO Partial & Total; MED-EL, Innsbruck, Austria), were performed to determine the forces such a prosthesis can withstand.

Assessment of the surgical usability and the comparison of the results from the literature research and the destructive pull tests indicate that the prostheses can withstand loads markedly higher than the forces which typically occur, within the human middle ear.

PS20

Technical background of the Vibrogram in-situ measurement for the VIBRANT SOUNDBRIDGE

Hamidreza Mojallal, MED-EL Medical Electronics

Introduction: The Vibrogram is integrated as an in-situ measurement tool in the SYMFIT fitting software for the VIBRANT SOUNDBRIDGE (VSB) active middle ear implant. It was introduced in 2012, but it is still considered sometimes as a black box for some experts. The aim of this presentation is to provide the professional user with some information about the technical background of the Vibrogram development and its application in the clinical workflow.

Method: The output quantification of AMEIs is based on ASTM standard [1]. The output quantification of the VSB's floating mass transducer (FMT) is based on temporal bone measurements by Geoffrey Ball et al. in 1990s. In several temporal bone measurements, the vibration of the stapes footplate by electrical excitation of the FMT coupled to the long process of the incus was measured and compared to the middle ear transfer function with constant sound pressure in the ear canal [2]. These values were used as the fundamental magnitudes for the calculation of output curves and fitting procedures in the software and has been adapted for all frequencies and levels in the Vibrogram. However, as the values were in dB SPL, they needed to be converted into the equivalent dB HL (dB HL eq) magnitudes. For this purpose, the ANSI standard for conversion from dB SPL to dB HL was used [3]. The same calibration has been used in the software for all types of audio processors (i. e. Lo and Hi). However, since different APs show different output characteristics, for development of the Vibrogram these differences had to be considered.

Result: According to mentioned procedures, the corresponding excitation voltage for 100 dB HL eq at 1 kHz is about -15.5 dB V or about 168 mV rms (i. e. 100 dB SPL: -23 dB V)

Conclusion: Despite proven benefits of the Vibrogram, there are some potentials for improvement. Further research is in progress to investigate the influence of different coupling positions and their impact on Vibrogram measurement and consequently on device fitting. Two limitations of the Vibrogram in former SYMFIT software versions have been improved upon in the new SYMFIT 8 generation. The first is better user friendliness regarding measurement and data entry. The other improvement relates to the direct implementation of the bone conduction audiometric thresholds and Vibrogram thresholds in target gain calculation. This leads to a streamlined and more comfortable first fit, especially for patients with moderate-to-severe mixed hearing loss. For more details, the white paper on this topic can be found under: https://www.medel.pro/online-resources/white-papers

References:
1. Standard practice for describing system output of implantable middle ear hearing devices, ASTM F 2504-05,2005
2. Dietz, TG; Ball, GR; Katz, BH. Partially Implantable Vibrating Ossicular Prosthesis. International Conference on Solid-State Sensors and Actuators, 1997, p. 433-436
3. ANSI-standard S3.6-1996. Specification for Audiometers.

PS21

Development of a new stapes head coupler for the Vibrant Soundbridge

Kathrin Sonntag, MED-EL Medical Electronics
Frauke Niewöhner, MED-EL Medical Electronics

Background: The Vibrant Soundbridge (MED-EL Medical Electronics, Austria) is an active middle ear implant with a floating mass transducer (FMT) that is connected to a middle ear structure. In case of a discontinuous ossicular chain with an intact stapes, the FMT can be coupled on top of the stapes suprastructure via a Vibroplasty Clip-Coupler (MED-EL Medical Electronics). For middle ears where space between the head of the stapes and the tympanic membrane is reduced, an alternative coupler has been developed. The new Stapes-SH-Coupler (SH-Coupler) has been designed to fit middle ears where a reduced functional height is required without losing transmission performance.

Methods: Micro-CT data of temporal bones have been analyzed to find the optimal placement for the coupler and FMT in relation to the stapes and the available space. 3D-model variants of the SH-Coupler were virtually positioned to the stapes to find the ideal design. To estimate the pressure when coupling the SH-Coupler to the stapes, a FEM simulation was performed. The dimension and design of the titanium coupler legs have been considered to achieve an optimal clamping connection to the stapes head and crura. Usability placement tests on temporal bones were conducted. 17 surgeons performed handling tests by placing the SH-Coupler to the stapes.

Results: The new SH-Coupler has a reduced functional height of 0.5 mm compared to the Vibroplasty Clip-Coupler. Instead of placing the FMT with the Clip-Coupler above the stapes head, the FMT is now placed lateral to the stapes with the SH-Coupler. The actual protrusion of the SH-Coupler above the stapes head now measures 1.9 mm. For a perfect and stable coupling to the stapes, a 6-legs-design was developed. 4 legs clamp the stapes crura, 2 legs the stapes head. The SH-Coupler passed the handling test and all usability related acceptance criteria were fulfilled.

Conclusions: The new developed SH-Coupler provides an alternative with more stable fixation to the stapes when placement of the current Vibroplasty Clip-Coupler is limited. With the new SH-Coupler, the FMT is positioned on the inferior side of the stapes instead of the top of the stapes head to reduce the functional height. The new SH-Coupler includes coupling to the stapes crura in addition to coupling to the stapes head to enhance stability of angular positioning of the FMT.

PS22

Design, Fabrication, Benchtop, and Cadaveric Temporal Bone Testing of Ultraminiature MEMS Implantable Middle Ear Accelerometers

Panagiota Kitsopoulos, University of Michigan
Alison E. Hake, University of Michigan
Emily Z. Stucken, University of Michigan
Christopher M. Welch, University of Michigan
Karl Grosh, University of Michigan

Background: Hearing loss is a debilitating condition that affects over 5% of the world's population. Hearing aids (HAs) positively impact patients' lives, but HA adoption and use rates are very low. Negative issues associated with the external elements of traditional auditory prostheses, such as safety, appearance, and ease of use, are among those most cited by patients either for not adopting a HA or for abandoning their use. A completely implantable auditory prostheses (CIAP) could help to ameliorate these issues. For the same reasons, cochlear implant (CI) patients could also benefit from the development of a completely implantable device. Blocking progress toward this goal is the lack of a completely implantable acoustic sensor capable of matching or exceeding the performance of external microphones. Previous studies have indicated that, with their small size and performance, piezoelectric microelectromechanical systems (MEMS) accelerometers have the potential to function as implantable sensors within the middle ear, thus replacing the external components. A low-noise implantable accelerometer is yet to be built, but we are on the critical path towards meeting the necessary specifications.

Methods: Our ultraminiature accelerometer designs consist of proof-mass-loaded piezoelectric cantilever bimorph beams in either a single or dual resonance configuration. We test our sensors in benchtop experiments (actuation and sensitivity) where the output of the MEMS accelerometer was compared to that of a laser doppler vibrometer for calibration and verification. These experiments are used to validate analytical models that predict our sensors' performance due to different directional excitations. We have performed cadaveric temporal bones testing accessing the middle ear using a mastoidectomy with posterior tympanotomy approach to avoid disturbing the tympanic membrane) and affixing the accelerometer to the umbo.

Results: Previous results have validated the analytical model for transverse excitations. Our models now have identified a dual bandwidth sensor design that meets low noise and low mass specifications. Rapid prototyping has enabled us to develop packaging that encapsulates our sensor and fits within the middle ear cavity thereby allowing for quick experimental testing of new design concepts. Preliminary testing in cadaveric temporal bones with a commercial, ultraminiature, narrow bandwidth sensor shows promising results, and we are interested in extending this cadaveric experiment to our own prototypes.

Conclusion: Validated modeling and testing show promise for our small (<10mg) packaged piezoelectric MEMS accelerometers. While our theoretical results point the way forward, experimental validation of the packaged devices is needed to realize this promise.

PS23

Relevance of tympanic membrane lesion at different locations and of different sizes for the middle ear transfer function

Thomas Effertz, University of Göttingen
Nicholas Bevis, University of Göttingen
Benjamin Sackmann, University of Reutlingen
Michael Lauxmann, University of Reutlingen
Dirk Beutner, University of Göttingen

Perforations of the tympanic membrane (TM) can occur as a result of injury or inflammation of the middle ear. These perforations can lead to conductive hearing loss (HL), where in in some cases the magnitude of HL exceeds that attributable to the observed TM perforation alone. We aim with this study to better understand the effects of location and size of TM perforations on the sound transmitting properties of the middle ear.
The middle ear transfer function (METF) of six human temporal bones (TB; freshly frozen specimen of body donors) were compared before and after perforation of the TM at different locations (anterior or posterior lower quadrant) and of different sizes (1mm, ¼ of the TM, ½ of the TM, and full ablation). The METF were correlated with a Finite Element (FE) model of the middle ear, in which similar alterations were simulated.
The measured and simulated FE model METFs exhibited frequency and perforation size dependent amplitude losses at all locations and severities. In direct comparison, posterior TM perforations affected the transmission properties to a larger degree than perforations of the anterior quadrant. This could possibly be caused by an asymmetry of the TM, where the malleus-incus complex rotates and results in larger deflections in the posterior TM half than in the anterior TM half. The FE model of the TM with a sealed cavity suggest that small perforations result in a decrease of TM rigidity and thus to an increase in oscillation amplitude of the TM, mostly above 1 kHz.
The location and size of TM perforations influence the METF in a reproducible way. Correlating our data with the FE model could help to better understand the pathologic mechanisms of middle-ear diseases. If small TM perforations with uncharacteristically significant HL are observed in daily clinical practice, additional middle ear pathologies should be considered. Further investigations on the loss of TM pretension due to perforations may be informative.

PS24

Application of Wideband-Tympanometry for the Evaluation of Passive Middle-Ear Prostheses

Nicholas Bevis, University of Göttingen
Thomas Effertz, University of Göttingen
Dirk Beutner, University of Göttingen

Application of Wideband-Tympanometry for the Evaluation of Passive Middle-Ear Prostheses
The mechanical properties of the middle ear and the behavior of new prostheses are studied in temporal bones using Laser-Doppler Vibrometry (LDV) and simulated using the finite element method (FEM). However, these do not represent middle-ear characteristics during atmospheric pressure fluctuations. Wideband tympanometry (WBT) provides a noninvasive method for monitoring the acoustic properties of the middle ear. We have investigated the use of WBT in the evaluation of passive middle ear prostheses.
We utilized LDV and WBT (Interacoustics Titan-Tympanometer) measurements to test two partial ossicular replacement prostheses (PORP) in tympanoplasty under different pressure conditions (± 300 daPa). One prosthesis had the design of a rigid titanium prosthesis, whereas the other prosthesis had a ball joint centered in the prosthesis headplate.
Both prostheses showed equivalent sound transmission characteristics in the LDV measurements. Differences in the behavior of the prostheses were observed during the WBT measurements. Changes in static pressure in the ear canal caused movements of the tympanic membrane, which affected the acoustic admittance of the reconstruction.
WBT provides new insights on the evaluation and development of passive middle-ear prostheses, as the dynamic movements of the ossicular chain can be observed during atmospheric pressure variations. This allows prediction of prosthesis movement under physiological conditions and should be further investigated.

Author Index

Fierens, Guy	PS11
Firzlaff, Daniel	PD2.7
Fridberger, Anders	PD7.4
Furhapter, Severin	PS18
Furlong, Cosme	PS9
Gan, Rong	PD6.3 , PD8.1 , PD8.2
Geerardyn, Alexander	PS11
Ghoncheh, Mohammad	PD5.2 , PD7.3 , PS4
Golde, Jonas	PD11.3
Graf, Lukas	PD10.6, PS6
Grais, Emad M	PD11.2
Greene, Nathaniel	PD1.2, PD8.3 , PS8
Grosh, Karl	PD2.1 , PS22
Gruninger, Ivo	PS3, PS13
Guan, Xiying	PS7
Hake, Alison E	PD2.1 , PS22
Harre, Kathrin	PD2.7
Hayashi, Masaaki	PS10
Higo, Takenobu	PS10
Honegger, Flurin	PS6
Hoon Sim, Jae	PD1.2, PD1.4 , PD1.5
Horton, Nicholas	PS16
Hu, Yihan	PD3.2
Huber, Alexander	Keynote, PD1.4 , PD1.5 , PS14
Huettenbrink, Karl Bernd	PD11.1
Hyun Cho, Nam	PD1.6
Ikegami, Hajime	PS10
Irie, Yuuka	PS10
Jenkins, Herman	PS8
Jiang, Shangyuan	PD6.3 , PD8.1 , PD8.2
Jie Ren, Liu	PD1.2
Kanzaki, Sho	PD6.4 , PS10
Keat, Chee Sze	PS10
Keefe, Douglas	PS16
Kempa, Stephan	PS12
Kerckhofs, Greet	PD4.2
Kerkhofs, Lore	PD4.2 , PD4.3
Kieswetter, Klaas	PS18
Kim, Namkeun	PD7.1
Kim, Jongwoo	PD7.1
Kirsten, Lars	PD11.3
Kitsopoulos, Panagiota	PD2.1 , PS22
Kleemann, Hans	PD2.7
Knlke, Nicole	PD10.5
Koch, Martin	PD1.2, PD2.6
Koch, Edmund	PD11.3
Koike, Takuji	PD6.4 , PS10
Kuen, Clemens	PS19
Kymissis, Ioannis	PD10.6
Lang, Jeffrey	PD10.6
Lauxmann, Michael	PD2.4 , PD6.1 , PD6.2 , PS23
Lechleitner, Thomas	PS19
Lee, Sinyoung	PD6.4 , PS10
Lenarz, Thomas	PD5.3 , PD10.3, PD10.4, PD10.5, PS4

Leo, Karl	PD2.7
Li, Chenlong	PS1
Liang, Junfeng	PS7
Livens, Pieter	PD1.1, PD4.1
Lorenz, Korinna	PD11.5
Ludke, Theresa	PD2.7
Maas, Patrick	PD7.3
Macke, Jakob	PD11.4
Maier, Hannes	PD1.2, PD2.3, PD5.2, PD5.3, PD7.3, PD9.2, PD10.3, PD10.4, PD10.5, PS4
Martin, Michael	PS12
Mason, Matt	Plenary Lecture 3
McHugh, Christopher	PD1.6, PD10.6
Mohallal, Hamidreza	PD2.3
Mojallal, Hamidreza	PS20
Molenda, Carmen	PS13
Morgenstern, Joseph	PD11.3
Morita, Yoji	PD6.4
Mosshammer, Klara	PD2.7
Motallebzadeh, Hamid	PD11.4, PS7, PS15
Muller, Christoph	PD11.5
Muller, Joachim	PS3, PS13
Muller-Gerbl, Magdalena	PS6
Muyshondt, Pieter	PD1.1
Myoung2, Soomin	PS16
Nakajima, Hideko Heidi	PD1.6, PD10.6
Neudert, Marcus	PD1.2, PD1.3, PD2.5, PD2.6, PD2.7, PD3.3, PD11.3, PD11.5
Nie, Leixin	PD11.2
Niewhner, Frauke	PS21
O'Connell-Rodwell, Caitlin	PD3.2
Ohoyama, Kenji	PS10
Olson, Elizabeth	PD10.6
Ossman, Steffen	PD1.3
Ossmann, Steffen	PD3.3
Peacock, John	PD3.1, PS2
Pfiffner, Flurin	PD5.1, PD7.2
Polk, Marie-Luise	PD11.5
Prenzler, Nils	PD5.3
Prochazka, Lukas	PD1.4
Prodanovic, Srdan	PD5.2, PD7.4
Puria, Sunil	PD3.2, PD9.1, PD11.4, PS7, PS15
Putzeys, Tristan	PD4.2, PD4.3, PS11
Pyka, Grzegorz	PD4.2
Rahim, Tariq	PD11.2
Rainer, Stefan	PS17
Ravicz, Michael	PD1.6, PD3.2, PD9.1
Remenschneider, Aaron	PS9, PS16
Ren, Liu Jie	PS1, PS5
Rocha F,lix, Tiago	PD4.2, PD5.3
Rsli, Christof	PD1.4, PD1.5, PD5.1, PD7.2
Rose-Eichberger, Karin	PS18
Rosowski, John	PS9
Sackmann, Benjamin	PD2.4, PD6.1, PD6.2, PS23
Salcher, Rolf Benedikt	PD5.3

Sanders, Sarah	PD8.2
Scandurra, Francesca	PS18
Schr, Merlin	PD1.4, PD1.5, PS14
Schnleitner, Florian	PD11.4
Schurzig, Daniel	PD9.2
Secchia, Paul	PD1.6
Sertich, Joe	Banquet Presentation
Shimizu, Yuki	PS10
Sim, Jae Hoon	PS14
Sok, Mealaktey	PS16
Song, Yew	PD10.6
Sonntag, Kathrin	PS21
Spellman, Garth	PD3.1, PS2
Spitzner, Sarah	PD2.7
Starovoyt, Anastasiya	PD4.2, PD4.3
Stauske, David	PD2.3
Steinhardt, Uwe	PS19
Stenfelt, Stefan	Plenary Lecture 4, PD5.2, PD7.3, PD7.4, PS5
Stieger, Christof	PS6
Stoessel, Alexander	PD3.3
Strenger, Tobias	PD10.2
Stucken, Emily Z	PD2.1, PS22
Surendran, Sudeep	PS5
Tang, Haimi	PS9
Timm, Max Eicke	PD5.3, PD9.2
Tollin, Daniel	PD3.1, PD8.3, PS2, PS8
Urban, Michael	PS18
Verhaert, Nicolas	PD4.2, PD4.3, PS11
Voss, Susan	PS16
Waldmann, Bernd	PD5.3
Walilko, Tim	PD8.3
Wang, Fang	PD11.6
Wang, Shuqi	PS1
Waool-Kornherr, Edwin	PS19
Warnecke, Athanasia	PD9.2
Warnholtz, Birthe	PD1.4
Welch, Christopher M	PD2.1, PS22
Wils, Irina	PS11
Wirth, Markus	PD11.6
Xie, Youzhou	PS1, PS5
Xu, Jingqi	PS1, PS5
Yao, Wenjuan	PS1, PS5
Yeiser, Aaron	PD10.6
You, Hyeonsik	PS10
Zahnert, Thomas	PD2.5, PD2.7, PD11.3, PD11.5
Zhang, John	PD10.6
Zhang, Tianyu	PS1, PS5
Zhao, Mingdou	PD7.4
Zhao, Fei	PD11.2
Zhe-Xi, Luo	Plenary Lecture 1
Zosuls, Aleksandrs	PD1.6

The Grace ALTO line offers a unique patented method that makes the ALTO the only non-crimp adjustable length titanium design in otology today. This advantage allows the surgeon to adjust the prosthesis even after initial sizing, trimming and placement. The prosthesis can be lengthened or shortened in precise .25mm increments. The Grace Medical product line offers a vast array of options for the medical professional including titanium and titanium with hydroxlapatite (HA) heads, integrated footplate shoes and elaborate innovative head designs that interface with cartilage or the tympanic membrane (TM).

Visit **www.gracemedical.com** to learn more.

Grace Medical We Listen.

8500 Wolf Lake Drive, Suite 110 | Memphis, TN 38133 | Toll-Free 1.866.472.2363 | www.gracemedical.com

Kurz Middle Ear Surgery Solutions

Precision in the Middle Ear Where it Matters Most!

- ✓ Developed By Surgeons/Middle Ear Mechanics Engineers
- ✓ Long History of Helping Surgeons Safely Deliver Excellent Hearing Outcomes Since 1993
- ✓ Evidence Based Middle Ear Surgery Solutions is Our Passion
- ✓ New Innovations coming in late 2022/early 2023

Variac Adjustable Partial and Total with Footplate Shoe

Nitibond Heat Activated Self Crimping Stapes Prosthesis

The Original Clip Partial

Nitiflex Stapes Prosthesis

Heinz Kurz GmbH
Tuebinger Strasse 3 | 72144 Dusslingen | Germany
Phone: +49 (0)7072/9179-0
E-Mail: info@kurzmed.com

Kurz Medical, Inc
5126 South Royal Atlanta Drive
Tucker, GA 30084
Phone: (770) 349-6330
Email: info@kurzmed.com

MED-EL

BONEBRIDGE BCI 602

Always A Step Ahead

With a reduced drilling depth of almost 50%*, straightforward surgery, plus excellent hearing and healthy skin for your patients, find out why BONEBRIDGE is the world's most advanced active bone conduction implant.

Discover more at https://go.medel.pro/BONEBRIDGE

M00886 r1.0

hearLIFE

*in comparison to the previous BCI 601 implant

medel.com

Oticon Medical

Ponto 5 Family of Sound Processors

Still the smallest

- Ponto 5 Mini - Still the world's smallest sound processor
- Ponto 5 SuperPower - The world's smallest and still the most powerful abutment-level SuperPower sound processor

BrainHearing™ benefits

- Better hearing starts with the brain
- Designed to support the cognitive processes we use to make sense of sound: Orient, Separate, Focus and Analyze
- Aims to make listening easier and free up mental energy

OpenSound Navigator™

- Reduced listening effort for your patients
- Preserves speech and provides access to sound from 360°

OpenSound Optimizer™

- Feedback management with no audible feedback and stable gain throughout the day
- Improved sound quality

Oticon RemoteCare for Oticon Medical

- A secure, convenient and focused solution for remote follow-up care
- Flexible appointment options for your patients

Learn more about the Ponto™ System

www.oticonmedical.com/us

oticon MEDICAL

Venue Area

University Memorial Center

UNIVERSITY OF COLORADO **BOULDER**

Second Floor

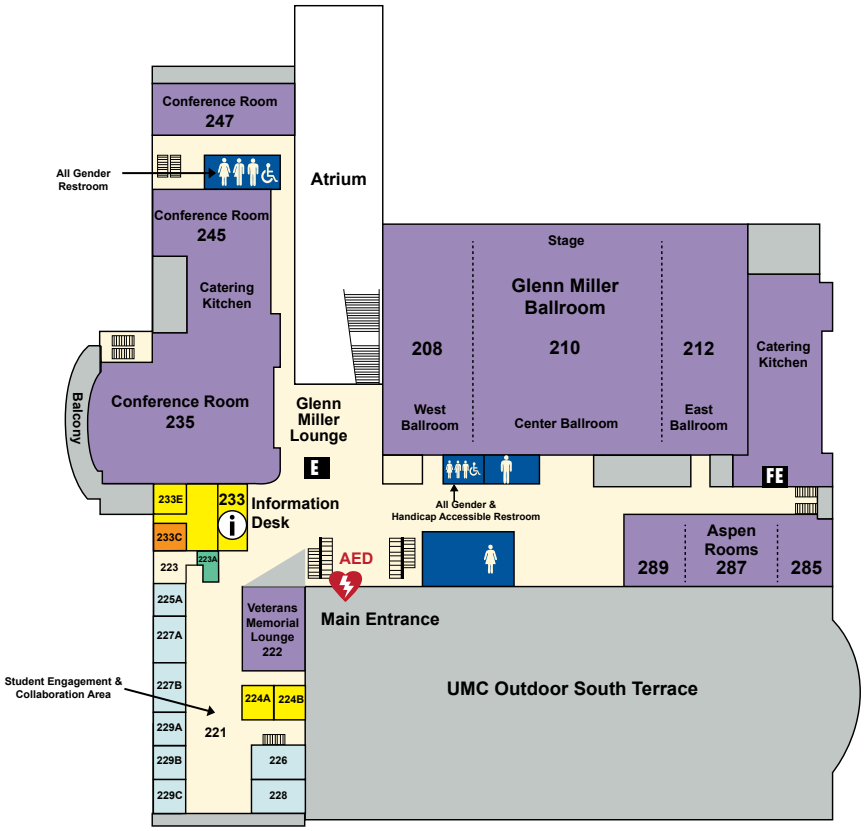

OFFICE	ROOM #
Aspen Rooms	285, 287, 289
Conference Rooms	235, 245, 247
CU NightRide	233C
Glenn Miller Ballroom	208, 210, 212
Quiet Space	223
Student Engagement & Collaboration Area	221
UMC Information Desk	233
UMC Security	233E
Veterans Memorial Lounge	222
Washroom (CU affiliates only)	223A

- Administrative Office
- Conference Room
- Restroom
- Washroom
- Student Organization Meeting Space
- Student Service
- Automated External Defibrillator (AED)
- E Elevator
- FE Freight Elevator
- Information

MEMRO 2022
Hearing Research

Dear Colleagues,

For those wishing to contribute to a special edition of Hearing Research highlighting research presented at MEMRO 2022, please submit manuscripts (see procedure below) for review by **August 1, 2022**. This deadline will be strictly enforced to ensure timely review and publication of this work.

Details for assisting your manuscript preparation.
Papers in special issues can be either review or new research papers tied to your presentation. Papers should be substantial but not longer than 10 printed pages, including Figures, Tables, etc. This corresponds to approximately 10,000 words (where every figure/table reduces this by approximately 350 words). We suggest you not drop below 6,000 words.
Elsevier will provide free color in the print issue for up to four Figures (all figures are free on the Web version).
Papers must be submitted online via www.sciencedirect.com/journal/hearing-research. Follow the instructions and select MEMRO 2022 from the Article Type menu. This will ensure the paper is routed for review for the MEMRO special edition.
Submissions will be reviewed in the same manner as regular submissions to the journal, but to ensure the accepted manuscripts have high quality and interest to the broader Hearing Research community, the editors will assess each submission for excellence in quality, novelty, interest (to the broader hearing research community), and representation of the MEMRO meeting prior to sending each out for review. Hearing Research normally sends reviews back within 3-4 weeks of the submission date. In order to speed publication, revisions should be submitted within 4 weeks of receipt of the initial decision. A second round of revision may be required. Accepted papers appear as submitted on the Hearing Research website within days, and corrected proofs typically appear within 6 weeks. The print edition will appears sometime in the middle of 2023.
Anticipated timeline:

a. First submission	**August 1, 2022**
b. Initial decision	October 1, 2022
c. Revised version submisstion	October 15, 2022
d. (Final) decision	December 1, 2022
e. Accepted paper on the web	December 15, 2022
f. Corrected proofs on the web	January 15, 2023

Guidelines for authors can be found at: https://www.elsevier.com/journals/hearing-research/0378-5955/guide-for-authors

Thank you for your contribution.

Stephen Cass, Nathaniel Greene, and Daniel Tollin
Editors for this Special Edition

NOTES